Hormonal responsiveness underlies trait diversification in *Sceloporus* lizards

Christopher David Robinson

San Antonio, Texas

Master of Science, University of Central Arkansas, 2017

Bachelor of Science, Trinity University, 2014

A Dissertation presented to the Graduate Faculty of the University of Virginia in Candidacy for the Degree of Doctor of Philosophy

Department of Biology

University of Virginia

March 27, 2024

Abstract

Testosterone plays a central role in regulating the development of male traits across vertebrates. Although this role is well-established, how androgen regulation evolves to influence the development of traits differently across species remains less clear. In my dissertation, I use lizards in the genus *Sceloporus* to test how hormone-phenotype couplings and hormone-genome interactions evolve to facilitate the evolution of male traits and of sexual dimorphism. In Chapter 1, I perform a testosterone manipulation experiment in juveniles from two species: *S. undulatus*, which exhibits the ancestral state of sexually dimorphic ventral coloration that develops when testosterone induces melanin synthesis in males, and *S. virgatus*, which exhibits a derived sexually monomorphic coloration where testosterone does not induce color development and melanin is absent from the dermis. I find that ventral skin in the sexually dimorphic *S. undulatus* is significantly more responsive to testosterone than ventral skin in the sexually monomorphic *S. virgatus*, as quantified by the number of genes up- or downregulated by testosterone. In particular, genes related to melanin synthesis are strongly upregulated by testosterone in the sexually dimorphic species, but not in the sexually monomorphic species. My results suggest that tissue- and gene-level sensitivity to testosterone can evolve to facilitate the evolution of male traits. In Chapter 2, I use immunohistochemistry to test whether the abundance and distribution of androgen receptor protein differ in the skin of unmanipulated adults of both species, predicting that androgen receptor localizes to melanophores (the cell type that produces melanin) in *S. undulatus* but to a different cell type in *S. virgatus*. I find that skin from *S. undulatus* males has abundant androgen receptor that is localized to the most superficial part of the dermis. However, *S. virgatus*

males exhibit very little androgen receptor, which is mostly observed in deeper parts of the dermis. Using antibodies for proteins characteristic of melanophores, I find that androgen receptor in *S. undulatus* males likely colocalizes within this cell type, which would facilitate androgen-induced melanin synthesis. However, I do not detect any melanophore markers in skin from *S. virgatus* males. This result suggests that the reduced androgen sensitivity in *S. virgatus* may be due to a significant reduction in androgen receptor expression, possibly driven by the loss of a single cell type crucial for androgen-induced melanin synthesis. In Chapter 3, I shift focus to test for sex- and species-specific effects of testosterone on the liver transcriptome. Using three species of *Sceloporus* (*S. undulatus*, *S. virgatus*, and *S. merriami*), I perform a testosterone manipulation experiment in juveniles and analyze gene expression in the liver. I find that males consistently have a stronger transcriptomic response to testosterone than females, but that the direction of testosterone-mediated gene expression is concordant between the sexes. However, I find that testosterone-mediated gene expression between species is evolutionarily labile, such that genes that are upregulated (or downregulated) by testosterone in one species are conversely downregulated (or upregulated) by testosterone in another. Further, the number of genes with significant treatment-by-species interactions increases with phylogenetic distance, suggesting that individual genes evolve to respond to testosterone in species-specific ways. Together, these results suggest that the transcriptome is characterized by evolutionary potential, facilitating the evolution of male traits and sexual dimorphism despite pleiotropic effects of testosterone.

Acknowledgements

I have many people to thank for their contributions to this dissertation. First and foremost, thanks to my advisor Bob Cox for pushing me to always think deeper. My dissertation is very different than I initially envisioned, but it is something that I am incredibly proud of. I could not have gotten here without your insight and dedication to rigorous science and logic. Thanks to my many collaborators and co-authors, Ian Clifton, Christian Cox, Matthew Hale, Henry John-Alder, Matthew Milnes, and Tyler Wittman. I would not have gotten through all of this work without your effort and unique perspectives on science. Thanks to all of my other lab mates, Rachana Bhave, Ashlyn Crain, Pietro de Mello, Myles Davoll, and Daniel Nondorf for discussions on my drafts of each chapter. And thank you to my committee, Butch Brodie, Dave Parichy, Alan Bergland, and Dave Carr, for asking insightful questions and giving advice as my dissertation took shape.

A special thanks to everyone who helped make Charlottesville home. Tyler Wittman, Maura Austin, and Ryan Sangston were with me from start to end. You all contributed so much to six years of joy, even when I was bad at collaborative board games. I am so fortunate to have made many great friends: Kim Arena, Kendall Branham, Audrey Brown, Luke Dilliard, Keric Lamb, Adam Lenhart, Hanna Makowski, Liza Mitchem, Connor Murray, Daniel Nondorf, Taylor Nystrom, and Phil Tubergen, and certainly others. Thank you all for the memories and making my time at UVA incredible.

Finally, thank you to my family for supporting me throughout this process.

I love you all so much.

Table of Contents

Introduction

Sexual dimorphism is a pervasive phenomenon despite the challenge of producing two distinct phenotypes from one underlying genome (Badyaev 2002). While numerous mechanisms have evolved to facilitate the development of sexually dimorphic traits, a commonly used (and studied) mechanism is differential regulation of transcription (Waxman and O'Connor 2006; Mank 2009; Williams and Carroll 2009; Cox et al. 2017; Wright et al. 2019; Gazda et al. 2020; Khalil et al. 2020). In vertebrates, sex differences in transcription are often regulated by estrogens and androgens (Rinn and Snyder 2005; van Nas et al. 2009; Xu et al. 2012; Frankl-Vilches et al. 2015; Cox et al. 2017; Anderson et al. 2020; Ansai et al. 2021; Hale et al. 2022). In my dissertation, I test how the steroid hormone testosterone regulates the development of sexually dimorphic phenotypes, and explore how hormonally mediated trait regulation can evolve to result in novel patterns of sexual dimorphism across closely related species.

Testosterone is a sex-steroid hormone produced primarily in the testes. Consequently, testosterone generally circulates at higher concentrations in males than in females, contributing to the development of male-typical traits. Biologically active testosterone (often converted by 5α-reductase into the more potent androgen 5α-dihydrotestosterone) exerts genomic effects by binding to the androgen receptor, which becomes activated upon binding and translocates to the nucleus. Here, the activated receptor acts as a transcription factor, altering patterns of gene expression by binding to androgen response elements (AREs) in the promoter, enhancer, or repressor region of target genes (Bennett et al. 2010; Cox 2020). Tissue-specific factors then modulate whether testosterone can bind to its receptor and alter transcription by interacting with an

ARE. Consequently, testosterone influences the expression of dozen to thousands of genes simultaneously, depending on ligand binding, chromatin accessibility, and coregulatory recruitment and receptor modulation (reviewed in Pihlajamaa et al. 2015). This phenomenon, known as hormonal pleiotropy, is thought to act as an evolutionary constraint if selection on the expression of a hormonally regulated gene causes maladaptive change in the expression of a second hormonally regulated gene (Stearns 1989; Flatt et al. 2005; Hau 2007; Mauro and Ghalambor 2020). By decoupling from androgen regulation, gene expression is "freed up" to contribute to phenotypic evolution across species without a corresponding change in circulating hormone levels (Hau 2007; McGlothlin and Ketterson 2008; Ketterson et al. 2009; Fuxjager and Schuppe 2018; Cox 2020; Cox et al. 2022).

In this dissertation, I use hormone manipulation experiments, RNA sequencing, and immunohistochemistry to investigate how androgen sensitivity, hormone receptor abundance, and hormone-phenotype couplings can evolve to facilitate the evolution of sexual dimorphism.

Sceloporus *lizards as a model system*

Fence and spiny lizards of the genus *Sceloporus* provide an ideal system to address this fundamental issue in evolutionary endocrinology because of their evolutionary history. The genus *Sceloporus* contains more than 100 recognized species found in North and Central America. The ancestral state of *Sceloporus* is characterized by male-biased sexual size dimorphism (John-Alder and Cox 2007) and the presence of sexually dimorphic ventral coloration in males (Wiens 1999; Ossip-Drahos et al. 2016).

Experimental work has illustrated that the steroid hormone testosterone is involved in the development of these sexually dimorphic phenotypes. In species with male-biased sexual size dimorphism, testosterone promotes skeletal growth (Cox and John-Alder 2005; John-Alder et al. 2007), and in species with ventral coloration, testosterone stimulates color production (Kimball and Erpino 1971; Cox et al. 2005b, 2008) through the synthesis of melanin (Quinn and Hews 2003).

However, sex differences in body size and coloration are evolutionarily labile. Across the sceloporine phylogeny, a derived state of female-biased sexual size dimorphism has evolved approximately six times (Jiménez-Arcos et al. 2017). In species where females are larger, testosterone has an inhibitory effect on growth rates (Abell 1998; Klukowski and Nelson 2001; Cox and John-Alder 2005; Cox et al. 2005a; Pollock et al. 2017). While the mechanisms underlying these evolutionary reversals are unknown, testosterone downregulates the expression of *IGF1* in the female-larger *S. undulatus* (Duncan et al. 2020). An analogous comparison has not been conducted in a male-larger *Sceloporus* species, but in the male-larger brown anole lizard (*Anolis sagrei*), testosterone promotes the development of male-biased sexual size dimorphism by upregulating *IGF1* (Cox et al. 2017). Therefore, it is reasonable to assume that the evolutionary reversal in sexual size dimorphism in *Sceloporus* is driven, at least in part, by novel genetic regulation of growth pathway genes by testosterone. Similarly, ventral coloration in males has been lost approximately 13 times across *Sceloporus*, resulting in a derived sexually monomorphic state (Wiens 1999). In the sexually monochromatic *S. virgatus*, testosterone no longer stimulates the production of melanin (Abell 1998; Quinn and Hews 2003). Again, the mechanism facilitating this evolutionary decoupling is unknown.

However, evolution of androgen regulation within the melanophore (the pigment cell that produces melanin) itself offers a plausible explanation, as ventral skin from *S. virgatus* (which has lost ventral coloration) retains guanine-filled iridophores (a second pigment cell type necessary for the expression of ventral coloration; Morrison et al. 1995; Hews and Quinn 2003).

In my dissertation, I use three species of *Sceloporus* lizards to test for mechanisms that contribute to the evolution of male traits and, consequently, the evolution of sexual dimorphism (Figure 1). The Eastern Fence Lizard, *S. undulatus*, is a female-larger species with sexually dimorphic ventral coloration. It is quickly becoming a model organism in evolutionary ecology and endocrinology, and the recent assembly and annotation of its genome (Westfall et al. 2021) has facilitated new investigations into the genetic responses to ecological stimuli (e.g., Assis et al. 2023). The Striped Plateau Lizard, *S. virgatus*, is a female-larger species that has lost male ventral coloration, representing the derived sexually monomorphic state. It is nested within the *undulatus* clade and diverged from the *S. undulatus* lineage approximately 12 million years ago (Wiens 1999; Ossip-Drahos et al. 2016). The Canyon Lizard, *S. merriami*, represents a basal lineage of *Sceloporus* and is characterized by the ancestral state for both traits: *S. merriami* exhibits male-biased sexual size dimorphism and has ventral coloration only in males. The most recent common ancestor between *S. merriami* and the *undulatus* clade was approximately 30 million years ago (Wiens 1999; Leaché et al. 2016; Ossip-Drahos et al. 2016). In Chapters 1 and 2, I compare *S. undulatus* and *S. virgatus* to test for mechanisms underlying the evolution of hormonally regulated coloration, using RNAseq to identify genetic pathways that differ in hormonal responsiveness between these two

species (Chapter 1), and immunohistochemistry to examine how differences in androgen receptor abundance and distribution can explain the observed transcriptomic differences in the skin (Chapter 2). In Chapter 3, I use all three species to test whether androgen regulation of gene expression is evolutionarily labile, then use results from this experiment to draw inferences about the evolutionary potential hypothesis (described below). Altogether, my dissertation advances our understanding of how hormonally regulated phenotypes can evolve through alterations to androgen sensitivity of gene expression. I show that molecular pathways related to phenotypic development evolve alternative regulatory relationships with androgens, and that the hormonally mediated transcriptome is defined by significant evolutionary potential.

Circulating hormones and hormone sensitivity as targets of selection

Historically, the perspective that changes to circulating hormone levels are correlated with phenotypic evolution across species has received much attention, largely because of the ease of measuring circulating hormone levels (Møller et al. 2005; Hau et al. 2008; Husak and Lovern 2014; Husak et al. 2021). However, circulating hormone levels alone often do not explain phenotypic variation observed in nature. For example, in two subspecies of *Junco hyemalis* that differ in testosterone-mediated aggressive behavior and ornamentation, gonadotropin-releasing hormone and luteinizing hormone both lead to the production of similar testosterone levels in each population (Bergeon Burns et al. 2014). However, levels of mRNA for luteinizing hormone receptor in the testes and androgen receptor in the hypothalamus differ, suggesting that autoregulation of hormone detection can lead to differences in testosterone sensitivity between subspecies

(Bergeon Burns et al. 2014). Tissue-specific sensitivity differences can facilitate phenotypic development that is decoupled from circulating testosterone levels in other tissues, allowing for evolutionary change (Hau 2007; Ketterson et al. 2009; Lipschutz et al. 2019). Because hormones can act pleiotropically throughout the body, change to hormone sensitivity in target tissues offers a compelling mechanism by which phenotypes can evolve in lieu of changes to circulating hormone levels themselves. Indeed, in the species of *Sceloporus* I use in my dissertation, circulating testosterone levels are similar (Cox and John-Alder 2005; John-Alder et al. 2009; Hews et al. 2012). This suggests that the evolution of androgen mediated traits is unlikely to be explained without examining processes that contribute to gene- and tissue-level sensitivity.

Androgen receptor and the evolution of male traits

Recently, evolutionary endocrinologists have begun to appreciate that aspects beyond circulating hormone levels can facilitate the development and evolution of hormonally mediated traits. Because androgens exert the majority of their effects through genomic action, meaning that they alter transcription, it is reasonable to conclude that the nexus between the hormone and genome is a target of selection. In this case, the androgen receptor is the target. Here I discuss two possible mechanisms by which androgen receptor can evolve to facilitate phenotypic diversity across species: sequence evolution and tissue- or cell-specific expression.

The androgen receptor (AR) is comprised of four major domains, each with unique and overlapping functions. The N-terminal domain (NTD) interacts with various cofactors, such as the coactivator SRC1 and the corepressor NCOR1, to alter gene

expression after activation and dimerization (Bevan et al. 1999; Cheng et al. 2002). It is further thought to help recruit heat shock proteins that stabilize the unbound receptor (Smith and Toft 2008). The ligand binding domain (LDB) contains the hormone binding region of the receptor and also helps recruit cofactors (Claessens et al. 2008). The hinge domain facilitates translocation into the nucleus (Zhou et al. 1994; Haelens et al. 2007) and helps the final domain, the DNA binding domain (DBD), to interact with AREs (Shaffer et al. 2004; Helsen et al. 2012), which are nucleotide motifs in promoter or enhancer regions of genes that alter patterns of expression. Across these domains, rates of evolutionary change are variable. In an analysis of eight taxa representing organisms across vertebrates, the NTD and the hinge domain have higher sequence variation than do the LDB and the DBD (Thornton and Kelley 1998; Schuppe et al. 2020). In particular, the LDB exhibits its greatest variation between teleost fishes and non-fishes, which primarily bind 11-ketotestosterone and 5α-dihydrotestosterone, respectively (Schuppe et al. 2020), yet displays 80% or higher sequence conservation among amniotes. Similarly, the DBD exhibits 100% homology among amniotes, with only minor variation between amniotes and fishes (Schuppe et al. 2020). Collectively, these results suggest that androgen- and ARE-binding are highly conserved, yet mechanisms that regulate transcription (such as cofactor recruitment by the NTD) can be fine-tuned readily in a species-specific manner. Mutations within these domains can lead to partial-to-complete androgen insensitivity, or over sensitivity to androgens and the development of cancers (Marcelli et al. 2000; Gottlieb et al. 2012; Chauhan et al. 2018; Fujita and Nonomura 2019). Therefore, selection likely purges mutations in the AR effectively because of the systemic nature of androgens regulating many life history traits simultaneously. Indeed,

the rate at which substitutions occur in these domains is low. Thornton and Kelley (1998) estimated the rates of substitution to be 1.25 per billion years for the NTD, 0.86 for the hinge domain, 0.19 for the LBD, and 0.04 for the DBD between *Xenopus* and human. Similarly, sequence homology is greater than 82% for the hinge region among 44 species of birds, greater than 92% for the DMD, and greater than 96% in the LBD (the NTD was not examined; Schuppe et al. 2020). Importantly for my work, AR shares 100% peptide homology between *S. undulatus* and *S. virgatus* (Nondorf, unpublished data). Therefore, while investigations into AR sequence evolution will likely unveil important patterns of evolution at the macroevolutionary scale, studies that aim to identify mechanisms of evolutionary change among closely related species should focus on other aspects of AR biology, such as receptor abundance.

Alterations to the abundance of AR in target tissues provide a compelling mechanism by which androgen-mediated traits can evolve. Behavioral traits used in sexual signaling can vary remarkably even among closely related species. Therefore, the neuromuscular systems underlying sexually dimorphic behaviors may coevolve with hormone receptor expression levels to facilitate behavioral diversification in predictable ways. Indeed, AR expression in the biceps of six anole lizard species positively covaries with the rate of push-up displays in males (Johnson et al. 2018). Similarly, in an analysis among seven bird species that range from using simple to complex wing movement displays, bird species with higher complexity scores had higher AR expression in muscles that control wing movement than did bird species with lower complexity scores (Fuxjager et al. 2015). Between the species with the highest and lowest complexity scores among these species, androgens up- and downregulate significantly more genes in the high AR,

high complexity species than in the low AR, low complexity species, suggesting that muscular expression of AR facilitates the production of sexually dimorphic behaviors (Fuxjager et al. 2016). Importantly, AR expression differences were only found in musculature that corresponds with the display behaviors, and not in other areas, suggesting that tissue specificity of AR expression facilitates the development and evolution of sexually dimorphic behaviors (Fuxjager et al. 2015). Finally, these findings extend to behaviors that arise convergently across taxa. In the frog *Staurois parvus*, males use a recently evolved foot flagging behavior not present in other members of the Ranidae family. The emergence of this novel behavior corresponds with significantly higher expression of AR in the leg muscles of this species relative to another ranid (*Rana pipiens*) and to the distant *Xenopus laevis*, neither of which uses foot flagging displays (Mangiamele et al. 2016). When expanding similar analyses to species with convergently evolved foot flagging behavior in other families, increased AR in leg muscle consistently coevolves with this behavior, although the magnitude can differ among taxa, suggesting that increased AR abundance cannot fully explain these evolutionary patterns (Anderson et al. 2021). Together, these studies illustrate that tissue-specific receptor abundances can evolve to facilitate the evolution of male-specific traits and, by extension, sexual dimorphism. While this has yet to be examined beyond behavioral phenotypes, it is easy to extend these results to make predictions about AR abundance and the development and evolution of sexually dimorphic morphological phenotypes.

Evolution of hormone-phenotype couplings

While the AR serves as the nexus between androgens and the genome, the efficacy by which a hormone can induce a transcriptomic response involves many additional elements, including (but not limited to) binding globulins that regulate hormone binding efficiency, cofactors that enhance or repress transcriptional ability of the activated hormone receptor, and nucleotide motifs proximal to the transitional start site of a gene to which hormone receptors bind and influence transcription (Fuxjager and Schuppe 2018; Cox et al. 2022). It is easy to envision a simplified scenario in which two individuals have identical circulating hormone levels and identical abundances of hormone receptor. All else being equal, the magnitude of transcriptomic regulation by the hormone, then, should also be identical. However, if a mutation in one individual altered the presence of binding globulins that prevent a hormone from interacting with its cognate receptor, then the downstream transcriptome for these two individuals would now vary; genes regulated by the hormone in the ancestral state would be expressed at basal levels (i.e., the level at which the gene would be expressed in the absence of the hormonal cue) in the mutant individual. Changes like this can be incredibly complex, resulting in novel phenotypic outcomes among individuals and species. These ideas, albeit overly simplified in this framework, illustrate potential mechanisms by which hormone-phenotype couplings can evolve.

Hormonal pleiotropy imposes covariance among phenotypes and coexpression patterns in the transcriptomes underlying those traits (Pavličev and Cheverud 2015). However, as illustrated above, evolution of many molecular mechanisms can erode this covariance and allow for the evolution of phenotypic independence (Ketterson et al.

2009). The evolutionary constraint hypothesis and the evolutionary potential hypothesis represent two ends of a continuum that attempt to explain how pleiotropically regulated traits can evolve (Hau 2007). If traits are tightly linked (constrained), then entire networks evolve as the pleiotropic regulator (for example, testosterone) increases or decreases in response to selection on one trait. However, this often imposes trade-offs and can slow evolutionary response (Hau 2007). Alternatively, selection may be able to act independently on pleiotropically regulated traits if the hormone-phenotype coupling exhibits evolutionary lability in the strength of this relationship (Hau 2007; Fuxjager and Schuppe 2018; Cox et al. 2022). Indeed, tissue-specific alterations to AR abundances (Fuxjager et al. 2015; Mangiamele et al. 2016; Johnson et al. 2018; Mangiamele and Fuxjager 2018; Anderson et al. 2021) illustrate one way that phenotypes can alter the magnitude of a hormone-phenotype coupling to facilitate diversification. Studies that explicitly test the alternative constraint and potential hypotheses are difficult to design, but measuring the strength of hormonal pleiotropy and examining how labile hormonal responses are across species represents one way in which we can gain inferences about mechanisms that allow for the evolution of hormone-phenotype couplings.

Dissertation contributions

In Chapter 1, I use *S. undulatus* and *S. virgatus* to test how testosterone induces the development of coloration in one species but not in the other. I perform a testosterone manipulation experiment, which results in the same circulating hormone concentrations between species. Therefore, the species-specific phenotypic effects and underlying genetic response that I measure are not due to differences in circulating hormone levels

themselves and instead are due to differences in how testosterone regulates transcription. As expected, testosterone induces the development of coloration in *S. undulatus* but not in *S. virgatus*. At the level of the transcriptome, testosterone induces significantly more differentially expressed genes in *S. undulatus* than in *S. virgatus*, suggesting that ventral skin of *S. virgatus* is less responsive to testosterone than ventral skin of *S. undulatus*. Potentially, this result could be explained by local differences in bioavailable 5α-dihydrotestosterone. I found that one of the genes encoding 5α-reductase, which converts testosterone into the more potent androgen 5α-dihydrotestosterone, is expressed higher in the skin of the sexually dimorphic *S. undulatus* than in the skin of the sexually monomorphic *S. virgatus*. Similarly, the gene encoding sex-hormone binding globulin, which binds to sex hormones and prevents them from being available to bind their cognate receptors, is expressed higher in the sexually monomorphic skin of *S. virgatus* than in the sexually dimorphic skin of *S. undulatus*. Together, these proteins could modulate the sensitivity of ventral skin in a species-specific manner to decouple local melanin synthesis from androgen control. Further, I find that genes upregulated by testosterone in *S. undulatus* are enriched for biological processes related to melanin synthesis. Specific genes related to melanin synthesis, such as *TYR*, *TYRP1*, and *OCA2* are upregulated in *S. undulatus*, but are unaffected by testosterone (and lowly expressed) in *S. virgatus*. This species-specific hormonal regulation is despite the gene encoding AR being expressed significantly higher in *S. virgatus* than in *S. undulatus*, and molecular markers for melanophores (*MITF*, *KIT*, and *DCT*) being expressed equivalently between species. Collectively, Chapter 1 illustrates how gene- and tissue-level processes regulated by androgens can evolve to facilitate the evolution of male traits and sexual dimorphism.

In Chapter 2, I use immunohistochemistry to test whether the observed transcriptomic differences from Chapter 1 result from differences in the abundance and distribution of AR protein in unmanipulated adults of these species. Based on RNAseq data from Chapter 1, I predict that AR abundance would be similar in each species, but that AR would localize to the melanin-producing melanophores only in *S. undulatus*. Surprisingly, I find remarkably little AR in the skin of the sexually monomorphic *S. virgatus*, in conflict to the mRNA results from Chapter 1. In contrast, AR is highly abundant in the skin of the sexually dimorphic *S. undulatus*, albeit in males to a much higher degree than in females. The AR in *S. undulatus* males localizes to the superficial dermis, where melanophores are found (Morrison et al. 1995). To test whether melanophores are present in the superficial dermis, I visualize the presence and distribution of three proteins that are markers for melanophores (microphthalmia-associated transcription factor, dopachrome tautomerase, and tyrosinase) and find that they localize to the same superficial area of the dermis that exhibited AR staining in *S. undulatus* males. Also in contrast to RNAseq results from Chapter 1, I find no evidence for these same three melanophore markers in the skin of the sexually monomorphic *S. virgatus* when using immunohistochemistry, suggesting that unpigmented melanophores are not present in the ventral skin of this species. Collectively, these results suggest that the loss of the AR in the superficial dermis may have facilitated the evolutionary loss of sexually dimorphic ventral coloration in *S. virgatus*, and that this loss of AR may be due to the loss of melanophores.

In Chapter 3, I use a testosterone manipulation experiment in three species (*S. undulatus*, *S. virgatus*, and *S. merriami*) to test for sex- and species-specific responses to

testosterone on liver transcriptome. Like in Chapter 1, my manipulation results in the same circulating hormone concentrations across species and in both sexes. I find that males consistently up- and downregulate more genes in response to testosterone than did females, regardless of species. This result suggests that some sexual dimorphism may arise due to early organizational differences that affect how an individual can respond to circulating hormone levels (Phoenix et al. 1959). Despite this sex difference in the magnitude in response, the direction of response is concordant between females and males, with no genes exhibiting sex-by-treatment interactions, as expected if females and males share genetic architecture that structures the response to a hormonal cue (Wittman et al. 2021). However, each species responds to testosterone somewhat differently. In pairwise species comparisons, dozens to hundreds of genes exhibit treatment-by-species interactions, with the comparisons comprised of closely related *S. undulatus* and *S. virgatus* having fewer significant interactions than either pairwise comparison of these species with the more distantly related *S. merriami*. Together, these results suggest that the transcriptome is characterized by evolutionary potential and that regulatory architecture evolves between species to facilitate the evolution of hormone-phenotype couplings.

Synthesis and implications

Collectively, my dissertation provides novel insight into mechanisms contributing to the evolution of hormonally mediated sexual dimorphism. An emerging perspective in evolutionary endocrinology is that hormone-phenotype couplings are characterized by considerable evolutionary potential. These couplings are substrates upon which selection

can shape individual phenotypes independent of the constraints imposed by hormonal pleiotropy. I provide multiple lines of evidence in support of the hypothesis that the regulation of hormone-phenotype couplings can evolve to facilitate the evolution of sexual dimorphism. While testosterone has similar suppressive effects on growth in *S. undulatus* and *S. virgatus*, resulting in female-biased sexual size dimorphism (Abell 1998; Cox and John-Alder 2005; Cox et al. 2005a; Pollock et al. 2017), testosterone stimulates the production of melanin on the abdomen only in *S. undulatus* (Quinn and Hews 2003; Chapter 1). This phenotypic difference is characterized by underlying transcriptomic differences in the response to testosterone in abdominal skin, where testosterone upregulates gene expression contributing to melanin synthesis in *S. undulatus*, but not *S. virgatus* (Chapter 1). Largely, the direction of gene expression in response to testosterone is similar in the skin between these two species, but testosterone induces more differentially expressed genes in the skin of the sexually dimorphic *S. undulatus*. Potentially, this difference is explained by remarkably less AR in the skin of the sexually monomorphic *S. virgatus*, which may localize to the pigment-producing melanophore (Chapter 2). The lack of AR in the abdominal skin of *S. virgatus* would "unplug" it from the regulatory effects of testosterone, leading to the development of a tissue-specific, sexually monomorphic phenotype without affecting other tissues. Indeed, in Chapter 3, I show that transcriptomic regulation by testosterone is more strongly correlated in the liver than in the skin of these two species, suggesting that different tissues can evolve to uniquely detect and respond to the hormonal environment in which genotypes are converted into realized phenotypes. Finally, I show that differences in hormonal regulation of gene expression were most pronounced between distantly related

species, suggesting that species-specific transcriptomic regulation accumulates with evolutionary time (Chapter 3). This result implies that the regulatory mechanisms by testosterone are evolutionarily labile.

References

Abell AJ. 1998. The effect of exogenous testosterone on growth and secondary sexual character development in juveniles of *Sceloporus virgatus*. Herpetologica 54:533-543. (https://www.jstor.org/stable/3893445)

Anderson AP, E Rose, SP Flanagan, and AG Jones. 2020. The estrogen-responsive transcriptome of female secondary sexual traits in the gulf pipefish. Journal of Heredity 111:294-306. (doi:10.1093/jhered/esaa008)

Anderson NK, ER Schuppe, KV Gururaja, LA Mangiamele, JCC Martinez, H Priti, R von May, D Preininger, and MJ Fuxjager. 2021. A common endocrine signature marks convergent evolution of an elaborate dance display in frogs. American Naturalist 198:522-539. (doi:10.1086/716213)

Ansai S, K Mochida, S Fujimoto, DF Mokodongan, BKA Sumarto, KWA Masengi, RK Hadiaty, AJ Nagano, A Toyoda, K Naruse, K Yamahira, and J Kitano. 2021. Genome editing reveals fitness effects of a gene for sexual dichromatism in Sulawesian fishes. Nature Communications 12:1350. (doi:10.1038/s41467-021-21697-0)

Assis BA, AP Sullivan, S Marciniak, CM Bergey, V Garcia, ZA Szpiech, T Langkilde, and GH Perry. 2023. Genomic signatures of adaptation in native lizards exposed to human-introduced fire ants. bioRxiv 2023.09.24.559217. (doi:10.1101/2023.09.24.559217)

Badyaev AV. 2002. Growing apart: an ontogenetic perspective on the evolution of sexual size dimorphism. Trends in Ecology & Evolution 17:369-378. (doi:10.1016/S0169-5347(02)02569-7)

Bennett NC, RA Gardiner, JD Hooper, DW Johnson, and GC Gobe. 2010. Molecular cell

biology of androgen receptor signalling. International Journal of Biochemistry &

Cell Biology 42:813-827. (doi:10.1016/j.biocel.2009.11.013)

Bergeon Burns CM, KA Rosvall, TP Hahn, GE Demas, and ED Ketterson. 2014.

Examining sources of variation in HPG axis function among individuals and

populations of the dark-eyed junco. Hormones and Behavior 65:179-187.

(doi:10.1016/j.yhbeh.2013.10.006)

Bevan CL, S Hoare, F Claessens, DM Heery, and MG Parker. 1999. The AF1 and AF2

domains of the androgen receptor interact with distinct regions of SRC1.

Molecular and Cellular Biology 19:8383-8392. (doi:10.1128/MCB.19.12.8383)

Chauhan P, A Rani, SK Singh, and AK Rai. 2018. Complete androgen insensitivity

syndrome due to mutations in the DNA-binding domain of the human androgen

receptor gene. Sexual Development 12:269-274. (doi:10.1159/000492261)

Cheng S, S Brzostek, SR Lee, AN Hollenberg, and SP Balk. 2002. Inhibition of the

dihydrotestosterone-activated androgen receptor by nuclear receptor corepressor.

Molecular Endocrinology 16:1492-1501. (doi:10.1210/mend.16.7.0870)

Claessens F, S Denayer, N Van Tilborgh, S Kerkhofs, C Helsen, and A Haelens. 2008.

Diverse roles of androgen receptor (AR) domains in AR-mediated signaling.

Nuclear Receptor Signaling 6:e008. (doi:10.1621/nrs.06008)

Cox RM. 2020. Sex steroids as mediators of phenotypic integration, genetic correlations,

and evolutionary transitions. Molecular and Cellular Endocrinology 502:110668.

(doi:10.1016/j.mce.2019.110668)

Cox RM and HB John-Alder. 2005. Testosterone has opposite effects on male growth in
lizards (*Sceloporus* spp.) with opposite patterns of sexual size dimorphism.
Journal of Experimental Biology 208:4679-4687. (doi:10.1242/jeb.01948)

Cox RM, CL Cox, JW McGlothlin, DC Card, AL Andrew, and TA Castoe. 2017.
Hormonally mediated increases in sex-biased gene expression accompany the
breakdown of between-sex genetic correlations in a sexually dimorphic lizard.
American Naturalist 189:315-332. (doi:10.1086/690105)

Cox RM, MD Hale, TN Wittman, CD Robinson, and CL Cox. 2022. Evolution of
hormone-phenotype couplings and hormone-genome interactions. Hormones and
Behavior 114:105216. (doi:10.1016/j.yhbeh.2022.105216)

Cox RM, SL Skelley, and HB John-Alder. 2005a. Testosterone inhibits growth in juvenile
male eastern fence lizards (*Sceloporus undulatus*): implications for energy
allocation and sexual size dimorphism. Physiological and Biochemical Zoology
78:531-545. (doi:10.1086/430226)

Cox RM, SL Skelley, A Leo, and HB John-Alder. 2005b. Testosterone regulates sexually
dimorphic coloration in the eastern fence lizard, *Sceloporus undulatus*. Copeia
2005:597-608. (doi:10.1643/CP-04-313R)

Cox RM, V Zilberman, and HB John-Alder. 2008. Testosterone stimulates the expression
of a social color signal in Yarrow's spiny lizard, *Sceloporus jarrovii*. Journal of
Experimental Zoology A: Ecological and Integrative Physiology 309A:505-514.
(doi:10.1002/jez.481)

Duncan CA, WS Cohick, and HB John-Alder. 2020. Testosterone reduces growth and
hepatic *IGF-1* mRNA in a female-larger lizard, *Sceloporus undulatus*: evidence of

an evolutionary reversal in growth regulation. Integrative Organismal Biology 2:obaa036. (doi:10.1093/iob/obaa036)

Flatt T, M-P Tu, and M Tatar. 2005. Hormonal pleiotropy and the juvenile hormone regulation of *Drosophila* development and life history. BioEssays 27:999-1010. (doi:10.1002/bies.20290)

Fujita K and N Nonomura. 2019. Role of androgen receptor in prostate cancer: a review. World Journal of Mens Health 37:1130518. (doi:10.5534/wjmh.180040)

Fuxjager MJ and ER Schuppe. 2018. Androgenic signaling systems and their role in behavioral evolution. Journal of Steroid Biochemistry and Molecular Biology 184:47-56. (doi:10.1016/j.jsbmb.2018.06.004)

Fuxjager MJ, J Eaton, WR Lindsay, LH Salwiczek, MA Rensel, J Barske, L Sorenson, LB Day, and BA Schlinger. 2015. Evolutionary patterns of adaptive acrobatics and physical performance predict expression profiles of androgen receptor – but not oestrogen receptor – in the forelimb musculature. Functional Ecolology 29:1197-1208. (doi:10.1111/1365-2435.12438)

Fuxjager MJ, J-H Lee, T-M Chan, JH Bahn, JG Chew, X Xiao, and BA Schlinger. 2016. Research resource: hormones, genes, and athleticism: effects of androgens on the avian muscle transcriptome. Molecular Endocrinology 30:254-271. (doi:10.1210/me.2015-1270)

Gazda MA, PM Araújo, RJ Lopes, MB Toomey, P Andrade, S Afonso, C Marques, L Nunes, P Pereira, S Trigo, and GE Hill. 2020. A genetic mechanism for sexual dichromatism in birds. Science 368:1270-1274. (doi:10.1126/science.aba0803)

Gottlieb B, LK Beitel, A Nadarajah, M Paliouras, and M Trifiro. 2012. The androgen receptor gene mutations database: 2012 update. Human Mutation 33:887-894. (doi:10.1002/humu.22046)

Haelens A, T Tanner, S Denayer, L Callewaert, and F Claessens. 2007. The hinge region regulates DNA binding, nuclear translocation, and transactivation of the androgen receptor. Cancer Research 67:4514-4523. (doi:10.1158/0008-5472.CAN-06-1701)

Hale MD, CD Robinson, CL Cox, and RM Cox. 2022. Ontogenetic change in male expression of testosterone-responsive genes contributes to the emergence of sex-biased gene expression in *Anolis sagrei*. Frontiers in Physiology 13:886973. (doi:10.3389/fphys.2022.886973)

Hau M. 2007. Regulation of male traits by testosterone: implications for the evolution of vertebrate life histories. BioEssays 29:133-144. (doi:10.1002/bies.20524)

Hau M, SA Gill, and W Goymann. 2008. Tropical field endocrinology: ecology and evolution of testosterone concentrations in male birds. General and Comparative Endocrinology 157:241-248. (doi:10.1016/j.ygcen.2008.05.008)

Helsen C, S Kerkhofs, L Clinckemalie, L Spans, M Laurent, S Boonen, D Vanderscueren, and F Claessens. 2012. Molecular and Cellular Endocrinology 348:411-417. (doi:10.1016/j.mce.2011.07.025)

Hews DK and VS Quinn. 2003. Endocrinology of species differences in sexually dichromatic signals. Pp 253-277 in SF Fox, JK McCoy, and TA Baird, eds. Lizard Social Behavior. John Hopkins University Press, Baltimore, MD.

Hews DK, E Hara, and MC Anderson. 2012. Sex and species differences in plasma testosterone and in counts of androgen receptor-positive cells in key brain regions

of *Sceloporus* lizard species that differ in aggression. General and Comparative Endocrinology 176:493-499. (doi:10.1016/j.ygcen.2011.12.028)

Husak JF and MB Lovern. 2014. Variation in steroid hormone levels among Caribbean *Anolis* lizards: endocrine system convergence? Hormones and Behavior 65:408-415. (doi:10.1016/j.yhbeh.2014.03.006)

Husak JF, MJ Fuxjager, MA Johnson, MN Vitousek, JW Donald, CD Francis, W Goymann, M Hau, BK Kircher, R Knapp, LB Martin, ET Miller, LA Schoenle, and TD Williams. 2021. Life history and environment predict variation in testosterone across vertebrates. Evolution 75:1003-1010. (doi:10.1111/evo.14216)

Jiménez-Arcos VH, S Sanabria-Urbán, and R Cueva del Castillo. 2017. The interplay between natural and sexual selection in the evolution of sexual size dimorphism in *Sceloporus* lizards (Squamata: Phrynosomatidae). Ecology and Evolution 7:905-917. (doi:10.1002/ece3.2572)

John-Alder HB and RM Cox. 2007. Development of sexual size dimorphism in lizards: testosterone as a bipotential growth regulator. Pp 195-204 in DJ Fairbairn, T Szekely, and WU Blanckenhorn, eds. Sex, Size and Gender Roles: Evolutionary Studies of Sexual Size Dimorphism. Oxford University Press, Oxford.

John-Alder HB, RM Cox, and EN Taylor. 2007. Proximate developmental mediators of sexual size dimorphism: case studies from squamate reptiles. Integrative and Comparative Biology 47258-271. (doi:10.1093/icb/icm010)

John-Alder HB, RM Cox, GJ Haenel, and LC Smith. 2009. Hormones, performance and fitness: natural history and endocrine experiments on a lizard (*Sceloporus*

undulatus). Integrative and Comparative Biology 49:393-407. (doi:10.1093/icb/icp060)

Johnson MA, BK Kircher, and DJ Castro. 2018. The evolution of androgen receptor expression and behavior in *Anolis* lizard forelimb muscles. Journal of Comparative Physiology A 204:71-79. (doi:10.1007/s00359-017-1228-y)

Ketterson ED, JW Atwell, and JW McGlothlin. 2009. Phenotypic integration and independence: hormones, performance, and response to environmental change. Integrative and Comparative Biology 49:365-379. (doi:10.1093/icb/icp057)

Khalil S, JF Welklin, KJ McGraw, J Boersma, H Schwabl, MS Webster, and J Karubian. 2020. Testosterone regulates *CYP2J19*-linked carotenoid signal expression in male red-backed fairywrens (*Malurus melanocephalus*). Proceedings of the Royal Society of London B: Biological Sciences 287:20201687. (doi:10.1098/rspb.2020.1687)

Kimball FA and MJ Erpino. 1971. Hormonal control of pigmentary sexual dimorphism in *Sceloporus occidentalis*. General and Comparative Endocrinology 16:375-384. (doi:10.1016/0016-6480(71)90050-5)

Klukowski M and CE Nelson. 2001. Ectoparasite loads in free-ranging northern fence lizards, *Sceloporus undulatus hyacinthinus*: effects of testosterone and sex. Behavioral Ecology and Sociobiology 49:289-295. (doi:10.1007/s002650000298)

Leaché AD, BL Banbury, CW Linkem, and A Nieto-Montes de Oca. 2016. Phylogenomics of a rapid radiation: is chromosomal evolution linked to increased diversification in North American spiny lizards (genus *Sceloporus*)? BMC Evolutionary Biology 16:63. (doi:10.1186/s12862-016-0628-x)

Lipschutz SE, EM George, AB Bentz, and KA Rosvall. 2019. Evaluating testosterone as a

>phenotypic integrator: from tissues to individuals to species. Molecular and

>Cellular Endocrinology 496:110531. (doi:10.1016/j.mce.2019.110531)

Mank JE. 2009. Sex chromosomes and the evolution of sexual dimorphism: lessons from

>the genome. The American Naturalist 173:141-150. (doi:10.1086/595754)

Marcelli M, M Ittmann, S Mariani, R Sutherland, R Nigam, L Murthy, Y Zhao, and D

>DiConcini. 2000. Androgen receptor mutations in prostate cancer. Cancer

>Research 60:944-949. (doi:

Mauro AA and CK Ghalambor. 2020. Trade-offs, pleiotropy, and shared molecular

>pathways: a unified view of constraints on adaptation. Integrative and

>Comparative Biology 60:332-347. (doi:10.1093/icb/icaa056)

McGlothlin JW and ED Ketterson. 2008. Hormone-mediated suites as adaptations and

>evolutionary constraints. Philosophical Transactions of the Royal Society B:

>Biological Sciences 363:1611-1620. (doi:10.1098/rstb.2007.0002)

Møller AP, LZ Garamszegi, S Hurtrez-Boussès, and M Eens. 2005. Correlated evolution

>of male and female testosterone profiles in birds and its consequences. Behavioral

>Ecology and Sociobiology 58:534-544. (doi:10.1007/s00265-005-0962-2)

Morrison RL, MS Rand, and SK Frost-Mason. 1995. Cellular basis of color differences in

>three morphs of the lizard *Sceloporus undulatus erythrocheilus*. Copeia 1995:397-

>408. (doi:10.2307/1446903)

Ossip-Drahos AG, JR Oyola Morales, C Vital-García, JJ Zúñiga-Vega, DK Hews, and EP

>Martins. 2016. Shaping communicative colour signals over evolutionary time.

>Royal Society Open Science 3:160728. (doi:10.1098/rsos.160728)

Pavličev M and JM Cheverud. 2015. Constraints evolve: context dependency of gene effects allows evolution of pleiotropy. Annual Reviews of Ecology, Evolution, and Systematics 46:413-434. (doi:10.1146/annurev-ecolsys-120213-091721)

Phoenix CH, RW Goy, AA Gerall, and WC Young. 1959. Organizing action of prenatally administered testosterone propionate on the tissues mediating mating behavior in the female guinea pig. Endocrinology 65:369-382. (doi:10.1210/endo-65-3-369)

Pihlajamaa P, B Sahu, and OA Jänne. 2015. Determinants or receptor- and tissue-specific actions in androgen signaling. Endocrine Reviews 36:357-384. (doi:10.1210/er.2015-1034)

Pollock NB, S Feigin, M Drazenovic, and HB John-Alder. 2017. Sex hormones and the development of sexual size dimorphism: 5α-dihydrotestosterone inhibits growth in a female-larger lizard (*Sceloporus undulatus*). Journal of Experimental Biology 220:4068-4077. (doi:10.1242/jeb.166553)

Quinn VS and DK Hews. 2003. Positive relationship between abdominal coloration and dermal melanin density in phrynosomatid lizards. Copeia 2003:858-864. (doi:10.1643/h202-116.1)

Rinn JL and M Snyder. 2005. Sexual dimorphism in mammalian gene expression. Trends in Genetics 21:298-305. (doi:10.1016/j.tig.2005.03.005)

Schuppe ER, MC Miles, and MJ Fuxjager. 2020. Evolution of the androgen receptor: perspectives from human health to dancing birds. Molecular and Cellular Endocrinology 499:110577 (doi:10.1016/j.mce.2019.110577)

Shaffer PL, A Jivan, and DE Dollins. 2004. Structural basis of androgen receptor binding to selective androgen response elements. Proceedings of the National Academy of Sciences 101:4758-4763. (doi:10.1073/pnas.0401123101)

Smith DF and DO Toft. 2008. The intersection of steroid receptors with molecular chaperones: observations and questions. Molecular Endocrinology 22:2229-2240. (doi:10.1210/me.2008-0089)

Stearns SC. 1989. Trade-offs in life-history evolution. Functional Ecology 3:259-268. (doi:10.2307/2389364)

Thornton JW and DB Kelley. 1998. Evolution of the androgen receptor: structure-function implications. BioEssays 20:860-869. (doi:10.1002/(SICI)1521-1878(199810)20:10<860::AID-BIES12>3.0.CO;2-S)

van Nas A, D GuhaThakurta, SS Wang, N Yehya, S Horvath, B Zhang, L Ingram-Drake, G Chaudhuri, EE Schadt, TA Drake, AP Arnold, and AJ Lusis. 2009. Elucidating the role of gonadal hormones in sexually dimorphic gene coexpression networks. Endocrinology 150:1235-1249. (doi:10.1210/en.2008-0563)

Waxman DJ and C O'Connor. 2006. Growth hormone regulation of sex-dependent liver gene expression. Molecular Endocrinology 20:2613-2629. (doi:10.1210/me.2006-0007)

Westfall AK, RS Telemeco, MB Grizante, DS Waits, AD Clark, DY Simpson, RL Klabacka, AP Sullivan, GH Perry, MW Sears, CL Cox, RM Cox, ME Gifford, HB John-Alder, T Langkilde, MJ Angilletta Jr, AD Leaché, M Tollis, K Kusumi, and TS Schwartz. 2021. A chromosome-level genome assembly for the eastern fence

lizard (*Sceloporus undulatus*), a reptile model for physiological and evolutionary ecology. GigaScience 10:giab066. (doi:10.1093/gigascience/giab066)

Wiens JJ. 1999. Phylogenetic evidence for multiple losses of a sexually selected character in phrynosomatid lizards. Proceedings of the Royal Society of London B: Biological Sciences 266:1529-1535. (doi:10.1098/rspb.1999.0811)

Williams TM and SB Carroll. 2009. Genetic and molecular insights into the development and evolution of sexual dimorphism. Nature Reviews Genetics 10:797-804. (doi:10.1038/nrg2687)

Wittman TN, CD Robinson, JW McGlothlin, and RM Cox. 2021. Hormonal pleiotropy structures genetic covariance. Evolution Letters 5:397-407. (doi:10.1002/ev13.240)

Wright AE, TF Rogers, M Fumagalli, CR Cooney, and JE Mank. 2019. Phenotypic sexual dimorphism is associated with genomic signatures of resolved sexual conflict. Molecular Ecology 28:2860-2871. (doi:10.1111/mec.15115)

Xu X, JK Coats, CF Yang, A Wang, OM Ahmed, M Alvarado, T Izumi, and NM Shah. 2012. Modular genetic control of sexually dimorphic behaviors. Cell 148:596-607. (doi:10.1016/j.cell.2011.12.018)

Zhou Z-X, M Sar, JA Simental, MV Lane, and EM Wilson. 1994. A ligand-dependent bipartite nuclear targeting signal in the human androgen receptor. Journal of Biological Chemistry 18:13115-13123. (doi:10.1016/S0021-9258(17)36806-0)
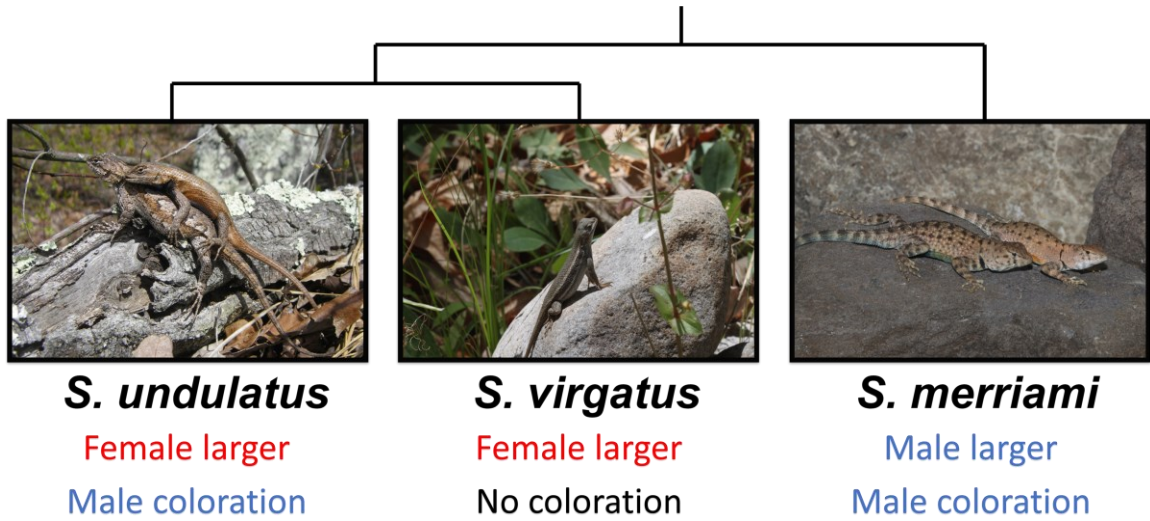
Figure 1. Photograph of the three species of *Sceloporus* used in this dissertation. The ancestral male-larger dimorphism is represented by *S. merriami*, while the ancestral male coloration is represented by *S. merriami* and *S. undulatus*. Cladogram represents the evolutionary relationships from Wiens (1999). Photograph of *S. undulatus* by Lukáš Kratochvíl and photographs of *S. virgatus* and *S. merriami* by Christian Cox.

Chapter 1:

Species differences in hormonally mediated gene expression underlie the evolutionary

loss of sexually dimorphic coloration in *Sceloporus* lizards[1]

Abstract

Phenotypic sexual dimorphism often involves the hormonal regulation of sex-biased expression for underlying genes. However, it is generally unknown whether the evolution of hormonally mediated sexual dimorphism occurs through upstream changes in tissue sensitivity to hormone signals, downstream changes in responsiveness of target genes, or both. Here, we use comparative transcriptomics to explore these possibilities in two species of *Sceloporus* lizards exhibiting different patterns of sexual dichromatism. Sexually dimorphic *S. undulatus* develops blue and black ventral coloration in response to testosterone, while sexually monomorphic *S. virgatus* does not, despite exhibiting similar sex differences in circulating testosterone levels. We administered testosterone implants to juveniles of each species and used RNAseq to quantify gene expression in ventral skin. Transcriptome-wide responses to testosterone were stronger in *S. undulatus* than in *S. virgatus*, suggesting species differences in tissue sensitivity to this hormone signal. Species differences in the expression of genes for androgen metabolism and sex hormone binding globulin were consistent with this idea, but expression of the androgen receptor gene was higher in *S. virgatus*, complicating this interpretation. Downstream of androgen signaling, we found clear species differences in hormonal responsiveness of genes related to melanin synthesis, which were upregulated by testosterone in *S. undulatus,* but not in *S. virgatus*. Collectively, our results indicate that hormonal regulation of melanin synthesis pathways contributes to the development of sexual dimorphism in *S. undulatus*, and that changes in the hormonal responsiveness of these genes in *S. virgatus* contribute to the evolutionary loss of ventral coloration.

Introduction

  Although female and male conspecifics share the vast majority of their genomes, differential regulation of transcription can result in the development of remarkably different phenotypes in each sex (Waxman and O'Connor 2006; Mank 2009; Williams and Carroll 2009; Cox et al. 2015; Cox et al. 2017; Wright et al. 2019; Gazda et al. 2020; Khalil et al. 2020). In vertebrates, estrogens and androgens are produced primarily in the gonads and then circulate to target tissues, where they bind nuclear receptors and thereby influence gene expression by interacting with hormone response elements in the genome. Consequently, sex differences in the production of estrogens and androgens lead to sex differences in gene expression, which in turn lead to the development of sexually dimorphic traits (Rinn and Snyder 2005; van Nas et al. 2009; Xu et al. 2012; Frankl-Vilches et al. 2015; Cox et al. 2017; Anderson et al. 2020; Ansai et al. 2021; Hale et al. 2022). Phenotypic responses to steroid hormones can evolve, such that different populations or species exhibit unique responses to the same hormonal stimulus (Cox and John-Alder 2005; Hau 2007; Rosvall et al. 2016; Lipshutz et al. 2019; Blázquez et al. 2020; Anderson et al. 2022; Enbody et al. 2022). This evolutionary lability can reflect multiple mechanisms, including upstream changes in the sensitivity of target tissues to hormonal signals (*e.g.*, changes in hormone receptor expression) or downstream changes in the responsiveness of specific genes and pathways to the activated hormone receptor (Cox et al. 2022). However, data directly linking evolutionary changes in phenotypes to differences in the hormonal regulation of underlying genes are generally lacking. To provide such data, we combined comparative transcriptomics and hormone manipulations in two closely related species representing ancestral (sexually dimorphic) and derived (monomorphic) states for coloration (Ossip-Drahos et al. 2016). We use this framework

to test whether the evolutionary loss of hormonally regulated sexual dimorphism occurs through upstream changes in tissue sensitivity to a hormonal signal, downstream changes in the responsiveness of specific genes and pathways to a hormonal signal, or a combination of these mechanisms.

Fence and spiny lizards (genus *Sceloporus*) provide an ideal comparative system because they exhibit repeated evolutionary transitions in sexual dimorphism for traits such as body size and coloration (Wiens 1999; John-Alder and Cox 2007; Ossip-Drahos et al. 2016; Jiménez-Arcos et al. 2017). The effects of testosterone on color and growth phenotypes are known to differ across species with different patterns of dimorphism (Quinn and Hews 2003; Cox and John-Alder 2005; Cox et al. 2005a,b, 2007, 2009). For example, *S. undulatus* males have vibrant blue and black patches on their abdomens and throats, whereas this coloration is absent or greatly reduced in females (Fig. 1). These patches can be induced by exogenous androgens in juveniles of both sexes, but they only develop naturally in males due to organizational effects of rising testosterone levels during maturation (Cox et al. 2005a; Pollock et al. 2017), and the vibrant blue color characteristic of breeding males requires further activational effects of elevated testosterone in adulthood (Cox et al. 2005a; Robinson and Gifford 2019). Conversely, *S. virgatus* males do not develop abdominal coloration naturally or in response to exogenous testosterone (Abell 1998b; Quinn and Hews 2003) and their white abdomens are virtually indistinguishable from those of females (Fig. 1). Whereas many *Sceloporus* species have independently evolved a derived state of vibrant ventral coloration in females, suggesting cross-sexual transfer (West-Eberhard 2003; Anderson and Falk 2023), *S. virgatus* has instead lost the ancestral state of vibrant ventral colorations in

males that is retained by *S. undulatus*. These two species diverged approximately 12 million years ago (Wiens 1999; Ossip-Drahos et al. 2016) and adult males of both species have similarly high levels of circulating testosterone during the breeding season (Abell 1998a; Cox et al. 2005a; Cox and John-Alder 2005, 2007; John-Alder et al. 2009; Hews et al. 2012). Therefore, the evolutionary loss of blue ventral coloration in *S. virgatus* males is due to the loss of color production, either generally or specifically in response to testosterone, rather than a change in circulating testosterone as a signal mediating sexual dichromatism. However, it is unknown whether this loss of color production in *S. virgatus* has occurred via the upstream loss of tissue sensitivity to testosterone, via downstream changes in the responsiveness of specific genes and pathways that underlie color production, or both.

In *Sceloporus* and other lizards, blue abdominal coloration is produced through the organization of two distinct pigment cells. In the dermis, a layer of iridophores sits superficial to a layer of melanophores (Taylor and Hadley 1970; McLean et al. 2017; Nicolaï et al. 2021), the ectotherm homologues of mammalian melanocytes. The iridophores contain orderly stacks of guanine platelets that reflect different wavelengths of light depending upon their orientation, and the underlying melanophores produce melanin granules that absorb any light that is not reflected by the iridophores (Morrison et al. 1995). This cellular arrangement is exemplified by the blue skin of adult *S. undulatus* males*, which results from both the reflection of blue light by iridophores and the absorption of other wavelengths by underlying melanophores (Fig. 1A-C). The presence of a similar iridophore layer in *S. undulatus* juveniles (C. D. Robinson, personal observation) and adult females (Fig. 1D-F), as well as in *S. virgatus* adults of either sex

(Fig. 1G-L), suggests that elevated testosterone is not necessary for iridophore development, and that iridophores alone are insufficient for the expression of blue color. In *S. undulatus* and closely related *S. consobrinus* (previously *S. undulatus consobrinus*), as well as other phrynosomatid lizards in which males develop blue ventral coloration, testosterone stimulates melanin production in the dermis (Kimball and Erpino 1971; Quinn and Hews 2003; Cox et al. 2005, 2008). Consequently, the evolutionary loss of sexually dimorphic coloration in *S. virgatus* likely occurred primarily through the loss of melanin synthesis in ventral skin, rather than through changes in the iridophore layer (Fig. 2A-B). Therefore, we focus our *a priori* tests (see below) on genes and pathways that are involved in melanocortin production and melanin synthesis (Table 1, Fig. 2C) as likely candidates for the evolutionary loss of responsiveness to androgen signaling. In addition to these specific downstream genes and pathways involved in melanin synthesis, we also focus on upstream pathways related to androgen metabolism, androgen availability, and androgen receptor expression (Table 1, Fig. 2C).

To examine species differences in responsiveness to androgen signaling, we manipulated circulating testosterone levels in *S. undulatus* and *S. virgatus* juveniles and then used bulk RNAseq of ventral skin to compare gene expression between controls and individuals with experimentally elevated testosterone within each species. We conducted this experiment in juveniles to test for effects on gene expression prior to sexual divergence in circulating testosterone, which avoids any confounding effects of endogenous testosterone and allows us to assess the development of coloration prior to any natural induction by testosterone. We first characterized genes and pathways responsive to testosterone in *S. undulatus* to identify those that potentially contribute to

the development of vibrant coloration in this sexually dimorphic species. We then

explored which of these genes and pathways have different expression patterns or fail to

respond to testosterone in *S. virgatus*, potentially explaining the loss of vibrant ventral

color in this sexually monomorphic species. We approached this comparison using a

combination of unbiased analyses across the entire skin transcriptome and targeted

analyses of specific genes selected *a priori* to test several potential mechanisms for the

evolutionary loss of hormonally mediated ventral coloration (Table 1, Fig. 2C).

Specifically, we tested whether these two closely related species differ in the expression

of 1) upstream genes that mediate tissue sensitivity to androgens, 2) genes downstream

from androgen signaling that regulate the production of melanin pigment, and 3) marker

genes that indicate the presence of melanophores or melanophore precursors.

Collectively, these analyses allow us to address an issue of general significance in

evolutionary endocrinology (Cox et al. 2022): whether evolutionary changes in

hormonally mediated phenotypes occur via upstream changes in tissue sensitivity to

hormonal signals, downstream changes in hormonal responsiveness of target genes, or a

combination of these mechanisms.

Methods

Experimental design and sample collection

      We collected wild juvenile Eastern Fence Lizards (*Sceloporus undulatus*; sexually

dichromatic) and Striped Plateau Lizards (*S. virgatus*; sexually monochromatic) at

approximately one month of age and transported them to the University of Virginia,

where they were housed individually in small terraria. After a one-month acclimation

period, we split individuals of each species and sex into two size-matched treatment groups: one receiving a small intraperitoneal implant filled with 100 µg crystalline testosterone and one receiving an empty implant as a control. Implant construction and surgical procedures followed previous studies (Cox et al. 2015, 2017; Wittman et al. 2021) and were designed to elevate circulating testosterone to levels typical of breeding adult males of each species (Cox and John-Alder 2005; Cox et al. 2005a; John-Alder et al. 2009; Hews et al. 2012). Further details about sample collection, animal care, environmental conditions in captivity, methods for implant design, and protocols for surgery are provided as Supplementary Materials. Eight weeks after treatment, we quantified color development by taking ventral photographs of each animal and using Fiji (ImageJ 1.52v) software (Schindelin *et al.*, 2012) and R v4.2.1 (R Core Team 2022) to estimate hue, saturation, and brightness. Hue represents the dominant wavelength, saturation represents a metric of color purity, and brightness represents closeness to white. For further details about color quantification, see the Supplementary Materials. The following day, we euthanized each animal via decapitation and immediately collected blood to confirm treatment effects on circulating testosterone levels via radioimmunoassay (see Supplementary Materials). We also immediately collected ventral skin from areas in which colorful abdominal patches develop in adult *S. undulatus* males (abdominal patches are absent in *S. virgatus* and in unmanipulated *S. undulatus* juveniles) into RNAlater (ThermoFisher Scientific) on ice, then refrigerated them for 24 h at 4°C and stored them at -80°C until RNA extraction.

We extracted RNA from skin of 48 juvenile lizards ($n = 6$ per treatment, per sex, per species) using Illustra™ RNAspin Mini RNA Isolation Kit (GE Healthcare)

following manufacturer specifications with minor modifications (see Supplementary Materials). RNA quality was assessed using a Nanodrop spectrophotometer (ThermoFisher Scientific, Waltham MA, USA) and Agilent 2100 BioAnalyzer (RNA 600 Pico; Agilent Biotechnologies, Santa Clara, CA, USA). Library preparation and sequencing were carried out by the Georgia Genomics and Bioinformatics Core (University of Georgia; Athens, GA). Two libraries (one *S. undulatus* control male, one *S. virgatus* testosterone male) were not sequenced due to low RNA concentrations. cDNA libraries were prepared from total RNA (~500 ng per sample) using KAPA Biosystems (Wilmington, MA) RNA library preparation chemistry with poly(A) selection. Libraries were sequenced on an Illumina NextSeq 2000 (2 × 100 bp paired-end sequencing) using P3 high-output flow cells. We assessed read quality and trimmed reads using Fastp (Chen et al. 2018) with paired-end base correction, low complexity filtering, 3' end tail quality trimming (average phred threshold = 20; window size = 5), and poly(g) and poly(x) trimming enabled. We also applied an overall minimum length filter of 36 bp and minimum phred score threshold of 25, then aligned reads to the *S. undulatus* genome (Westfall et al. 2021; GCA_019175285.1, SceUnd_v1.1) using subread-align (Liao et al. 2013), with *S. undulatus* transcripts used as an alignment guide (GCF_019175285.1). Following alignment, we assigned both uniquely mapped fragments and singleton reads to annotated *S. undulatus* genes using featureCounts (Liao et al. 2014) to generate a matrix of read counts.

Identification and functional characterization of testosterone-responsive genes

All statistical analyses were run in R v4.2.1 (R Core Team 2022). To characterize transcriptome-wide responses to testosterone in each species and identify testosterone-responsive genes with an unbiased approach, we conducted differential gene expression analysis on read counts from both species using the package edgeR v3.30.3 (Robinson et al. 2010). Prior to analysis, two libraries were removed due to low read counts (316k reads for a *S. undulatus* control female and 4.3M reads for a *S. virgatus* control male). We removed genes with low expression using *filterByExpr* in edgeR, which retained 18,017 genes. We then conducted principal components analysis using *robpca* within rospca v1.0.4 (Reynkens 2018) to test for outlier libraries. Three *S. virgatus* libraries (one control female, one testosterone female, and one control male) were subsequently removed. In total, 41 libraries were included in differential expression analyses, with $n = 4$–6 libraries per treatment, per sex, per species (Table 2) and an average library size of 19.9M reads in *S. undulatus* and 19.5M reads in *S. virgatus*. We normalized read counts using trimmed mean of M-values (TMM) normalization and used *glmQLFit* in edgeR to fit a negative binomial model to our data, specifying robust = TRUE to reduce the influence of hypervariable genes (see Phipson et al. 2016). Finally, we used the function *glmQLFTest* to calculate quasi-likelihood *F*-tests for paired contrasts between treatment groups (testosterone versus control) within each species, retaining the effect of sex in each species comparison. We conducted these same analyses without the effect of sex, and results were largely similar. We chose to present results from analyses including sex because an additional 787 genes pass filtration with this added biological information. Genes were considered significantly differentially expressed genes (hereafter, DEGs) if

their *P*-value was less than 0.05 following Benjamini-Hochberg correction for false discovery (Benjamini-Hochberg 1995).

To infer functions of genes that were differentially expressed in response to testosterone, we used gene ontology (GO) analysis (Ashburner et al., 2000; The Gene Ontology Consortium et al., 2021). Specifically, we used the PANTHER Overrepresentation Test (PANTHER17.0; GO Ontology database DOI: 10.5281/zenodo.6799722) with Fisher's exact test to examine GO biological processes and cellular components. We tested for enrichment of biological processes with DEGs using all protein-coding genes from three species: *Homo sapiens* (human) as the default GO reference species; *Anolis carolinensis* (green anole) as a comparison to another lizard; and *Danio rerio* (zebrafish) as a comparison to a model organism for pigment cell development (Parichy 2021). Green anoles and zebrafish both have dermal iridophores, which are absent in mammals, so including these species facilitates the identification of biological processes and cellular components related to iridophore development that would not be detectable using only the default human database. We used these GO analyses to characterize genes and pathways that respond to testosterone in *S. undulatus* and identify those likely to underlie the development of ventral coloration in this sexually dimorphic species. We predicted that any pathways related to color that were enriched for DEGs in *S. undulatus* would not be enriched for DEGs in sexually monomorphic *S. virgatus*, in which testosterone does not induce vibrant ventral color.

Species differences in transcriptome-wide responsiveness to testosterone

To explore whether the loss of color in *S. virgatus* reflects a tissue-wide loss of transcriptomic responsiveness to testosterone, we first tested whether the total number of DEGs differed between species using a chi-square test with one degree of freedom. Because of differences in our statistical power to identify DEGs due to species differences in sample size (22 *S. undulatus* libraries, 19 *S. virgatus* libraries), we extended this analysis by iteratively dropping three *S. undulatus* libraries and recalculating the number of DEGs 1,540 times, covering all possible combinations in which three out of 22 individuals could be removed to achieve equal sample sizes between species. For each iteration, we used a chi-square test to compare the total number of DEGs between species, then calculated the proportion of comparisons in which the number of DEGs differed ($P < 0.05$) between species.

To assess the overall similarity of transcriptomic responsiveness to testosterone between species, we asked whether DEGs that were significantly up- or down-regulated by testosterone in one species had $\log_2$-fold change ($\log_2FC$) values that were similarly different from zero in the other species. Specifically, we used Wilcoxon signed-rank tests to determine whether the median $\log_2FC$ values of the DEGs upregulated by testosterone in one species were significantly greater than zero in the other species, and whether the median $\log_2FC$ values of the DEGs downregulated by testosterone in one species were significantly less than zero in the other species. We conducted these analyses reciprocally using the sets of DEGs identified independently in each species. A significant P-value with the same fold-change direction would indicate that many of the genes that are responsive to testosterone in one species are similarly responsive to testosterone in the

other species. When analyzing whether genes upregulated by testosterone in *S. undulatus* were upregulated in *S. virgatus*, we excluded any DEGs identified by GO analysis as residing within pigment-related biological pathways (Table 3) because we were interested specifically in testing whether other DEGs unrelated to melanin synthesis exhibited similar transcriptomic responses between species.

Species differences in expression of a priori *candidate genes*

To analyze effects of sex, species, and treatment on a gene-by-gene basis for the candidate genes that we selected *a priori* for their roles in tissue sensitivity to androgens, melanin synthesis, and melanophore differentiation (Table 1), we converted read counts to transcripts per million (TPM). We first conducted separate ANOVAs on each gene (17 total genes) by including effects of sex, species, and treatment, plus all pairwise and three-way interactions. Because we were primarily interested in the effects of treatment and species, we conducted an additional analysis excluding sex and its interactions from the model. We then used the function *lrtest* from the lmtest package (Zeileis and Hothorn 2002) to test whether the full (including sex) or reduced (excluding sex) model best fit our data. We report results from the full model when the likelihood ratio test was significant and results from the reduced model when the likelihood ratio test was not significant. Consequently, sex and its interactions were only retained in analyses of expression for the genes *SRD5A3*, *POMC*, and *PCSK1N*.

Although we selected these genes *a priori,* we conservatively applied Bonferroni corrections to any *P*-values that could be viewed as multiple tests of the same mechanistic hypothesis (see below) when conducting these gene-specific analyses.

Unadjusted *P*-values are reported unless results are no longer significant after Bonferroni correction, in which case the adjusted value (P_{adj}) is also reported. First, we used an adjusted critical value of 0.0083 (6 tests) when assessing differences in the expression of 6 genes related to upstream androgen availability and/or tissue responsiveness to androgens. Second, we used an adjusted critical value of 0.01 (5 tests) when assessing differences in the expression of 5 genes related melanocortin production and signaling. Third, we used an adjusted critical value of 0.016 (3 tests) when assessing differences in the expression of 3 genes related to melanin synthesis and when assessing differences in the expression of 3 other genes used as molecular markers for melanophores.

We selected 6 genes to test for species differences in upstream androgen metabolism, androgen availability, and tissue sensitivity to androgens (Table 1; Fig. 2C). First, because testosterone can be locally converted to either estradiol (which does not activate the androgen receptor) or the more potent androgen 5α-dihydrotestosterone (DHT), we analyzed the expression of genes encoding aromatase (*CYP19A1*) and 5α-reductase (*SRD5A1, SRD5A2, SRD5A3*), the enzymes that respectively mediate these steps in steroid metabolism. Second, because androgen signaling cannot be initiated when steroids are bound by globulins, we analyzed the expression of the gene encoding sex hormone binding globulin (*SHBG*). Third, we assessed tissue sensitivity by analyzing the expression of the gene encoding androgen receptor (*AR*), which mediates the genomic effects of androgens on downstream genes. Analogous tests for the genes encoding estrogen receptor-α (*ESR1*) and estrogen receptor-β (*ESR2*) are reported in the Supplementary Materials. If changes to the regulation of any of these genes contribute to the evolutionary loss of color, we predicted that *S. virgatus* would exhibit 1) higher

CYP19A1 expression, 2) lower *SRD5A1-3* expression, 3) higher *SHBG* expression, and 4) lower *AR* expression, relative to *S. undulatus* (Table 1).

Next, we tested for species differences in hormonal responsiveness of key color genes downstream from androgen signaling. First, we tested for differences in 5 genes whose products contribute to the production, regulation, and detection of α-melanocyte stimulating hormone (α-MSH). Specifically, we examined expression patterns of the proopiomelanocortin gene (*POMC*) and genes encoding enzymes that contribute to the conversion of POMC to α-MSH (*PCSK1*, *PCSK2*, and *PCSK1N*). While *POMC* is expressed primarily in the pituitary, it can also be locally produced by keratinocytes and melanocytes in the skin (Schauer et al. 1994; Chakraborty et al. 1996; Wintzen et al. 1996; Rousseau et al. 2007). POMC is cleaved into its peptide derivatives adrenocorticotropic hormone (ACTH) and α-MSH by prohormone convertases 1 (*PCSK1*) and 2 *(PCSK2)*, respectively (reviewed in Harno et al. 2018). Because α-MSH then binds to the melanocortin-1 receptor (MC1R) on the surface of melanophores to stimulate melanin synthesis, we also tested for differences in expression of *MC1R*, which encodes the MC1R receptor. Next, we tested for differences in the expression of 3 downstream genes involved in melanin synthesis within melanophores (*TYR*, *TYRP1*, *OCA2*). The products of these genes play critical roles in converting tyrosine into melanin precursors (TYR; Raper 1928), stabilizing tyrosinase in the melanosomal membrane and contributing to melanosome biosynthesis (TYRP1; Boissy et al. 1996; Kobayashi et al. 1998), and regulating pH within the melanosome at optimal levels for melanin synthesis (the P protein, encoded by *OCA2*; Bellono et al. 2014). For most of these genes, we predicted that expression would be higher in *S. undulatus* than in *S. virgatus* and/or that

testosterone would upregulate expression in *S. undulatus*, but not in *S. virgatus* (Table 1). However, because *PCSK1N* encodes an inhibitor of prohormone convertase 1 (Fricker et al. 2000; Qian et al. 2000), we predicted that expression would be lower in *S. undulatus* than in *S. virgatus* and/or that testosterone would downregulate expression in *S. undulatus,* but not in *S. virgatus* (Table 1).

Finally, we tested for expression of 3 genes used as molecular markers of melanophores: *DCT*, *KIT*, and *MITF*. In the context of melanophores, *DCT*, encoding dopachrome tautomerase, contributes to the regulation of melanophore survival, *KIT*, encoding a tyrosine kinase called the KIT protein, facilitates signaling that regulates cellular processes, and MITF, encoding microphthalmia-associated transcription factor, regulates melanophore processes. If these genes are not expressed in the skin of *S. virgatus*, this might suggest that any observed differences between these two species are due to the loss of this cell type in the ventral dermis. However, expression of these three genes would suggest that the cell type necessary for melanin synthesis is present, but does not attain a fully melanized state in *S. virgatus*. If the evolutionary loss of color is due to a loss of melanophore development in the skin, we would expect reduced or undetectable expression of these three genes in *S. virgatus*, relative to *S. undulatus* (Table 1).

Results

Confirming treatment effects on circulating testosterone and coloration

Our implants consistently elevated plasma testosterone concentrations measured at the end of the eight-week experiment, regardless of species or sex (Fig. 3). For *S.*

undulatus, there was a significant increase in circulating testosterone in the treatment group ($F_{1,16}$ = 74.23, P < 0.0001), with no sex effect ($F_{1,16}$ = 0.31, p = 0.589) or treatment × sex interaction ($F_{1,16}$ = 0.15, p = 0.705). Similarly, for *S. virgatus*, there was a significant increase in testosterone in the treatment group ($F_{1,15}$ = 75.51, p < 0.0001), with no sex effect ($F_{1,15}$ = 1.19, p = 0.293) or treatment × sex interaction ($F_{1,15}$ = 0.27, p = 0.614). In an omnibus model including sex, species, treatment, and all two- and three-way interactions, only treatment was significant ($F_{1,31}$ = 149.87, P < 0.0001; all other P > 0.44).

In the sexually dichromatic *S. undulatus*, testosterone treatment significantly decreased brightness (closeness to white; $F_{1,18}$ = 34.60, P < 0.001; Fig. 4A) and decreased hue (dominant wavelength; $F_{1,18}$ = 4.875, P = 0.041; Fig. 4B), yet had no effect on saturation (color purity; $F_{1,18}$ = 2.73, P = 0.116; Fig. 4C) of the lateral areas of ventral skin where patches develop. There were no sex effects or treatment × sex interactions for any aspect of skin coloration (all P > 0.14). In the sexually monochromatic *S. virgatus,* there were no treatment effects, sex effects, or treatment × sex interactions for any aspect of coloration (all P > 0.17; Fig. 4D-F). Lateral areas of melanized skin with faint blue color were evident on the abdomens of most *S. undulatus* juveniles that received testosterone implants, whereas the abdomens of all other groups were essentially white with little evidence of ventral patch formation (Fig. S1).

Identification and functional characterization of testosterone-responsive genes

In *S. undulatus*, the species in which maturing males develop vibrant blue and black ventral coloration, 278 genes were differentially expressed in the skin in response

to testosterone (Fig. 5A), with 74 upregulated by testosterone (Table S1) and 204

downregulated by testosterone (Table S2). For *S. virgatus*, the species in which neither

sex develops blue or black ventral coloration, only 55 genes were differentially expressed

in the skin (Fig. 5B), with 30 upregulated by testosterone (Table S3) and 25

downregulated by testosterone (Table S4). Among the 74 genes that were significantly

upregulated by testosterone in *S. undulatus*, GO enrichment revealed that pathways

related to the melanin biosynthetic process and melanocyte (i.e., melanophore)

differentiation were significantly enriched. Among the five total biological processes

enriched across *H. sapiens*, *D. rerio*, and *A. carolinensis*, these two were the only shared

processes across all three reference species (Table 3). Additionally, all but one of the

other enriched processes (peptidoglycan transport) were related to pigmentation (Table

3). Among the 204 genes downregulated by testosterone in *S. undulatus*, enriched

pathways included spermine biosynthesis process, mitotic spindle midzone assembly, and

positive regulation of ubiquitin protein ligase activity, among others (Table S5). There

were no enriched pathways in *S. virgatus*.

Species differences in transcriptome-wide responsiveness to testosterone

The number of testosterone-responsive DEGs in the sexually dichromatic *S.

undulatus* was significantly greater than in the sexually monochromatic *S. virgatus*

whether we compared all DEGs (278 vs. 55 genes; $\chi^2 = 161.88$, $P < 0.001$) or the subsets

that were upregulated (74 vs. 30; $\chi^2 = 18.615$, $P < 0.001$) or downregulated (204 vs. 25;

$\chi^2 = 139.92$, $P < 0.001$) by testosterone (Fig. 5A-B). When we iteratively excluded every

possible combination of three *S. undulatus* libraries to ensure equal statistical power in

each species, we found that the number of DEGs was significantly ($P < 0.05$) higher in *S. undulatus* than in *S. virgatus* for 1,487 of 1,540 iterations (96.6%), and that the mean ($\pm$ 1 SD) number of DEGs was 3.71 $\pm$ 1.93 times greater in *S. undulatus* ($\bar{x} = 153.7 \pm 96.1$) than in *S. virgatus* ($\bar{x} = 40.4 \pm 8.3$). There were no cases in which *S. virgatus* had significantly more DEGs than *S. undulatus*. Therefore, species differences in transcriptome-wide responsiveness to testosterone are robust to the minor difference in sample size between species (Fig. S2).

Seven of the genes that were significantly upregulated by testosterone in the sexually dichromatic *S. undulatus* are related to pigmentation and melanin synthesis pathways (Table 3), and these seven genes were completely unresponsive to testosterone in the sexually monochromatic *S. virgatus* (Fig. 5A-B, red symbols). When excluding these 7 genes, the remaining 67 genes that were significantly upregulated by testosterone in *S. undulatus* had log$_2$FC values that were significantly greater than zero in *S. virgatus* ($V = 1442$, $P = 0.016$; Fig. 5C). Likewise, genes that were significantly downregulated by testosterone in *S. undulatus* had log$_2$FC values that were significantly less than zero in *S. virgatus* ($V = 7276$, $P < 0.001$; Fig. 5C). Reciprocally, genes that were significantly up- or downregulated by testosterone in *S. virgatus* also displayed similar patterns of upregulation ($V = 388$, $P < 0.001$; Fig. 5C) or downregulation ($V = 59$, $P = 0.004$; Fig. 5C) in *S. undulatus*. A total of 95 genes were upregulated by testosterone in either species, with nine genes significantly upregulated by testosterone in both species (Fig. 5D). A total of 225 genes were downregulated by testosterone in either species, with four of these genes were significantly downregulated by testosterone in both species (Fig. 5D). While the overall trend was for genes to respond similarly in response to testosterone

between species, many genes were responsive in one species yet unresponsive in the other.

Species differences in genes mediating androgen availability and tissue sensitivity

$SRD5A2$, one of the three genes encoding the 5α-reductase enzyme that converts testosterone to the more potent androgen 5α-DHT, was expressed at higher levels in the sexually dichromatic *S. undulatus* than in the sexually monochromatic *S. virgatus* ($F_{1,37} = 17.11$, $P < 0.001$), was downregulated by testosterone ($F_{1,37} = 24.75$, $P < 0.001$), and had no treatment × species interaction ($F_{1,37} = 1.29$, $P = 0.263$; Fig. 6B). Neither $SRD5A1$ nor $SRD5A3$ exhibited a significant treatment effect, species effect, or treatment × species interaction (all $P > 0.089$), although males exhibited higher expression of $SRD5A3$ than females ($F_{1,33} = 9.34$, $P = 0.004$). $CYP19A1$, which encodes the aromatase enzyme that converts testosterone to estradiol, was not expressed at detectable levels in the skin of either species. $SHBG$, which encodes sex hormone binding globulin, was expressed at higher levels in *S. virgatus* than in *S. undulatus* ($F_{1,37} = 20.72$, $P < 0.001$), with no effect of testosterone ($F_{1,37} = 0.86$, $P = 0.359$) or treatment × species interaction ($F_{1,37} = 0.07$, $P_{adj} = 1$; Fig. 6A). AR, which encodes the androgen receptor, was expressed at higher levels in *S. virgatus* than in *S. undulatus* ($F_{1,37} = 14.65$, $P < 0.001$) and was downregulated by testosterone ($F_{1,37} = 10.86$, $P = 0.002$) similarly in both species (treatment × species interaction: $F_{1,37} = 1.44$, $P = 0.238$; Fig. 6C).

Species differences in genes mediating melanocortin production and signaling

Our expression data collectively suggest that the production of POMC and its conversion to α-MSH are both stimulated by testosterone in the sexually dichromatic *S. undulatus*, but not in the sexually monochromatic *S. virgatus*, and that the α-MSH signal is more likely to be detected in *S. undulatus* due to relatively higher expression of the gene for its MC1R receptor. *POMC,* which encodes proopiomelanocortin, was expressed at much higher levels in *S. undulatus* than in *S. virgatus,* in which its expression was barely detectable in control animals ($F_{1,33} = 43.15$, $P < 0.001$). *POMC* expression was significantly increased by testosterone ($F_{1,33} = 7.92$, $P = 0.008$) in both species (treatment × species interaction: $F_{1,33} = 3.60$, $P = 0.066$), although its expression was much lower in *S. virgatus* than in *S. undulatus* even in the presence of exogenous testosterone (Fig. 6D). *PCSK1,* which encodes the enzyme that converts POMC to adrenocorticotrophic hormone (ACTH), was expressed at higher levels in *S. virgatus* than in *S. undulatus* ($F_{1,37} = 9.44$, $P = 0.004$), but exhibited no treatment effect ($F_{1,37} = 0.51$, $P = 0.482$) or treatment × species interaction ($F_{1,37} = 0.94$, $P = 0.338$). *PCSK2,* which encodes the enzyme that subsequently converts ACTH to α-MSH, did not differ in expression by species ($F_{1,37} = 0.57$, $P = 0.454$) or treatment ($F_{1,37} = 2.68$, $P = 0.110$), but had a significant treatment × species interaction ($F_{1,37} = 8.59$, $P = 0.006$; Fig. 6E), such that testosterone increased *PCSK2* expression in *S. undulatus* but not in *S. virgatus*. *PCSK1N,* which encodes proSAAS, an inhibitor of the conversion of POMC to ACTH, was expressed at higher levels in *S. virgatus* than in *S. undulatus* ($F_{1,33} = 13.26$, $P < 0.001$), but was unaffected by testosterone ($F_{1,33} = 5.60$, $P = 0.024$, $P_{adj} = 0.114$) and exhibited no treatment × species interaction ($F_{1,33} = 2.06$, $P = 0.160$). *MC1R,* which encodes the melanocortin-1 receptor,

was expressed at higher levels in *S. undulatus* than in *S. virgatus* ($F_{1,37}$ = 19.46, $P <$ 0.001; Fig. 6F), with no treatment effect ($F_{1,37}$ = 0.04, P = 0.846) or treatment × species interaction ($F_{1,37}$ = 0.04, P = 0.840).

Species differences in genes mediating melanin synthesis

Our expression data collectively suggest that melanin synthesis is stimulated at the transcriptional level by testosterone in the sexually dichromatic *S. undulatus*, but not in the sexually monochromatic *S. virgatus*. *TYR*, which encodes tyrosinase, was expressed at higher levels in *S. undulatus* than in *S. virgatus* ($F_{1,37}$ = 14.73, $P < 0.001$), upregulated by testosterone ($F_{1,37}$ = 10.24, P = 0.003), and upregulated more strongly in *S. undulatus* than in *S. virgatus* (treatment × species interaction: $F_{1,37}$ = 8.80, P = 0.005; Fig. 6G). We observed similar patterns for *TYRP1*, which encodes tyrosinase-related protein 1, such that it was expressed higher in *S. undulatus* ($F_{1,37}$ = 8.54, P = 0.006), upregulated by testosterone ($F_{1,37}$ = 6.88, P = 0.013), and upregulated more strongly in *S. undulatus* than in *S. virgatus* (treatment × species interaction: $F_{1,37}$ = 6.85, P = 0.013; Fig. 6H). *OCA2,* which encodes the P protein, exhibited a significant treatment × species interaction ($F_{1,37}$ = 8.28, P = 0.007; Fig. 6I), but no significant species ($F_{1,37}$ = 2.32, P = 0.137) or treatment ($F_{1,37}$ = 4.61, P_{adj} = 0.111, P = 0.038) effects.

Expression of marker genes for melanophores and their precursors

Genes selected as markers for melanophores or melanophore precursors were expressed in both species and were unresponsive to testosterone in either species. *DCT,* which encodes dopachrome tautomerase, was expressed similarly in both species ($F_{1,37}$ =

4.14, $P_{adj} = 0.127$, $P = 0.049$), with no treatment effect ($F_{1,37} = 1.84$, $P = 0.183$) or treatment × species interaction ($F_{1,37} = 0.01$, $P = 0.939$; Fig. 6J). *KIT,* which encodes a tyrosine kinase called the KIT protein, was expressed similarly in both species ($F_{1,37} = 4.33$, $P_{adj} = 0.127$, $P = 0.044$), with no treatment effect ($F_{1,37} = 0.17$, $P = 0.686$) or treatment × species interaction ($F_{1,37} = 0.76$, $P = 0.388$; Fig. 6K). *MITF,* which encodes the melanocyte-inducing transcription factor (also known as microphthalmia-associated transcription factor), was expressed similarly in both species ($F_{1,37} = 1.03$, $P = 0.318$), with no treatment effect ($F_{1,37} = 0.51$, $P = 0.480$) or treatment × species interaction ($F_{1,37} = 0.68$, $P = 0.415$; Fig. 6L).

Discussion

We found that the evolutionary loss of hormonally mediated ventral coloration is associated with the loss of transcriptional responsiveness to testosterone by genes putatively involved in the production of ventral coloration. Whereas several key melanin synthesis genes were upregulated in response to testosterone in sexually dichromatic *S. undulatus*, these same genes were unresponsive to exogenous testosterone in sexually monochromatic *S. virgatus*. This does not appear to be due to the absence of melanophores in the skin of *S. virgatus*, given that we detected the expression of genes characteristic of melanophores at similar levels in the skin of both species. Nor does it appear to be because the ventral skin of *S. virgatus* is insensitive to androgens, given that we detected higher relative expression of the androgen receptor in *S. virgatus* and that transcriptome-wide patterns of up- and downregulation by testosterone were directionally similar in both species. However, we did find some evidence for lower transcriptional

sensitivity to testosterone in the skin of *S. virgatus* than in *S. undulatus.* In particular, we found 3.7 times fewer genes that were differentially expressed in response to exogenous testosterone in *S. virgatus* relative to *S. undulatus*. We also found that *S. virgatus* skin expressed significantly less *SRD5A2*, which encodes the enzyme that converts testosterone into the more potent 5α-dihydrotestosterone, and significantly more *SHBG*, which encodes a binding globulin that prevents androgen signaling, relative to *S. undulatus*. Below, we discuss these mechanisms in greater detail and integrate them with recent theory and empirical work on the evolution of hormonally mediated sexual dimorphism.

The expression of genes that mediate melanin synthesis within melanophores (*i.e., TYR*, *TYRP1*, *OCA*) was generally stimulated by testosterone in the sexually dichromatic *S. undulatus*, but was low and unresponsive to testosterone in the sexually monochromatic *S. virgatus*. These genes are critical for the production of melanin, and mutations in these genes are associated with atypical melanin-based phenotypes across taxa, including clinical abnormalities in humans (Yokoyama et al. 1990; Kelsh et al. 1996; Passmore et al. 1999; Toyofuku et al. 2001; King et al. 2003; Lyons et al. 2005a,b; Oetting et al. 2005; Klaassen et al. 2018; Li et al. 2019). However, coding-sequence mutations typically result in systemic pigmentation effects rather than localized changes like those observed between *S. undulatus* and *S. virgatus*. In contrast, regulatory changes in gene expression can result in the evolution of morphology (Carroll 1995; Prud'homme et al. 2007; Wittkopp and Kalay 2012; Horton et al. 2014; Sackton et al. 2019; Merritt et al. 2020; Huang et al. 2022; Luecke et al. 2022), including phenotypes dependent upon melanin production (Gompel et al. 2005; Prud'homme et al. 2006; Werner et al. 2010;

Koshikawa et al. 2015; Kratochwil et al. 2018; Koshikawa 2020; Hughes et al. 2021). Our results therefore suggest that the loss of ventral color in *S. virgatus* is at least partially due to the loss of androgen-dependent expression of these key melanin synthesis genes in the ventral skin. However, the mechanisms that underlie this loss of androgen responsiveness are less clear.

One hypothetical mechanism for the loss of androgen responsiveness by melanin synthesis genes is that mature melanophores are absent from the ventral skin of sexually monochromatic *S. virgatus*. The loss of this cell type may alter the transcriptomic profile of the skin and therefore explain both the low expression of individual melanin synthesis genes and the overall reduction in androgen responsiveness of the skin transcriptome in *S. virgatus,* relative to sexually dichromatic *S. undulatus*. However, contrary to this hypothesis, we detected expression of three melanophore-specific lineage markers at comparable levels in the skin of both species (*DCT*, *KIT*, and *MITF;* Steel et al. 1992; Parichy et al. 1999; Bondurand et al. 2000; Kelsh et al. 2000; Quigley et al. 2004; Mort et al. 2015; Schartl et al. 2016). This result suggests that melanophores or their melanoblast precursors are present in the skin of *S. virgatus*, although we cannot determine their developmental stage. The reduced expression of both *POMC* and *MC1R* in *S. virgatus,* relative to *S. undulatus,* could indicate that melanophores are in an immature state and therefore unable to produce (POMC) and receive (MC1R) the necessary melanocortin signals to promote melanin synthesis. However, the location of POMC synthesis is unknown in our system and could occur in keratinocytes or melanophores (Schauer et al. 1994; Chakraborty et al. 1996; Wintzen et al. 1996; Rousseau et al. 2007), such that the use of *POMC* expression for inferences about melanophore development is tenuous.

Nonetheless, our data indicate that melanophores are present in the skin of *S. virgatus,* but do not receive the necessary signals to mature or to initiate melanin production.

The reduced expression of *MC1R* that we observed in the skin of *S. virgatus* is one potential mechanism for the failure of melanophores to express melanin synthesis genes. Generally, MC1R binds α-MSH, which induces a cAMP cascade, resulting in increased expression of *MITF* and downstream melanin synthesis pathways (reviewed in Park et al. 2009). Therefore, the reduction in *MC1R* expression that we observed in *S. virgatus* could explain some of the observed species differences in the expression of *TYR*, *TYRP1*, and *OCA2*. Coding sequence mutations in *MC1R* have been shown to underlie whole-body color evolution in several vertebrates (Nachman et al. 2003; Rosenblum et al. 2004; Mundy 2005; Rosenblum et al. 2010; Jin et al. 2020). Upstream from MC1R, reductions in the production and processing of POMC into α-MSH, which binds MC1R to initiate melanin synthesis, could also explain the low expression of *TYR*, *TYRP1*, and *OCA2* in *S. virgatus*. Our data support this possibility in that the expression of *POMC* is extremely low in *S. virgatus* relative to *S. undulatus*, and is stimulated by testosterone in *S. undulatus,* but not *S. virgatus*. Moreover, some genes whose products are involved in the processing of POMC into α-MSH are only responsive to androgens in *S. undulatus*. For example, *PCSK2* is upregulated by testosterone in *S. undulatus,* but it is not responsive to testosterone in *S. virgatus*. Therefore, the production of α-MSH in response to testosterone is likely greater in *S. undulatus*, increasing activation of the MC1R receptor and promoting melanin synthesis. Collectively, our data suggest that the loss of ventral coloration in *S. virgatus* occurs partly through the loss of *POMC* expression and

processing in response to androgens, and partly through reductions in *MC1R* expression, resulting in the failure of testosterone to induce expression of melanin synthesis genes.

Finally, the question remains of whether and how overall sensitivity to androgens is reduced in the skin of the sexually monochromatic *S. virgatus*. Our data indicate that this is not due to the wholesale loss of androgen receptor expression in the skin, as *AR* was expressed robustly in both species, with slightly elevated expression in *S. virgatus*. However, we cannot eliminate the possibility of cell-specific changes in the expression of androgen receptor that are not captured by our bulk RNAseq approach. For example, *AR* could be expressed in *S. virgatus* keratinocytes and iridophores, but not in *S. virgatus* melanophores, preventing their maturation and subsequent melanization in response to androgen signaling (Schartl et al. 1982) while maintaining transcriptome-wide expression of *AR*. Rigorously addressing this possibility would require a more targeted approach, such as AR staining and localization via immunohistochemistry, *in situ* hybridization, or single-cell RNAseq. Support for this hypothesis would represent a case of a single cell type within a tissue "unplugging" from hormonal control (Hau 2007; Ketterson et al. 2009). Although our data do not provide any evidence of reduced *AR* expression in *S. virgatus,* they do suggest that testosterone may be more readily converted to the more potent androgen 5α-DHT in *S. undulatus*, based on higher expression of *SRD5A2* (but not of *SRD5A1* or *SRD5A3*)*. Differences in the conversion of testosterone to 5α-DHT could lead to species-specific patterns of gene expression (Lin and Chang 1997; Dadras et al. 2001). Additionally, *SHBG* was expressed at higher levels in *S. virgatus* than in *S. undulatus*, potentially reducing the local availability of free androgens in the skin of *S. virgatus* (Anderson 1974; Breuner and Orchinik 2002).

The evolution of hormonally mediated sexual dimorphism proceeds not only through changes in circulating hormone levels (*e.g.*, Husak and Lovern 2014), but also through changes in hormone-phenotype couplings (Cox 2020; Cox et al. 2022). For example, evolutionary changes in tissue-specific expression of the androgen receptor in manakins (Fuxjager et al. 2015) and anole lizards (Johnson et al. 2018) correspond to evolutionary changes in male-typical behaviors across species. Likewise, changes in the genomic distribution of hormone response elements may contribute to the evolution of sex-specific songs and display behaviors in birds (Frankl-Vilches et al. 2015; Fuxjager and Schuppe 2018) and sexual size dimorphism in primates (Anderson and Jones 2022). Having genomes for both *Sceloporus* species would permit similar comparisons of hormone response elements in this system, but currently there is no genome available for *S. virgatus*. We contribute to this emerging perspective in evolutionary endocrinology by showing that the evolution of sexually dimorphic coloration is associated with 1) pronounced changes in the hormonal responsiveness of downstream genes that mediate coloration, and 2) potential upstream changes in tissue sensitivity to a hormonal cue. Further exploration of these mechanisms will help clarify how phenotypes become evolutionarily decoupled from their hormonal regulators, facilitating the evolution of hormone-phenotype couplings and sexual dimorphism.

Funding

Acknowledgements

Data Availability

Phenotypic data are available on Dryad at https://doi.org/10.5061/dryad.7d7wm381c. Reads from RNAseq are available under BioProject ID PRJNA1003887 at the National Center for Biotechnology Information Short Read Archive.

References

Abell AJ. 1998a. Reproductive and post-reproductive hormone levels in the lizard *Sceloporus virgatus*. Acta Zoológica Mexicana 74:43-57.

Abell AJ. 1998b. The effect of exogenous testosterone on growth and secondary sexual character development in juveniles of *Sceloporus virgatus*. Herpetologica 54:533-543.

Anderson AP and AG Jones. 2022. The relationship between sexual dimorphism and androgen response element proliferation in primate genomes. Evolution 76:1331-1346.

Anderson AP and JJ Falk. 2023. Cross-sexual transfer revisited. Integrative and Comparative Biology icad021.

Anderson AP, E Rose, SP Flanagan, and AG Jones. 2020. The estrogen-responsive transcriptome of female secondary sexual traits in the gulf pipefish. Journal of Heredity 111:294-306.

Anderson DC. 1974. Sex-hormone-binding globulin. Clinical Endocrinology 3:69-96.

Ansai S, K Mochida, S Fujimoto, DF Mokodongan, BKA Sumarto, KWA Masengi, RK Hadiaty, AJ Nagano, A Toyoda, K Naruse, K Yamahira, and J Kitano. 2021. Genome editing reveals fitness effects of a gene for sexual dichromatism in Sulawesian fishes. Nature Communications 12:1350.

Ashburner M, CA Ball, JA Blake, D Botstein, H Butler, JM Cherry, AP Davis, K Dolinski, SS Dwight, JT Eppig, MA Harris, DP Hill, L Issel-Tarver, A Kasarskis, S Lewis, JC Matese, JE Richardson, M Ringwald, GM Rubin, and G Sherlock. 2000. Gene ontology: tool for the unification of biology. Nature Genetics 25:9.

Bellono NW, IE Escobar, AJ Lefkovith, MS Marks, and E Oancea. 2014. An intracellular anion channel critical for pigmentation. eLife 3:e04543.

Benjamini Y and Y Hochberg. 1995. Controlling the false discovery rate: a practical and powerful approach to multiple testing. Journal of the Royal Statistical Society 57:289-300.

Blázquez MA DC Nelson, and D Wijers. 2020. Evolution of plant hormone response pathways. Annual Review of Plant Biology 71:327-353.

Boissy RE, H Zhao, WS Oetting, LM Austin, SC Wildenberg, YL Boissy, Y Zhao, RA Sturm, VJ Hearing, RA King, and JJ Nordlund. 1996. Mutation in and lack of expression of tyrosinase-related protein-1 (TRP-1) in melanocytes from an individual with brown oculocutaneous albinism: a new subtype of albinism classified as "OCA3". American Journal of Human Genetics 58:1145-1156.

Bondurand N, V Pingault, DE Goerich, N Lemort, E Sock, C Le Caignec, M Wegner, and M Goossens. 2000. Interaction among *SOX10*, *PAX3*, and *MITF*, three genes altered in Waardenburg syndrome. Human Molecular Genetics 9:1907-1917.

Breuner CW and M Orchinik. 2002. Plasma binding proteins as mediators of corticosteroid action in vertebrates. Journal of Endocrinology 175:99-112.

Carroll SB. 1995. Homeotic genes and the evolution of arthropods and chordates. Nature 376:479-485.

Chakraborty AK, Y Funasaka, A Slominski, G Ermak, J Hwang, JM Pawelek, and M Ichihashi. 1996. Production and release of proopiomelanocortin (POMC) derived peptides by human melanocytes and keratinocytes in culture: regulation by ultraviolet B. Biochemica et Biophysica Acta 1313:130-138.

Chen S, Y Zhou, Y Chen, and J Gu. 2018. fastp: an ultra-fast all-in-one FASTQ
preprocessor. Bioinformatics 34:i884-i890.

Cox CL, AF Hanninen, AM Reedy, and RM Cox. 2015. Female anoles retain
responsiveness to testosterone despite the evolution of androgen-mediated sexual
dimorphism. Functional Ecology 29:758-767.

Cox RM. 2020. Sex steroids as mediators of phenotypic integration, genetic correlations,
and evolutionary transitions. Molecular and Cellular Endocrinology 502:110668.

Cox RM and HB John-Alder. 2005. Testosterone has opposite effects on male growth in
lizards (*Sceloporus* spp.) with opposite patterns of sexual size dimorphism. Journal of
Experimental Biology 208:4679-4687.

Cox RM and HB John-Alder. 2007. Increased mite parasitism as a cost of testosterone in
male striped plateau lizards *Sceloporus virgatus*. Functional Ecology 21:327-334.

Cox RM, CL Cox, JW McGlothlin, DC Card, AL Andrew, and TA Castoe. 2017.
Hormonally mediated increases in sex-biased gene expression accompany the
breakdown of between-sex genetic correlations in a sexually dimorphic lizard. The
American Naturalist 189:315-332.

Cox RM, DS Stenquist, and R Calsbeek. 2009. Testosterone, growth, and the evolution of
sexual size dimorphism. Journal of Evolutionary Biology 22:1586-1598.

Cox RM, MA Butler, and HB John-Alder. 2007. The evolution of sexual size dimorphism
in reptiles. In: Sex, Size and Gender Roles: Evolutionary Studies of Sexual Size
Dimorphism, eds: DJ Fairbairn, WU Blanckenhorn, and T Szekely. Chapter 4:38-49.
Oxford University Press, Oxford.

Cox RM, MD Hale, TN Wittman, CD Robinson, and CL Cox. 2022. Evolution of hormone-phenotype couplings and hormone-genome interactions. Hormones and Behavior 114:105216.

Cox RM, SL Skelly, A Leo, and HB John-Alder. 2005a. Testosterone regulates sexually dimorphic coloration in the eastern fence lizard, *Sceloporus undulatus*. Copeia 2005:597-608.

Cox RM, SL Skelly, and HB John-Alder. 2005b. Testosterone inhibits growth in juvenile male eastern fence lizards (*Sceloporus undulatus*): implications for energy allocation and sexual size dimorphism. Physiological and Biochemical Zoology 78:531-545.

Cox RM, V Zilberman, and HB John-Alder. 2008. Testosterone stimulates the expression of a social color signal in Yarrow's spiny lizard, *Sceloporus jarrovii*. Journal of Experimental Zoology A: Ecological Genetics and Physiology 309:505-514.

Dadras SS, X Cai, I Abasolo, and Z Wang. 2001. Inhibition of 5α-reductase in rat prostate reveals differential regulation of androgen-response gene expression by testosterone and dihydrotestosterone. Gene Expression 9:183-194.

Enbody EK, SYW Sin, J Boersma, SV Edwards, S Ketaloya, H Schwabl, MS Webster, and J Karubian. 2022. The evolutionary history and mechanistic basis of female ornamentation in a tropical songbird. Evolution 76:1720-1736.

Frankl-Vilches C, H Kuhl, M Werber, S Klages, M Kerick, A Bakker, EHC de Oliveria, C Reusch, F Capuano, J Vowinckel, S Leitner, M Ralser, B Timmermann, and M Gahr. 2015. Using the canary genome to decipher the evolution of hormone-sensitive gene regulation in seasonal singing birds. Genome Biology 16:1-25.

Fricker LD, AA McKinzie, J Sun, E Curran, Y Qian, L Yan, SD Patterson, PL
Courchesne, B Richards, N Levin, N Mzhavia, LA Devi, and J Douglass. 2000.
Identification and characterization of proSAAS, a granin-like neuroendocrine peptide
precursor that inhibits prohormone processing. Journal of Neuroscience 20:639-648.

Fuxjager MJ and ER Schuppe. 2018. Androgenic signaling systems and their role in
behavioral evolution. Journal of Steroid Biochemistry and Molecular Biology 184:47-
56.

Fuxjager MJ, J Eaton, WR Lindsay, LH Salwiczek, MA Rensel, J Barske, L Sorenson,
LB Day, and BA Schlinger. 2015. Evolutionary patterns of adaptive acrobatics and
physical performance predict expression profiles of androgen receptor – but not
oestogen receptor – in forelimb musculature. Functional Ecology 29:1197-1208.

Gazda MA, PM Araújo, RJ Lopes, MB Toomey, P Andrade, S Afonso, C Marques, L
Nunes, P Pereira, S Trigo, and GE Hill. 2020. A genetic mechanism for sexual
dichromatism in birds. Science 368:1270-1274.

Gompel N, B Prud'homme, PJ Wittkopp, VA Kassner, and SB Carroll. 2005. Chance
caught on the wing: *cis*-regulatory evolution and the origin of pigment patterns in
Drosophila. Nature 433:481-487.

Hale MD, CD Robinson, CL Cox, and RM Cox. 2022. Ontogenetic change in male
expression of testosterone-responsive genes contributes to the emergence of sex-
biased gene expression in *Anolis sagrei*. Frontiers in Physiology 13:886973.

Harno E, TG Ramamoorthy, AP Coll, and A White. 2018. POMC: the physiological
power of hormone processing. Physiological Reviews 98:2381-2430.

Hau M. 2007. Regulation of male traits by testosterone: implications for the evolution of

    vertebrate life histories. BioEssays29:133-144.

Hews DK, E Hara, and MC Anderson. 2012. Sex and species differences in plasma

    testosterone and in counts of androgen receptor-positive cells in key brain regions of

    Sceloporus lizard species that differ in aggression. General and Comparative

    Endocrinology 176:493-499.

Horton BM, WH Hudson, EA Ortlund, S Shirk, JW Thomas, ER Young, WM Zinzow-

    Kramer, and DL Maney. 2014. Estrogen receptor α polymorphism in a species with

    alternative behavioral phenotypes. Proceedings of the National Academy of Sciences

    111:1443-1448.

Huang Y, R Shang, G-A Lu, W Zeng, C Huang, C Zou, and T Tang. 2022. Spatiotemporal

    regulation of a single adaptively evolving *trans*-regulatory element contributes to

    spermatogenetic expression divergence in *Drosophila*. Molecular Biology and

    Evolution 39:msac127.

Hughes JT, ME Williams, M Rebeiz, and TM Williams. 2021. Widespread *cis*- and *trans*-

    regulatory evolution underlies the origin, diversification, and loss of a sexually

    dimorphic fruit fly pigmentation trait. Journal of Experimental Zoology B: Molecular

    and Developmental Evolution 2021:1-19.

Husak JF and MB Lovern. 2014. Variation in steroid hormone levels among Caribbean

    Anolis lizards: endocrine system convergence? Hormones and Behavior 65:408-415.

Jiménez-Arcos VH, S Sanabria-Urbán, and R Cueva del Castillo. 2017. The interplay

    between natural and sexual selection in the evolution of sexual size dimorphism in

    Sceloporus lizards (Squamata: Phrynosomatidae). Ecology and Evolution 7:905-917.

Jin Y, H Tong, G Shao, J Li, Y Lv, Y Wo, RP Brown, and C Fu. 2020. Dorsal pigmentation and its association with functional variation in *MC1R* in a lizard from different elevations on the Qinghai-Tibetan Plateau. Genome Biology and Evolution 12:2303-2313.

John-Alder HB and RM Cox. 2007. Development of sexual size dimorphism in lizards: testosterone as a bipotential growth regulator. Pp. 195-204 in: Sex, Size and Gender Roles: Evolutionary Studies of Sexual Size Dimorphism. Edited by DJ Fairbairn, T Szekely, and WU Blanckenhorn. Oxford University Press.

John-Alder HB, RM Cox, GJ Haenel, and LC Smith. 2009. Hormones, performance and fitness: natural history and endocrine experiments on a lizard (*Sceloporus undulatus*). Integrative and Comparative Biology 49:393-407.

Johnson MJ, BK Kircher, and DJ Castro. 2018. The evolution of androgen receptor expression and behavior in *Anolis* lizard forelimb muscles. Journal of Comparative Physiology A 204:71-79.

Kelsh RN, B Schmid, and JS Eisen. 2000. Genetic analysis of melanophore development in zebrafish embryos. Developmental Biology 225:277-293.

Kelsh RN, M Brand, Y-J Jiang, C-P Heisenberg, S Lin, P Haffter, J Odenthal, MC Mullins, FJM van Eeden, M Furutani-Seiki, M Granato, M Hammerschmidt, DA Kane, RM Warga, D Beuchle, L Vogelsang, and C Nüsslein-Volhard. 1996. Zebrafish pigmentation mutations and the processes of neural crest development. Development 123:369-389.

Ketterson ED, JW Atwell, and JW McGlothlin. 2009. Phenotypic integration and

    independence: hormones, performance, and response to environmental change.

    Integrative and Comparative Biology 49:365-379.

Khalil S, JF Welklin, KJ McGraw, J Boersma, H Schwabl, MS Webster, and J Karubian.

    2020. Testosterone regulates *CYP2J19*-linked carotenoid signal expression in male

    red-backed fairywrens (*Malurus melanocephalus*). Proceedings of the Royal Society

    of London B: Biological Sciences 287:20201687.

Kimball FA and MJ Erpino. 1971. Hormonal control of pigmentary sexual dimorphism in

    Sceloporus occidentalis. General and Comparative Endocrinology 16:375-384.

King RA, J Pietsch, JP Fryer, S Savage, MJ Brott, I Russell-Eggitt, CG Summers, and

    WS Oetting. 2003. Tyrosinase gene mutations in oculocutaneous albinism 1 (OCA1):

    definition of the phenotype. Human Genetics 113:502-513.

Klaassen H, Y Wang, K Adamski, N Rohner, and JE Kowalko. 2018. CRISPR

    mutagenesis confirms the role of *oca2* in melanin pigmentation in *Astyanax*

    mexicanus. Developmental Biology 441:313-318.

Kobayashi T, G Imokawa, DC Bennett, and VJ Hearing. 1998. Tyrosinase stabilization by

    Tyrp1 (the *brown* locus protein). Journal of Biological Chemistry 273:31801-31805.

Koshikawa S. 2020. Evolution of wing pigmentation in *Drosophila*: diversity,

    physiological regulation, and *cis*-regulatory evolution. Development, Growth &

    Differentiation 62:269-278.

Koshikawa S, MW Giorgianni, K Vaccaro, VA Kassner, JH Yoder, T Werner, and SB

    Carroll. 2015. Gain of *cis*-regulatory activities underlies novel domains of *wingless*

gene expression in *Drosophila*. Proceedings of the National Academy of Sciences 112:7524-7529.

Kratochwil CF, Y Liang, J Gerwin, JM Woltering, S Urban, F Henning, G Machado-Schiaffino, CD Hulsey, and A Meyer. 2018. Agouti-related peptide 2 facilitates convergent evolution of stripe patterns across cichlid fish radiations. Science 362:457-460.

Li J, B Bed'hom, S Marthey, M Valade, A Dureux, M Moroldo, C Péchoux, J-L Coville, D Gourichon, A Vieaud, B Dorshorst, L Andersson, and M Tixier-Boichard. 2019. A missense mutation in *TYRP1* causes the chocolate plumage color in chicken and alters melanosome structure. Pigment Cell & Melanoma Research 31:381-390.

Liao Y, GK Smyth, and W Shi. 2013. The Subread aligner: fast, accurate and scalable read mapping by seed-and-vote. Nucleic Acid Research 41:e108.

Liao Y, GK Smyth, and W Shi. 2014. featureCounts: an efficient general purpose program for assigning sequence reads to genomic features. Bioinformatics 30:923-930.

Lin T-M and C Chang. 1997. Cloning and characterization of TDD5, an androgen target gene that is differentially repressed by testosterone and dihydrotestosterone. Proceedings of the National Academy of Sciences 94:4988-4993.

Lipshutz SE, EM George, AB Bentz, and KA Rosvall. 2019. Evaluating testosterone as a phenotypic integrator: from tissues to individuals to species. Molecular and Cellular Endocrinology 496:110531.

Luecke D, G Rice, and A Kopp. 2022. Sex-specific evolution of a *Drosophila* sensory

　　system via interacting *cis*- and *trans*-regulatory changes. Evolution & Development

　　24:37-60.

Lyons LA, DL Imes, HC Rah, and RA Grahn. 2005a. Tyrosinase mutations associated

　　with Siamese and Burmese patterns in the domestic cat (*Felis catus*). Animal

　　Genetics 36:119-126.

Lyons LA, IT Foe, HC Rah, and RA Grahn. 2005b. Chocolate coated cats: *TYRP1*

　　mutations for brown color in domestic cats. Mammalian Genome 16:356-366.

Mank JE. 2009. Sex chromosomes and the evolution of sexual dimorphism: lessons from

　　the genome. The American Naturalist 173:141-150.

McLean CA, A Lutz, KJ Rankin, D Stuart-Fox, and Adnan Moussalli. 2017. Revealing

　　the biochemical and genetic basis of color variation in a polymorphic lizard.

　　Molecular Biology and Evolution 34:1924-1935.

Merritt JR, KE Grogan, WM Zinzow-Kramer, D Sun, EA Ortlund, SV Yi, and DL Maney.

　　2020. A supergene-linked estrogen receptor drives alternative phenotypes in a

　　polymorphic songbird. Proceedings of the National Academy of Sciences 117:21673-

　　21680.

Morrison RL, MS Rand, and SK Frost-Mason. 1995. Cellular basis of color differences in

　　three morphs of the lizard *Sceloporus undulatus erythrocheilus*. Copeia 1995:397-

　　408.

Mort RL, IJ Jackson, and EE Patton. 2015. The melanocyte lineage in development and

　　disease. Development 142:620-632.

Mundy NI. 2005. A window on the genetics of evolution: *MC1R* and plumage colouration in birds. Proceedings of the Royal Society of London B: Biological Sciences 272:1633-1640.

Nachman MW, HE Hoekstra, and SL D'Agostino. 2003. The genetic basis of adaptive melanism in pocket mice. Proceedings of the National Academy of Sciences 100:5268-5273.

Nicolaï MPJ, L D'Alba, J Goldenberg, Y Gansemans, F Van Nieuwerburgh, S Clusella-Trullas, and MD Shawkey. 2021. Untangling the structural and molecular mechanisms underlying colour and rapid colour change in a lizard, *Agama atra*. Molecular Ecology 30:2262-2284.

Oetting WS, S Savage Garrett, M Brott, and RA King. 2005. P gene mutations associated with oculocutaneous albinism II (OCA2). Human Mutation 25:323-329.

Ossip-Drahos AG, JR Oyola Morales, C Vital- García, JJ Zúñiga-Vega, DK Hews, and EP Martins. 2016. Shaping communicative colour signals over evolutionary time. Royal Society Open Science 3:160728.

Parichy DM. 2021. Evolution of pigment cells and patterns: recent insights from teleost fishes. Current Opinions in Genetics & Development 69:88-96.

Parichy DM, JF Rawls, SJ Pratt, TT Whitfield, and SL Johnson. 1999. Zebrafish *sparse* corresponds to an orthologue of *c-kit* and is required for the morphogenesis of a subpopulation of melanocytes, but is not essential for hematopoiesis or primordial germ cell development. Development 126:3425-3436.

Park HY, M Kosmadaki, M Yaar, and BA Gilchrest. 2009. Cellular mechanisms regulating human melanogenesis. Cellular and Molecular Life Sciences 66:1493-1506.

Passmore LA, B Kaesmann-Kellner, and BHF Weber. 1999. Novel and recurrent mutations in the tyrosinase gene and the P gene in the German albino population. Human Genetics 105:200-210.

Phipson B, S Lee, IJ Majewski, ES Alexander, and GK Smyth. 2016. Robust hyperparameter estimation protects against hypervariable genes and improves power to detect differential expression. The Annals of Applied Statistics 10:946-963.

Pollock NB, S Feigin, M Drazenovic, and HB John-Alder. 2017. Sex hormones and the development of sexual size dimorphism: 5α-dihydrotestosterone inhibits growth in a female-larger lizard (*Sceloporus undulatus*). Journal of Experimental Biology 220:4068-4077.

Prud'homme B, N Gompel, A Rokas, VA Kassner, TM Williams, S-D Yeh, JR True, and SB Carroll. 2006. Repeated morphological evolution of *cis*-regulatory changes in a pleiotropic gene. Nature 440:1050-1053.

Prud'homme B, N Gompel, and SB Carroll. 2007. Emerging principles of regulatory evolution. Proceedings of the National Academy of Sciences 104:8605-8612.

Qian Y, LA Devi, N Mzhavia, S Munzer, NG Seidah, and LD Fricker. 2000. The C-terminal region of proSAAS is a potent inhibitor of prohormone convertase 1. Journal of Biological Chemistry 275:23596-23601.

Quigley IK, JM Turner, RJ Muckels, JL Manuel, EH Budi, EL MacDonald, and DM Parichy. 2004. Pigment pattern evolution by differential deployment of neural crest

and post-embryonic melanophore lineages in *Danio* fishes. Development 131:6053-6069.

Quinn VS and DK Hews. 2003. Positive relationship between abdominal coloration and dermal melanin density in phrynosomatid lizards. Copeia 2003:858-864.

R Core Team. 2022. R: a language and environment for statistical computing. R Foundation for Statistical Computing. Vienna, Austria.

Raper HS. 1928. The aerobic oxidases. Physiological Reviews 8:245-282.

Reynkens T. 2018. rospca: robust sparse PCA using ROSPCA algorithm. R package version 1.0.4.

Rinn JL and M Snyder. 2005. Sexual dimorphism in mammalian gene expression. Trends in Genetics 21:298-305.

Robinson CD and ME Gifford. 2019. Intraseasonal changes of patch color in prairie lizards (*Sceloporus consobrinus*). Herpetologica 75:79-84.

Robinson MD, DJ McCarthy, and GK Smyth. 2010. edgeR: a Bioconductor package for differential expression analysis of digital gene expression data. Bioinformatics 26:139-140.

Rosenblum EB, H Hoekstra, and MW Nachman. 2004. Adaptive reptile color variation and the evolution of the *MC1R* gene. Evolution 58:1794-1808.

Rosenblum EB, H Römpler, T Schöneberg, and HE Hoekstra. 2010. Molecular and functional basis of phenotypic convergence in white lizards at White Sands. Proceedings of the National Academy of Sciences 107:2113-2117.

Rosvall KA, CMB Burns, SP Jayaratna, and ED Ketterson. 2016. Divergence along the

    gonadal steroidogenic pathway: implications for hormone-mediated phenotypic

    evolution. Hormones and Behavior 84:1-8.

Rousseau K, S Kauser, LE Pritchard, A Warhurst, RL Oliver, A Slominski, ET Wei, AJ

    Thody, DJ Tobin, and A White. 2007. Proopiomelanocortin (POMC), the

    ACTH/melanocortin precursor, is secreted by human epidermal keratinocytes and

    melanocytes and stimulates melanogeneis. The FASEB Journal 21:1844-1856.

Sackton TB, P Grayson, A Cloutier, Z Hu, JS Liu, NE Wheeler, PP Gardner, JA Clarke,

    AJ Baker, M Clamp, and SV Edwards. 2019. Convergent regulatory evolution and

    loss of flight in paleognathous birds. Science 364:74-78.

Schartl A, M Schartl, and F Anders. 1982. Promotion and regression of neoplasia by

    testosterone-promoted cell differentiation in *Xiphophorus* and *Girardinus*.

    Carcinogenesis 7:427-434.

Schartl M, L Larue, M Goda, MW Bosenberg, H Hashimoto, and RN Kelsh. 2016. What

    is a vertebrate pigment cell? Pigment Cell & Melanoma Research 29:8-14.

Schauer E, F Trautinger, A Köck, A Schwarz, R Bhardwaj, M Simon, JC Ansel, T

    Schwarz, and TA Luger. 1994. Proopiomelanocortin-derived peptides are synthesized

    and released by human keratinocytes. Journal of Clinical Investigation 93:2258-2262.

Steel KP, DR Davidson, and IJ Jackson. 1992. TRP-2/DT, a new early melanoblast

    marker, shows that steel growth factor (c-kit ligand) is a survival factor. Development

    115:1111-1119.

Taylor JD and ME Hadley. 1970. Chromatophores and color change in the lizard, *Anolis carolinensis*. Zeitschrift Für Zellforschung Und Mikroskopische Anatomie 104:282-294.

The Gene Ontology Consortium. 2021. The gene ontology resource: enriching a GOld mine. Nucleic Acid Research 49:D325-D334.

Toyofuku K, I Wada, JC Valencia, T Kushimoto, VJ Ferrans, and VJ Hearing. 2001. Oculocutaneous albinism types 1 and 3 are ER retention diseases: mutation of tyrosinase or Tyrp1 can affect the processing of both mutant and wild-type proteins. FASEB 15:2149-2161.

van Nas A, D GuhaThakurta, SS Wang, N Yehya, S Horvath, B Zhang, L Ingram-Drake, G Chaudhuri, EE Schadt, TA Drake, AP Arnold, and AJ Lusis. 2009. Elucidating the role of gonadal hormones in sexually dimorphic gene coexpression networks. Endocrinology 150:1235-1249.

Xu X, JK Coats, CF Yang, A Wang, OM Ahmed, M Alvarado, T Izumi, and NM Shah. 2012. Modular genetic control of sexually dimorphic behaviors. Cell 148:596-607.

Waxman DJ and C O'Connor. 2006. Growth hormone regulation of sex-dependent liver gene expression. Molecular Endocrinology 20:2613-2629.

Werner T, S Koshikawa, TM Williams, and SB Carroll. 2010. Generation of a novel wing colour pattern by the Wingless morphogen. Nature 464:1143-1148.

West-Eberhard MJ. 2003. Developmental Plasticity and Evolution. New York: Oxford University Press.

Westfall AK, RS Telemeco, MB Grizante, DS Waits, AD Clark, DY Simpson, RL Klabacka, AP Sullivan, GH Perry, MW Sears, CL Cox, RM Cox, ME Gifford, HB

John-Alder, T Langkilde, MJ Angilletta Jr, AD Leaché, M Tollis, K Kusumi, and TS Schwartz. 2021. A chromosome-level genome assembly for the eastern fence lizard (*Sceloporus undulatus*), a reptile model for physiological and evolutionary ecology. GigaScience 10:giab066.

Wiens JJ. 1999. Phylogenetic evidence for multiple losses of a sexually selected character in phrynosomatid lizards. Proceedings of the Royal Society of London B: Biological Sciences 266:1529-1535.

Williams TM and SB Carroll. 2009. Genetic and molecular insights into the development and evolution of sexual dimorphism. Nature Reviews Genetics 10:797-804.

Wintzen M, M Yaar, JPH Burbach, and BA Gilchrest. 1996. Proopiomelanocortin gene product regulation in keratinocytes. Journal of Investigative Dermatology 106:673-678.

Wittkopp PJ and G Kalay. 2012. *Cis*-regulatory elements: molecular mechanisms and evolutionary processes underlying divergence. Nature Reviews Genetics 13:59-69.

Wittman TN, CD Robinson, JW McGlothlin, and RM Cox. 2021. Hormonal pleiotropy structures genetic covariance. Evolution Letters 5:397-407.

Wright AE, TF Rogers, M Fumagalli, CR Cooney, and JE Mank. 2019. Phenotypic sexual dimorphism is associated with genomic signatures of resolved sexual conflict. Molecular Ecology 28:2860-2871.

Yokoyama T, DW Silversides, KG Waymire, BS Kwon, T Takeuchi, and PA Overbeek. 1990. Conserved cysteine to serine mutation in tyrosinase is responsible for the classical albino mutation in laboratory mice. Nucleic Acids Research 18:7293-7298.

Zeileis A and T Hothorn. 2002. Diagnostic checking in regression relationships. R News 2:7-10.

Table 1. Genes selected *a priori* to test hypotheses for species differences in "Tissue sensitivity to testosterone", "melanocortin production and signaling", "mediation of melanin synthesis", and "presence of melanophores. "Tissue sensitivity" includes genes with products that influence androgen metabolism, androgen availability, and androgen receptor availability. "Melanocortin production and signaling" includes genes with products that produce and detect α-melanocyte stimulating hormone. "Mediation of melanin synthesis" includes genes with products that influence melanin synthesis. "Presence of melanophores" includes genes commonly used as molecular markers of melanophores and their cellular precursors. Bolded gene names and predictions indicate instances in which we find statistical support for our predictions.

Hypothesis	Gene	Product and function	Prediction for expression
Tissue sensitivity to testosterone	*CYP19A1*	Aromatase – converts testosterone (T) to estradiol, which cannot bind AR	Higher in *S. virgatus*
	SRD5A1 **SRD5A2** *SRD5A3*	5α-reductase – converts T to more potent androgen 5α-dihydrotestosterone (5α-DHT), which also binds AR	**Higher in *S. undulatus***
Conclusion: *Partial support*	**SHBG**	Sex hormone binding globulin – binds T and prevents androgen signaling	**Higher in *S. virgatus***
	AR	Androgen receptor (AR) – mediates gene expression when bound by T or 5α-DHT	Higher in *S. undulatus*
Melanocortin production and signaling	**POMC**	Proopiomelanocortin (POMC) – precursor to adrenocorticotropic hormone (ACTH) and α-melanocyte stimulating hormone (α-MSH)	**Higher in *S. undulatus*** and/or **upregulated by T in *S. undulatus***
	PCSK1	Prohormone convertase 1 (PC1) – cleaves POMC into ACTH	Higher in *S. undulatus* and/or upregulated by T in *S. undulatus*
	PCSK1N	proSAAS – inhibits PC1	**Lower in *S. undulatus*** and/or downregulated by T in *S. undulatus*
Conclusion: *Partial support*	**PCSK2**	Prohormone convertase 2 – cleaves ACTH into α-MSH	Higher in *S. undulatus* and/or **upregulated by T in *S. undulatus***
	MC1R	Melanocortin-1 receptor – binds ACTH and α-MSH to regulate melanin synthesis	**Higher in *S. undulatus*** and/or upregulated by T in *S. undulatus*
Mediation of melanin synthesis	**TYR**	Tyrosinase – converts tyrosine into melanin precursors	**Higher in *S. undulatus*** and/or **upregulated by T in *S. undulatus***
	TYRP1	Tyrosinase-related protein 1 – stabilizes tyrosinase in melanosomal membranes	**Higher in *S. undulatus*** and/or **upregulated by T in *S. undulatus***
Conclusion: *Strong support*	*OCA2*	P protein – regulates melanosome pH to facilitate melanin synthesis	Higher in *S. undulatus* and/or **upregulated by T in *S. undulatus***
Presence of melanophores	*DCT*	Dopachrome tautomerase – regulates melanophore survival	Not expressed in *S. virgatus*
	KIT	KIT protein – facilitates signaling to regulate cellular processes in melanophores	Not expressed in *S. virgatus*
Conclusion: *No support*	*MITF*	Microphthalmia-associated transcription factor – regulates melanophore processes	Not expressed in *S. virgatus*

Table 2. Sample sizes for each species, sex, and treatment group. We extracted RNA from skin from six individuals per treatment, per sex, per species (48 total). Values here represent the numbers used in analysis after libraries were removed due to low RNA concentrations, low read counts, and visual examination of robustPCA plots.

Species	Control			Testosterone		
	Female	Male	Total	Female	Male	Total
S. undulatus	5	5	10	6	6	12
S. virgatus	5	4	9	5	5	10

Table 3. Results from Gene Ontology enrichment analysis testing for enriched pathways from genes upregulated by testosterone in *S. undulatus* juveniles. Analyses were conducted three times, examining over enrichment of protein-coding genes from three reference species (source of GO terms). Genes listed include all genes represented within nested processes for a term. Genes in bold are represented in more than one biological process. FDR is the *P*-value after correction for False Discovery Rate.

Source of GO terms	Biological process	Fold Enrichment	Genes	FDR
Homo sapiens	Eye pigment biosynthetic process	>100	*EDN3, OCA2, PMEL, RAB27A, SLC45A2, TYR, TYRP1*	0.052
	Peptidoglycan transport	>100	*SLC15A2, SLC15A3*	0.045
	Melanin biosynthetic process	>100	*OCA2, PMEL, SLC45A2, TYR, TYRP1*	<0.001
	Melanocyte differentiation	80	*EDN3, OCA2, RAB27A, TYRP1*	<0.001
Anolis carolinensis	Melanin biosynthetic process	>100	*OCA2, TYR, TYRP1*	0.002
	Melanocyte differentiation	>100	*OCA2, PMEL, RAB27A, TYR*, TYRP1	0.005
	Cellular pigmentation	86	*PMEL, RAB27A, TYRP1*	0.014
Danio rerio	Melanin biosynthetic process	>100	*OCA2, TYR*	0.001
	Melanocyte differentiation	93	*OCA2, SLC45A2, TYR*	<0.001

4000X   10000X

S. undulatus

Male

Female

S. virgatus

Male

Female

2.5µm   1µm

Figure 1.

79
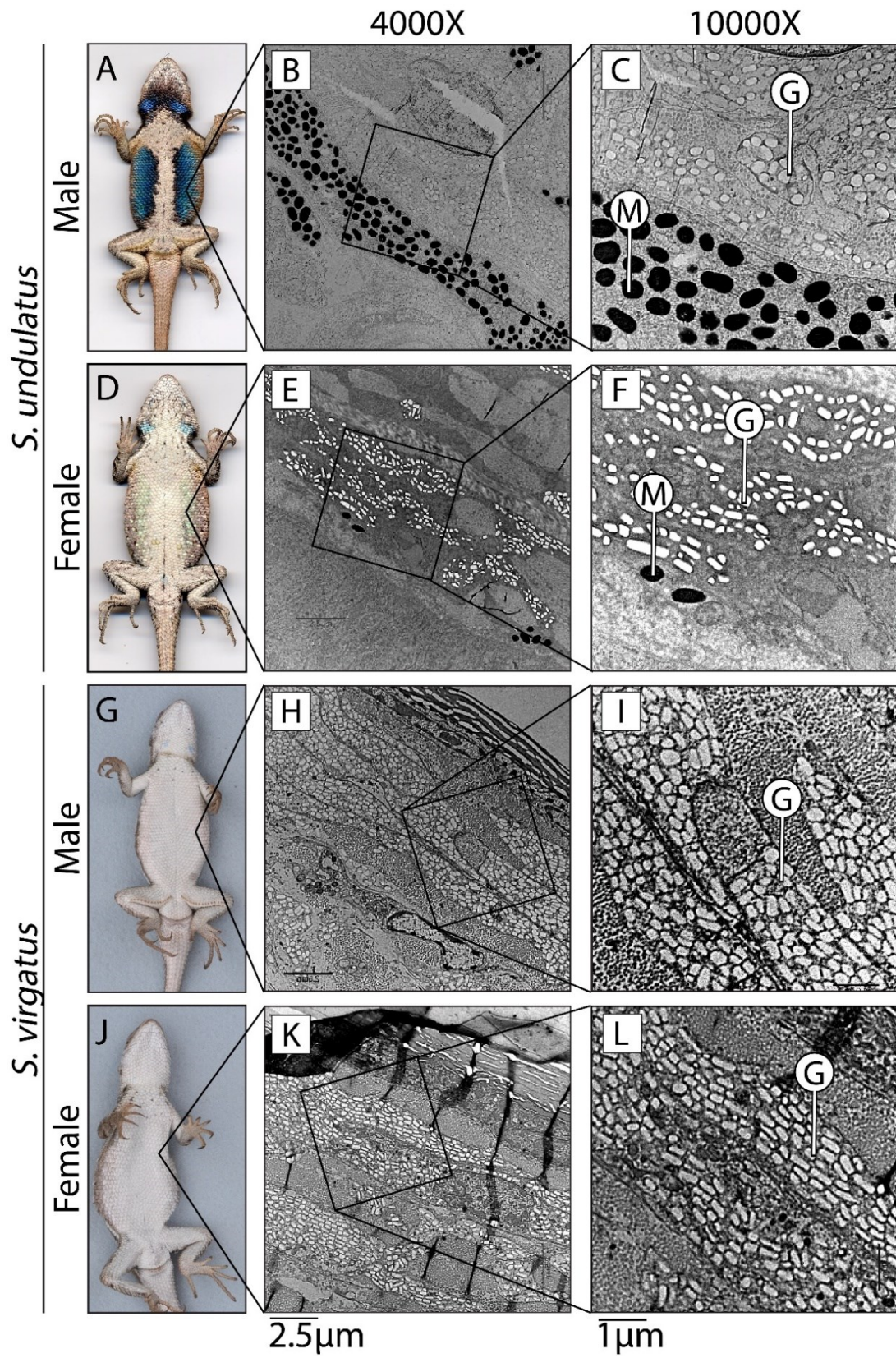
Figure 1. Photographs and transmission electron micrographs of ventral skin in (**A-C**) *S. undulatus* males, (**D-F**) *S. undulatus* females, (**G-I**) *S. virgatus* males, and (**J-L**) *S. virgatus* females. Blue skin in *S. undulatus* males results from reflection of blue light by organized guanine platelets (G) within iridophores, and from absorption of other wavelengths by an underlying layer of melanin-filled melanosomes (M) within melanophores. Organized guanine platelets are present within iridophores of all four groups, but a pronounced melanophore layer of melanin-filled melanosomes is only present in *S. undulatus* males. Images from panels A and D were originally published in Cox et al. (2005a) by the American Society of Ichthyologists and Herpetologists. They are being used under a Creative Commons CC BY license.
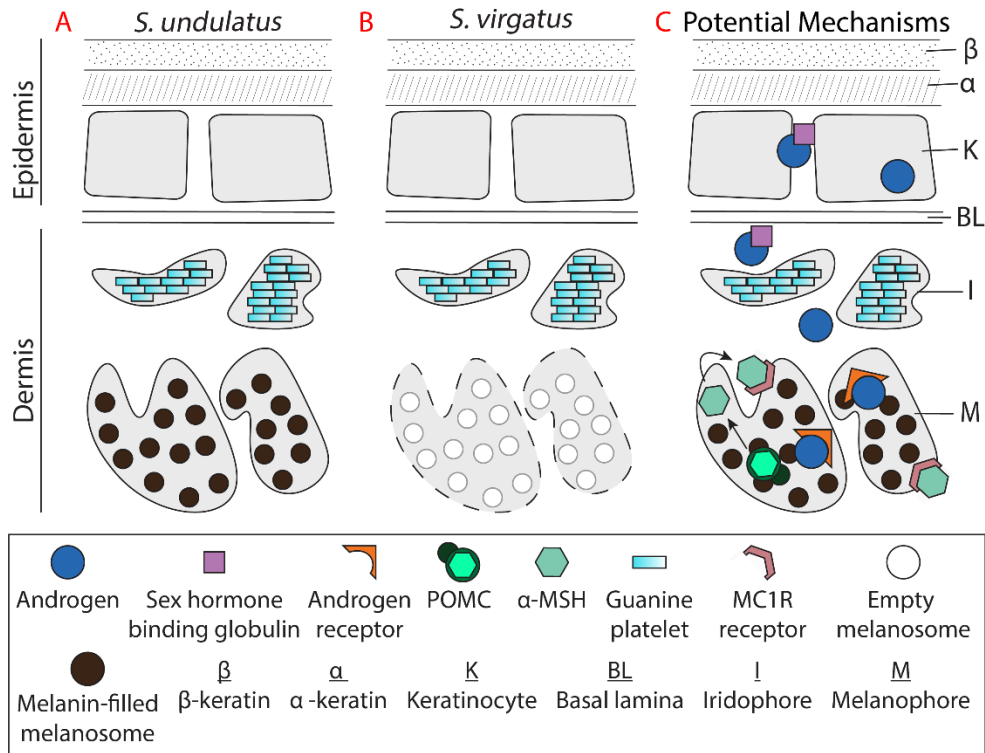
Figure 2. Proposed model of ventral skin in (**A**) *S. undulatus* and (**B**) *S. virgatus*. Adult *S. undulatus* males have a layer of melanized melanophores deep to the iridophore layer, whereas *S. virgatus* males do not. Melanophores in *S. virgatus* are illustrated with dashed lines to indicate that it is unknown whether *S. virgatus* retains unpigmented melanophores in its ventral skin. (**C**) In *S. undulatus*, we hypothesize that free androgens bind the androgen receptor (AR) to induce melanin synthesis via production of proopiomelanocortin (POMC), which is processed into α-melanocyte stimulating hormone (α-MSH) that binds the melanocortin-1 receptor (MC1R) on the surface of melanophores to stimulate melanin synthesis.
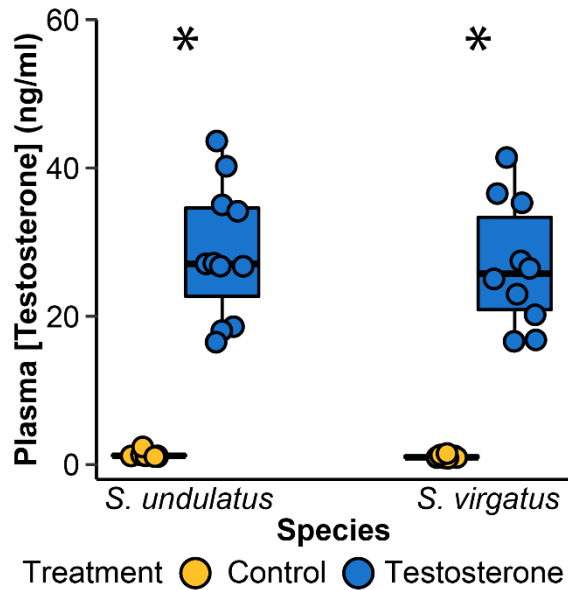
Figure 3. Circulating levels of plasma testosterone for *S. undulatus* and *S. virgatus* at the time of tissue collection, eight weeks after implantation. Each circle is an individual, with boxplots illustrating the median (horizontal line), first and third quartiles (box), and 1.5 times the interquartile range (whiskers) for each treatment group. Hormone implants significantly raised ($P < 0.05$, asterisks) circulating testosterone to similar levels in both species.
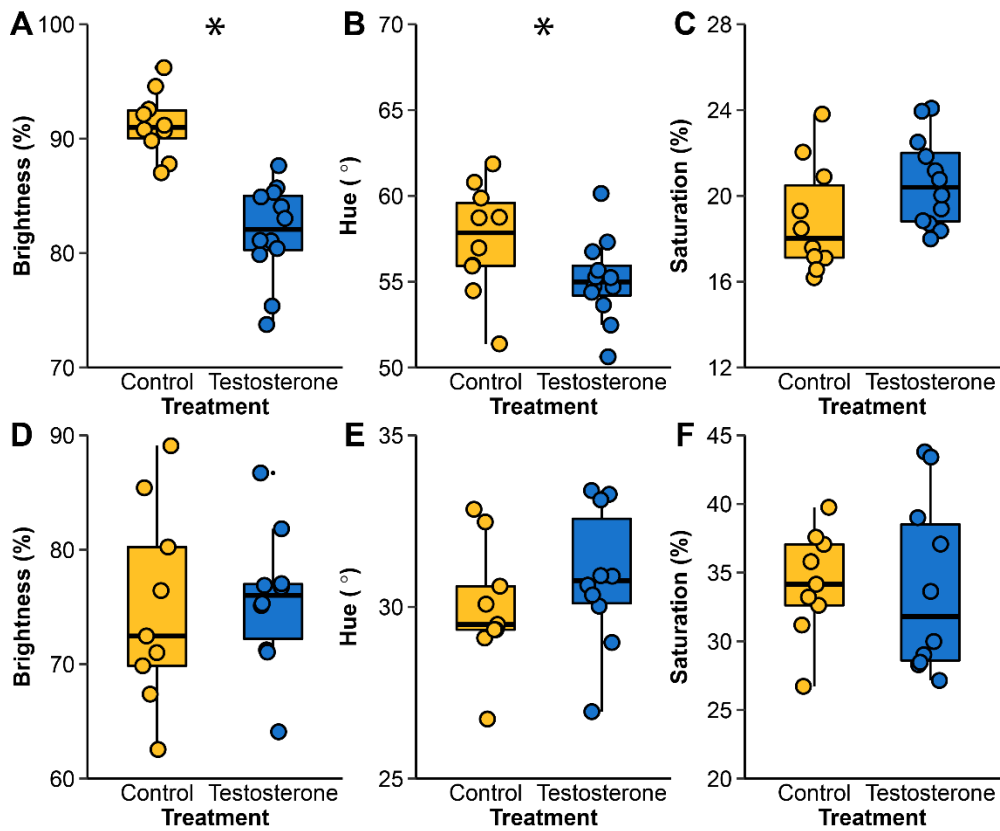
Figure 4. Effects of testosterone on three aspects of ventral color in (**A–C**) *S. undulatus*, and (**D–F**) *S. virgatus*. Each circle is an individual, with boxplots illustrating the median (horizontal line), first and third quartiles (box), and 1.5 time the interquartile range (whiskers) for each treatment group. Testosterone decreased brightness and hue ($P <$ 0.05, asterisks) in *S. undulatus*, but had no effect on coloration in *S. virgatus*.
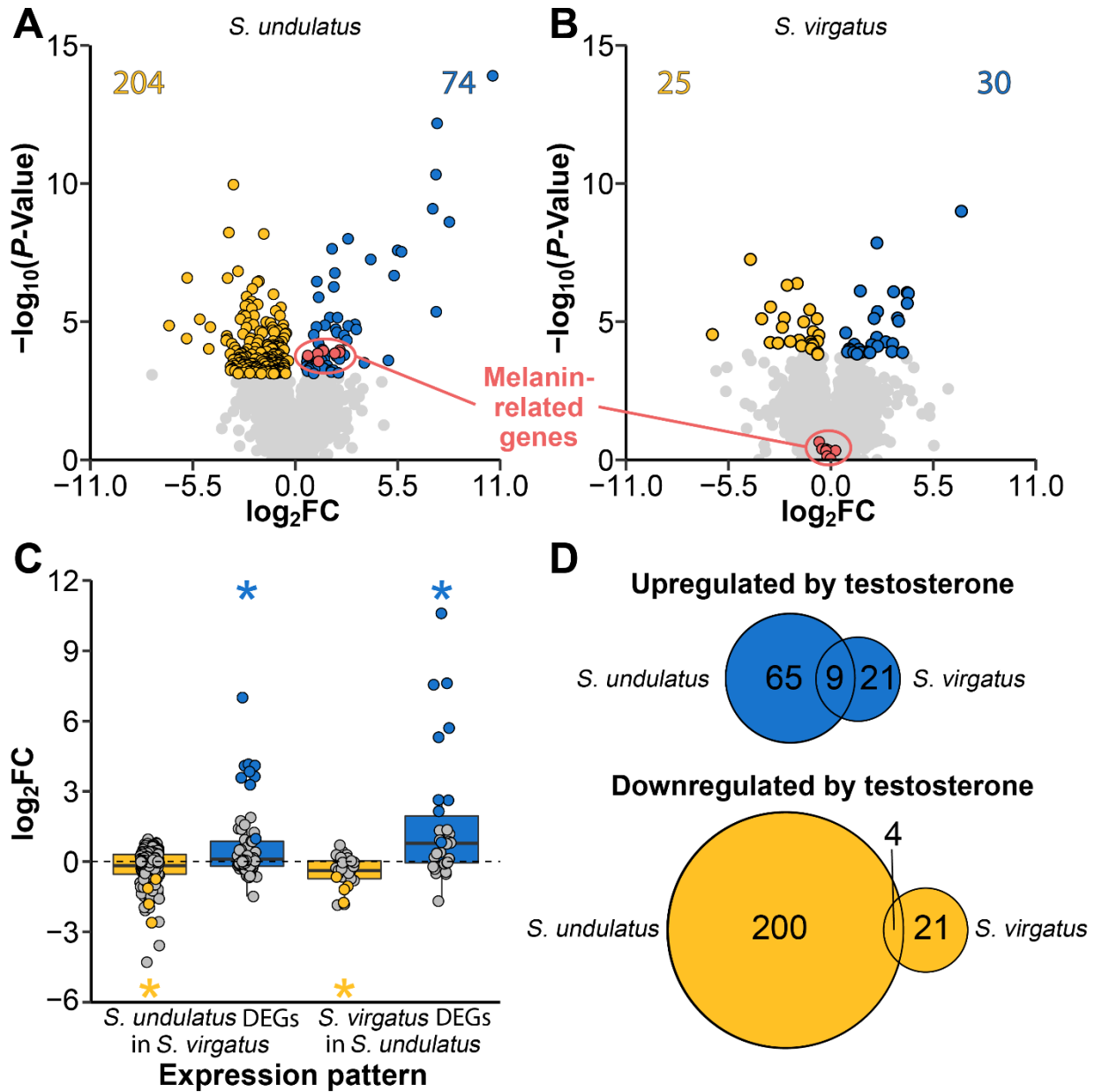
Figure 5. Volcano plots of the -$\log_{10}$ *P*-value for the effect of testosterone on expression against the $\log_2$ fold change (FC) between testosterone and control groups for 18,017 genes (circles) in (**A**) *S. undulatus,* and (**B**) *S. virgatus*. Positive values represent genes upregulated by testosterone while negative values represent genes downregulated by testosterone. Colored symbols and numbers at the top of each panel indicate genes that are significantly differentially expressed between treatment groups after Benjamini-

Hochberg correction. Red symbols represent melanin-related genes identified from GO analyses (Table 3). Gray symbols indicate genes that are not differentially expressed. (**C**) Distributions of $\log_2$FC values in the opposite species for the differentially expressed genes from panels **A-B**, with individual genes plotted as circles and boxplots reporting the median (horizontal line), first and third quartiles (box), and 1.5 times the interquartile range (whiskers) of values in each category. Blue boxplots represent genes that were upregulated by testosterone in panels **A-B**, while yellow boxplots represent genes that were downregulated by testosterone. Colored symbols represent genes that were differentially expressed in both species. Asterisks denote distributions that differ significantly from zero, indicating that effects of testosterone on expression are similar across species. (**D**) Venn diagrams illustrating the number of shared and unique DEGs up- or downregulated by testosterone between *S. undulatus* and *S. virgatus*.
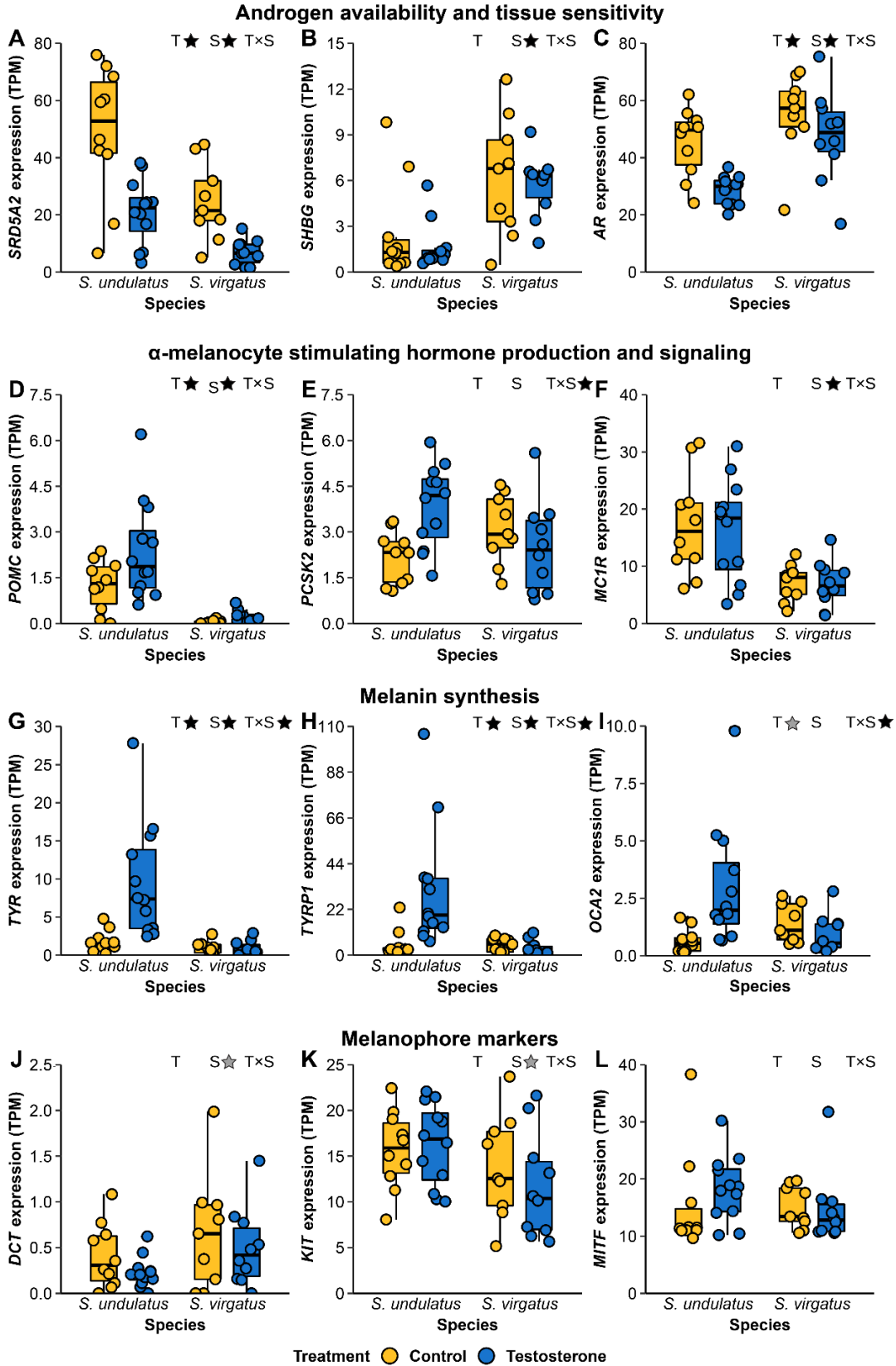
Figure 6.

Figure 6. Gene expression (transcripts per million, TPM) as a function of species and testosterone treatment for nine candidate genes selected *a priori* because of their roles mediating (**A-C**) androgen metabolism, availability, and signaling, (**D-F**) α-melanocyte stimulating hormone production, (**G-I**) production of melanin pigment, and (**J-L**) as molecular markers of melanophores at different stages of development. Boxplots illustrate the median (horizontal line), first and third quartiles (box edges) and 1.5 times the interquartile range (whiskers) for individual values (circles) in each group. Significant terms from ANOVA including hormone treatment (T), species (S), and treatment × species interactions (T×S) are represented by gray stars to the right of each model term when $P < 0.05$ and black stars to the right of each model term when $P_{adj} < 0.05$ (adjusting for multiple comparisons across several genes in a given mechanistic pathway).

Supplementary Methods

Animal collection and husbandry

Animals for the testosterone manipulation experiment were collected from the wild at approximately one month of age. We collected 30 (15 per sex) juvenile *S. undulatus* from Colliers Mills Wildlife Management Area, Jackson Township, NJ (40.07889, -74.43736) on 7 September, 2019, and 42 (21 per sex) juvenile *S. virgatus* from Cochise County, Arizona (31.89834, -109.21800) on 26 September, 2019. We transported animals to the University of Virginia and housed them in a dedicated animal facility. Each animal was housed individually in an 18 x 35 x 27 cm plastic cage with a brick for basking, a petri dish filled with aquarium rocks and deionized water for drinking, sand as a substrate, and a 15-cm segment of PVC pipe as a place to hide. Each cage was placed directly beneath two fluorescent bulbs for ultraviolet light (ReptiSun 10.0 UVB; Zoo Med Laboratories, Inc.) and one 45W incandescent spot bulb (Bulbrite 45W 120V R20 Reflector Bulb) to provide focused heat for basking. Lizards received fresh water daily and 5–7 crickets (*Gryllodes sigillatus,* 0.25-inch size, Ghann's Cricket Farm, Augusta, GA) three times per week. Each week, we rotated cages to mitigate any "shelf" effects arising from thermal stratification. Room lights and UV bulbs were set on a 12:12 light-dark cycle and spot bulbs were set on a second timer to provide 9 h of basking time each day. The room was set at an ambient temperature of 21°C to achieve a thermal gradient of approximately 7°C (range 24°C to 31°C) within each cage when basking lamps were on.

Implant design and surgery

We designed testosterone and control implants following previously published methods (Cox et al. 2015, 2017; Wittman et al. 2021). We constructed slow-release implants from 4 mm pieces of Silastic tubing (Dow Corning, Midland, MI, USA; 0.058 inner diameter x 0.077 outer diameter). We sealed one end of each tube with 100% waterproof silicone gel (General Electric; Boston, MA), allowed it to cure overnight, then added 1 µL of either (1) testosterone dissolved into dimethyl sulfoxide (DMSO) at a concentration of 100 µg µL^{-1} (testosterone implant), or (2) pure DMSO (control implant). We then sealed the other end of the implant with silicone gel and allowed the seal to cure and the DMSO to diffuse through the tubing and evaporate for 5 days, leaving behind 100 µg of crystallized testosterone in the lumen of testosterone implants, or an empty lumen in the case of control implants.

We measured the snout-vent length (nearest mm) and body mass (nearest 0.01 g) of each individual, then divided males and females of each species evenly between testosterone and control treatments while matching treatment groups for body size. We fasted animals for 2 days prior to surgery. Immediately prior to surgery, we administered a 1 µL subcutaneous injection of 0.25% Sensoricaine (Bupivacaine HCl) in the lower abdomen for local anesthesia and analgesia. We then held animals at -20°C for five minutes to immobilize them during surgery, which we performed on a semi-frozen gel pack. We cleaned the lower abdomen with alternating swabs of antiseptic (chlorohexidine gluconate 4% solution) and isopropyl alcohol. Finally, we made a 3-5 mm lateral incision in the lower abdomen, placed the appropriate implant (sterilized in 100% ethanol) into the body cavity, and sealed the incision using cyanoacrylate surgical adhesive

(VetClose®, Butler Schein Animal Health, Dublin, OH, USA). We allowed animals to recover in sterile plastic containers overnight before returning them to their home cages.

Color quantification

Eight weeks after we administered treatments, we took ventral photographs of each animal alongside a color standard (Kodak Gray Scale and Color Control Patches) under standardized lighting conditions (FE30050-10 28W fluorescent photography bulbs in reflecting hoods). Because color is thermally sensitive in *S. undulatus* (Langkilde and Boronow, 2012), we held animals at 30°C for one hour prior to taking photographs. For logistical reasons, we used a different camera for each species, making values comparable within a species, but not between species. Specifically, we used a Canon EOS Rebel T3i with 100 mm macro lens to photograph *S. undulatus*, and a Nikon D750 with a Nikkor AF-S VR 105mm f/2.8G IF-ED lens to photograph *S. virgatus*. We analyzed digital photographs using Fiji (ImageJ 1.52v) software (Schindelin *et al.*, 2012). We first outlined each patch (or the approximate location in which a color patch would develop, for those individuals without a visible phenotype) using the 'polygon' tool, then used the 'color histogram' package to extract mean red, green, and blue (RGB) values within the circumscribed area. We converted these mean RGB values into hue, saturation, and brightness using the *rgb2hsv* function in R v4.2.1 (R Core Team 2022). Hue is the dominant wavelength and is measured on a 360° color wheel. Saturation is a metric of color purity, with 100% representing complete saturation by the dominant color and 0% corresponding to gray. Brightness is a measure of closeness to white, with 100% brightness appearing white and 0% brightness appearing black.

Testosterone quantification

To quantify testosterone concentrations, we used radioimmunoassay following Smith and John-Alder (1999). We extracted samples twice using diethyl ether, dried them under a stream of ultra-filtered air, and reconstituted them in phosphate-buffered saline with gelatin (PBSG). Samples were then assayed using tritiated testosterone as a radiolabel (PerkinElmer Life Science Inc.) and a rabbit-derived testosterone antiserum (1:18,000 dilution). Intra-assay variation was $4.8 \pm 0.7\%$ (mean $\pm$ 1SD), inter-assay coefficient of variation was 6.6%, and the limit of detection was 6.5 pg.

RNA Extraction

We incubated skin tissue in lysis buffer for 10 min at room temperature, then homogenized it using a Qiagen TissueLyser II (Qiagen; Germantown, MD) with 5 mm sterile stainless-steel beads, with two homogenization bouts of two minutes each at 30 hz. We next added 10 µL of 20 mg/ml proteinase-K to the homogenate and incubated at 55°C for five minutes. We filtered the lysate through an RNAspin Mini Filter and centrifuged for 1 min at 11,000 g. We next added 70% ethanol to facilitate RNA binding, then added the lysate to an RNAspin Mini Column and centrifuged for 30 sec at $8000 \times$ g. Next, we added desalting buffer and centrifuged for 1 min at $11,000 \times$ g. We digested DNA in the sample using DNase I and allowed it to incubate for 15 min. We then washed the samples three times to inactivate DNase I with the wash buffer, centrifuging for 1 min at $11,000 \times$ g for the first two washes and for 2 min at $11,000 \times$ g for the third wash. Finally, we eluted RNA in RNase-free water.

Estrogen receptor analyses

To test for differences in estrogen signaling, we analyzed he expression of genes

encoding for estrogen receptor-α (*ESR1*) and estrogen receptor-β (*ESR2*). Each initial

model included sex, species, and treatment, plus all pairwise and three-way interactions.

The sex effect and all interactions with sex were dropped for *ESR2* after likelihood ratio

testing. No *P*-value adjusted were conducted for these analyses.

Supplementary Results

Estrogen receptor

We found that *ESR1* was expressed higher in *S. undulatus* than in *S. virgatus* ($F_{1,33} =$

4.185, $P = 0.049$) with no effect of treatment ($F_{1,33} = 2.40$, $P = 0.131$) or a treatment ×

species interaction ($F_{1,33} = 1.29$, $P = 0.264$; Fig. S3A). Similarly, we found that *ESR2* was

expressed higher in *S. undulatus* than in *S. virgatus* ($F_{1,37} = 18.61$, $P < 0.001$) with no

effect of treatment ($F_{1,37} = 0.01$, $P = 0.914$) or a treatment × species interaction ($F_{1,37} =$

0.10, $P = 0.763$; Fig. S3B).

Supplementary References

Cox CL, AF Hanninen, AM Reedy, and RM Cox. 2015. Female anoles retain responsiveness to testosterone despite the evolution of androgen-mediated sexual dimorphism. Functional Ecology 29:758-767.

Cox RM, CL Cox, JW McGlothlin, DC Card, AL Andrew, and TA Castoe. 2017. Hormonally mediated increases in sex-biased gene expression accompany the breakdown of between-sex genetic correlations in a sexually dimorphic lizard. The American Naturalist 189:315-332.

Langkilde T and KE Boronow. 2012. Hot boys are blue: temperature-dependent color change in male eastern fence lizards. Journal of Herpetology 46:461-465.

Schindelin J, I Arganda-Carreras, E Frise, V Kaynig, M Longair, T Pietzsch, S Peribisch, C Rueden, S Saalfeld, B Schmid, and JY Tinevez. 2012. Fiji: an open-source platform for biological-image analysis. Nature Methods 9:676.

Smith LC and HB John-Alder. 1999. Seasonal specificity of hormonal, behavioral, and coloration responses to within- and between-sex encounters in male lizards (*Sceloporus undulatus*). Hormones and Behavior 36:39-52.

Wittman TN, CD Robinson, JW McGlothlin, and RM Cox. 2021. Hormonal pleiotropy structures genetic covariance. Evolution Letters 5:397-407.

Table S1. Genes upregulated by exogenous testosterone in *S. undulatus* juveniles. Log$_2$FC represents the log$_2$ fold change in gene expression in the testosterone group relative to the control group. Log$_2$CPM represents the log$_2$ expression of each gene in counts per million averaged across all samples. *F* is the *F* statistic and *P*-value is the associated *P*-value, and FDR is the Benjamini-Hochberg corrected *P*-value from differential expression analyses.

Gene Symbol	log$_2$FC	log$_2$CPM	*F*	*P*-Value	FDR
LOC121920525	10.59777	2.906431	196.3842	1.26E-14	2.28E-10
LOC121923632	7.61414	1.176806	115.5032	6.67E-13	6.01E-09
LOC121920490	7.550993	1.540824	84.37299	4.74E-11	2.85E-07
LOC121914138	7.378676	1.262499	78.0442	8.19E-10	2.95E-06
LOC121923236	8.271428	5.043514	63.23469	2.47E-09	7.42E-06
LOC121933055	2.834601	2.237552	54.05269	1.00E-08	2.00E-05
LOC121934418	1.976519	4.558505	50.0807	2.31E-08	4.16E-05
GPR62	5.498249	-1.84896	52.63327	2.64E-08	4.32E-05
GRIN2B	5.702136	-0.36061	52.04443	2.96E-08	4.44E-05
CORIN	4.052551	0.624988	46.09258	5.58E-08	7.73E-05
VIL1	2.125467	1.575031	41.23691	1.73E-07	0.000208
LOC121920489	5.306539	-1.93231	45.60073	2.15E-07	0.000242
OPN5	1.158354	2.141525	38.36422	3.51E-07	0.000316
FXYD7	2.071083	2.055427	36.59465	5.50E-07	0.00045
LOC121937101	1.256227	4.376023	33.29024	1.31E-06	0.000909
LOC121934552	7.567038	-1.1815	53.02688	4.39E-06	0.002325
LOC121926756	1.854091	6.873359	27.40502	7.09E-06	0.003207
LOC121935580	2.269711	4.545647	27.44016	7.12E-06	0.003207
LOC121920288	3.208161	0.216132	26.10459	1.26E-05	0.004893
TSPAN10	1.596572	1.112261	25.19925	1.34E-05	0.004942
TRIM59	2.846274	3.512648	25.17401	1.42E-05	0.005014
NRCAM	1.13544	3.37163	24.75617	1.54E-05	0.005292
PDC	2.17288	2.10583	24.12272	1.88E-05	0.005919
NQO2	3.278233	1.110434	24.07511	1.91E-05	0.005919
XK	2.234383	0.062759	23.28262	2.45E-05	0.006997
ADRA2A	0.992768	3.519246	22.64317	3.00E-05	0.007953
LOC121927973	2.618058	1.070954	22.52724	3.12E-05	0.008136
LOC121917984	2.771892	0.974941	21.24639	4.73E-05	0.011217
FGF9	1.251672	2.160089	20.50946	6.04E-05	0.013187
LOC121923332	1.459066	1.932858	18.97811	0.000102	0.017623
TYRP1	2.39004	3.444518	18.95008	0.000106	0.018039
MLANA	1.511769	3.663855	18.67858	0.000113	0.018859

TYR	2.384181	1.5501	18.30643	0.000129	0.020702
B4GALNT2	2.148785	-0.34922	18.10573	0.000138	0.021593
OCA2	2.123274	1.513302	18.06125	0.00014	0.021744
PMEL	1.206461	7.363531	18.01145	0.000143	0.021775
LOC121920008	1.588437	4.71813	17.90286	0.00015	0.022225
LOC121921684	2.635588	2.756634	17.73257	0.000161	0.023072
RAB27A	0.674349	6.36236	17.54542	0.000168	0.023744
RXFP1	2.206855	-0.56255	17.37443	0.000179	0.024936
PCSK6	0.676558	4.551088	17.2341	0.000188	0.025505
GPD1L	0.65192	5.935812	17.09408	0.000197	0.025863
LOC121927137	2.37834	0.717534	16.74088	0.000224	0.027544
LOC121933040	1.560222	-0.51471	16.62954	0.000233	0.027843
LOC121919397	0.865653	4.979768	16.59513	0.000236	0.028007
LOC121918884	4.997434	1.297479	17.00665	0.000252	0.028392
TRPM1	0.842353	4.720591	16.41641	0.000252	0.028392
SLC15A2	1.409892	3.691603	16.36523	0.000257	0.028801
SLC45A2	1.251457	2.023172	16.19434	0.000273	0.0301
SIM2	0.973218	2.863183	16.18662	0.000274	0.0301
PLCL1	0.625029	3.338973	16.14452	0.000278	0.0301
CFI	3.706253	3.709781	16.05341	0.00031	0.031887
CEACAM5	0.823274	4.361642	15.70154	0.000328	0.032592
PCDH17	1.011171	3.073211	15.52416	0.00035	0.033541
FMN1	0.755507	4.432719	15.4485	0.00036	0.034035
EDN3	0.698631	5.493425	15.36388	0.000371	0.034035
LOC121922615	1.71931	-0.46539	15.21859	0.000392	0.035153
LOC121936217	1.265172	1.74215	15.12729	0.000406	0.036128
C2H3orf18	0.886192	3.144261	14.976	0.000429	0.036673
AP3M2	0.585228	3.842565	14.94724	0.000434	0.036897
LOC121933036	1.443606	2.9666	14.88665	0.000444	0.037173
FAM43B	1.368857	4.161524	14.87588	0.000448	0.037173
LOC121935237	1.521461	5.576409	14.80528	0.000468	0.037984
SLC15A3	0.764674	3.2313	14.73599	0.00047	0.037984
LRRC38	1.418386	2.42395	14.70629	0.000475	0.038241
TAFA4	1.526695	0.628703	14.60688	0.000494	0.03909
DIXDC1	1.038771	4.981867	14.48484	0.000517	0.040444
LOC121936725	0.733022	2.827038	14.44342	0.000525	0.040444
RTN4RL1	1.938594	-1.58306	14.2539	0.000565	0.042516
LRP1B	2.048997	-0.15839	14.23422	0.000569	0.042516
LOC121935044	0.661273	3.737105	14.0481	0.000611	0.043528
LOC121937354	1.936987	-1.55152	13.81665	0.000668	0.045926
CDHR3	2.315702	-0.69485	13.87598	0.000711	0.047813
ESM1	0.9874	1.295491	13.52941	0.000746	0.049109

Table S2. Genes downregulated by exogenous testosterone in *S. undulatus* juveniles. Log$_2$FC represents the log$_2$ fold change in gene expression in the testosterone group relative to the control group. Log$_2$CPM represents the log$_2$ expression of each gene in counts per million averaged across all samples. *F* is the *F* statistic and *P*-value is the associated *P*-value, and FDR is the Benjamini-Hochberg corrected *P*-value from differential expression analyses.

Gene symbol	log$_2$FC	log$_2$CPM	*F*	*P*-Value	FDR
LOC121934528	-3.31781	1.187045	78.93052	1.09E-10	4.93E-07
LOC121926170	-3.56409	4.870808	57.29161	5.96E-09	1.50E-05
IDI1	-1.6888	6.775612	56.0413	6.68E-09	1.50E-05
DHCR24	-3.07104	9.399493	42.26652	1.49E-07	0.000192
LOC121926006	-5.79894	4.935612	40.50559	2.61E-07	0.000265
LOC121929382	-3.63017	8.953421	40.08234	2.65E-07	0.000265
LOC121929303	-1.94964	4.295516	38.5027	3.41E-07	0.000316
LOC121929338	-2.03651	1.096194	38.1565	3.70E-07	0.000317
ATP2C2	-2.3035	3.088976	35.98832	6.43E-07	0.000504
STRIP2	-1.16886	5.929713	34.22959	1.02E-06	0.000766
LOC121915560	-2.61523	3.435407	33.59995	1.25E-06	0.000897
DNAH7	-2.34167	1.698759	32.03089	1.85E-06	0.001234
SLCO4C1	-2.01701	4.758464	31.23885	2.37E-06	0.001479
FOXN1	-2.52358	5.03536	31.38043	2.38E-06	0.001479
CSMD2	-2.67752	3.316251	30.8098	2.68E-06	0.001611
DBF4	-0.77116	4.827638	30.26778	3.02E-06	0.001756
SLC3A1	-2.33225	0.257753	29.94781	3.31E-06	0.001862
SYTL2	-1.05179	6.198807	29.22679	4.06E-06	0.002219
LOC121916912	-2.78797	6.692323	28.32663	5.83E-06	0.002957
CENPW	-2.21303	2.007757	27.85013	6.06E-06	0.002957
LANCL1	-0.81979	6.048322	27.84406	6.07E-06	0.002957
LOC121915301	-2.67562	1.794923	27.71977	6.30E-06	0.002988
CENPF	-2.94098	4.221216	27.1819	8.04E-06	0.003494
LOC121915080	-5.12457	-0.92719	26.85323	8.14E-06	0.003494
MCM5	-1.56077	5.647543	26.13042	1.03E-05	0.004295
LOC121915433	-2.50384	5.992445	26.07241	1.12E-05	0.004476
LPAR3	-1.32174	2.861279	25.80237	1.12E-05	0.004476
LOC121926693	-2.2409	5.021003	25.53943	1.28E-05	0.004893
AR	-0.64214	7.50211	25.24643	1.32E-05	0.004942
LOC121929284	-6.7734	4.073415	26.88751	1.38E-05	0.004981

ANKRD33	-4.55832	-2.07577	24.69539	1.57E-05	0.005292
LOC121934888	-1.21349	4.329273	24.6628	1.59E-05	0.005292
SOAT2	-2.62674	2.894465	24.66623	1.63E-05	0.005333
ADAMTS7	-0.65551	5.553597	24.21854	1.82E-05	0.00586
EDARADD	-1.19754	3.396728	23.86974	2.03E-05	0.006205
SLC66A3	-0.95425	5.606918	23.64203	2.18E-05	0.006532
FANCI	-1.89804	3.354572	23.62379	2.21E-05	0.006532
PRXL2A	-1.12325	6.903357	23.33558	2.41E-05	0.006991
CENPX	-1.76072	2.662634	23.19804	2.51E-05	0.007075
TRERF1	-0.48013	5.647644	23.07719	2.61E-05	0.00724
LOC121920314	-2.8008	3.534909	23.0424	2.80E-05	0.007573
SMS	-0.53705	6.664165	22.84161	2.82E-05	0.007573
LOC121927235	-3.67397	-0.28585	22.38712	3.26E-05	0.00839
LOC121923013	-0.60357	3.299837	21.80159	3.94E-05	0.009965
KIF2C	-2.39139	1.847074	21.77839	3.98E-05	0.009965
LOC121922333	-5.8283	-1.16728	23.99658	4.08E-05	0.010063
LOC121936001	-3.64118	3.111545	21.76909	4.27E-05	0.0104
PNLDC1	-1.96601	-0.36883	21.31591	4.62E-05	0.011108
LOC121932914	-3.70734	-1.52597	21.88282	4.81E-05	0.011259
LOC121920538	-1.18698	3.234663	21.0622	5.03E-05	0.011615
MIS18BP1	-2.44339	2.4314	20.98966	5.23E-05	0.011921
JPH4	-0.71149	5.239015	20.90238	5.30E-05	0.011942
MTFR2	-2.02543	1.454604	20.53575	5.99E-05	0.013187
IL17RD	-0.86979	3.641835	20.49461	6.08E-05	0.013187
EXO1	-3.40237	2.166066	20.54481	6.21E-05	0.013317
LRAT	-1.49757	0.184301	20.23519	6.63E-05	0.014049
CPNE9	-1.16044	3.77437	20.10023	6.94E-05	0.014532
LOC121925291	-1.4862	4.035098	20.05829	7.06E-05	0.01463
NTN4	-0.91594	4.184355	20.0063	7.16E-05	0.014659
LOC121923220	-0.86026	6.420818	19.95861	7.28E-05	0.01473
ADAMTS17	-1.04581	4.784807	19.90584	7.41E-05	0.014829
BRCA2	-1.44948	3.907371	19.6461	8.10E-05	0.01589
RASAL3	-1.00434	5.0768	19.63779	8.11E-05	0.01589
LOC121929088	-0.98374	6.013372	19.54884	8.36E-05	0.016203
LOC121925156	-3.2442	0.106715	19.49528	8.52E-05	0.01621
FMO5	-0.69267	5.767938	19.48526	8.55E-05	0.01621
LOC121916175	-2.15564	-0.29605	19.41116	8.77E-05	0.016452
B4GALNT4	-0.803	3.060866	19.34934	8.95E-05	0.016576
KCNIP2	-1.18986	1.95214	19.32906	9.02E-05	0.016576
CDCA7	-1.18291	5.38442	19.22236	9.36E-05	0.01698
POC1B	-1.25035	1.093784	19.19558	9.44E-05	0.01698
DIRAS3	-1.24152	1.213874	19.15154	9.58E-05	0.01698
LOC121931392	-4.64055	3.367784	19.31419	9.61E-05	0.01698
KIFC1	-2.56454	3.027629	19.19169	9.78E-05	0.0171
MST1R	-0.60046	5.698714	18.87945	0.000105	0.018039

KIF18A	-3.15407	0.864306	18.72209	0.000112	0.018816
PRC1	-1.53387	4.575022	18.53531	0.00012	0.01986
ESPL1	-2.15787	3.176305	18.49434	0.000123	0.020109
SKA3	-2.7343	1.798926	18.41846	0.000125	0.020326
LOC121918980	-1.85155	4.22348	18.28498	0.000133	0.021079
COL10A1	-2.88398	0.495082	18.19932	0.000133	0.021079
LOC121918466	-1.12838	1.093985	18.0122	0.000142	0.021775
CCNA2	-2.88336	2.84398	18.08485	0.000145	0.021912
CCNB3	-3.48041	2.526631	18.05867	0.000147	0.022093
G2E3	-2.34019	1.903753	17.86759	0.000151	0.022225
LOC121934762	-0.85352	4.011592	17.83285	0.000152	0.022225
LAYN	-1.15914	2.339816	17.80704	0.000153	0.022248
ASPM	-3.0169	3.264785	17.86238	0.000158	0.022804
EHHADH	-0.91204	6.646132	17.53385	0.000169	0.023744
PIF1	-2.58445	0.695017	17.28383	0.000184	0.025505
TENM2	-1.21008	1.872338	17.24506	0.000187	0.025505
LOC121933223	-2.63491	1.919723	17.26392	0.000188	0.025505
NEIL3	-1.50177	1.74376	17.20398	0.00019	0.025513
LOC121925924	-1.37942	4.102772	17.15636	0.000194	0.025848
KIF20A	-2.79768	3.39915	17.24489	0.000196	0.025863
MELK	-3.01666	1.068663	17.11373	0.000198	0.025863
ANO9	-0.65458	6.318616	17.00811	0.000204	0.026385
LOC121915775	-2.03986	10.85602	17.07047	0.000207	0.026434
CDCA8	-1.53928	2.90144	16.96323	0.000207	0.026434
CCNB1	-2.88074	3.143777	17.05449	0.000209	0.02657
LOC121931904	-0.57697	9.00909	16.78949	0.00022	0.027544
LOC121936079	-1.45863	5.234503	16.81025	0.000222	0.027544
RNF32	-1.63992	0.73937	16.72572	0.000225	0.027544
LOC121929282	-2.16722	1.946815	16.72812	0.000226	0.027544
PKMYT1	-1.21692	3.687755	16.71485	0.000226	0.027544
LOC121937485	-3.07597	4.115474	16.87594	0.000229	0.027737
KIF11	-3.30904	3.940527	16.84778	0.000233	0.027843
CDC20	-3.31651	2.074756	16.65697	0.00024	0.028225
LOC121926535	-0.84743	5.298243	16.51022	0.000244	0.028392
CKAP2	-3.02767	2.524842	16.60434	0.000245	0.028392
LOC121916229	-0.92577	5.127782	16.45947	0.000248	0.028392
SLC15A1	-1.82712	5.779304	16.54474	0.00025	0.028392
LOC121916828	-1.28838	2.881793	16.41736	0.000252	0.028392
MAP3K1	-0.36959	5.983294	16.30721	0.000262	0.029179
PBK	-1.51906	2.435024	16.16953	0.000276	0.0301
KIF14	-2.85673	1.70365	16.1884	0.000279	0.0301
LOC121929619	-0.95688	3.738649	16.11293	0.000282	0.030209
LOC121933112	-1.49155	2.986084	16.05693	0.000288	0.030485
GTSE1	-1.72551	2.202438	16.05578	0.000288	0.030485
RACGAP1	-2.7503	2.618916	16.11354	0.00029	0.030598

GAREM2	-1.35854	0.901324	15.93756	0.0003	0.031468
C2H1orf112	-0.92608	3.938215	15.91192	0.000303	0.031583
LOC121929955	-3.02911	-2.08307	16.14939	0.000309	0.031887
RAD51C	-1.2585	3.995671	15.81878	0.000314	0.032155
YDJC	-1.11964	2.453082	15.7793	0.000318	0.032267
CDCA2	-2.30107	2.116838	15.80512	0.000319	0.032267
BARD1	-0.86388	4.612639	15.75699	0.000321	0.032267
PRR11	-2.24446	1.356195	15.75024	0.000322	0.032267
LOC121915687	-1.42439	2.495278	15.68918	0.000329	0.032592
PLK1	-2.76245	2.304165	15.72277	0.000334	0.032691
COL14A1	-1.66037	5.66286	15.71885	0.000335	0.032691
LOC121926428	-2.32489	-1.15445	15.63673	0.000336	0.032691
LOC121932546	-3.3197	0.550302	15.63816	0.000339	0.032811
MID1	-0.59499	4.796562	15.58193	0.000343	0.033005
BUB1	-2.79725	3.098279	15.58924	0.000355	0.033879
TTC13	-0.84201	4.845944	15.43253	0.000362	0.034035
ESCO2	-1.32375	3.610511	15.41465	0.000365	0.034035
LOC121927093	-0.96518	5.607679	15.40192	0.000366	0.034035
TOP2A	-2.78695	4.731926	15.56669	0.000368	0.034035
WDHD1	-0.88977	3.306347	15.36445	0.000371	0.034035
IQGAP3	-2.57763	3.4738	15.46556	0.000372	0.034035
OIP5	-2.52471	-0.12596	15.28777	0.000382	0.034775
LOC121924074	-3.2765	2.92643	15.38614	0.000387	0.03504
POF1B	-0.62543	10.71061	15.23913	0.000389	0.035058
SH3GL3	-1.15843	1.922189	15.10675	0.000409	0.036128
LOC121934537	-2.10902	8.01246	15.20159	0.000411	0.036128
LOC121936788	-1.37371	1.276734	15.0903	0.000411	0.036128
LOC121925481	-1.56671	6.844206	15.14355	0.000413	0.036128
INHBB	-1.52482	2.871272	15.04771	0.000418	0.036352
OLIG1	-3.46842	-1.46544	15.0376	0.00042	0.036352
CENPI	-2.22886	1.712242	15.01683	0.000425	0.036605
C7H1orf167	-2.1671	0.197086	14.98788	0.000428	0.036673
LOC121932011	-2.29465	5.357469	15.05643	0.000439	0.037104
NUF2	-2.77914	2.425281	14.95538	0.000445	0.037173
TPX2	-2.39987	3.42066	14.97104	0.000446	0.037173
LOC121926779	-2.07654	3.968605	14.93122	0.000451	0.03726
FAM171B	-0.69622	4.235394	14.79448	0.00046	0.037833
NUSAP1	-2.51787	3.485794	14.84125	0.000469	0.037984
LPIN3	-1.24033	6.456235	14.76552	0.00047	0.037984
CEP192	-0.56964	5.358369	14.67072	0.000482	0.038587
LOC121926999	-3.37266	-0.22559	14.66002	0.000486	0.038712
FANCA	-2.15514	2.341686	14.62971	0.000495	0.03909
PHGDH	-0.99121	7.139815	14.57528	0.0005	0.039309
LOC121923062	-1.81448	-0.28058	14.46733	0.000521	0.040444
LOC121923710	-3.02001	5.064555	14.62213	0.000524	0.040444

CDHR4	-1.96185	0.896709	14.4441	0.000525	0.040444
NUAK2	-0.73989	4.85511	14.42787	0.000528	0.040511
MXD3	-2.62115	1.706266	14.45142	0.000531	0.040542
LOC121933639	-3.38385	-0.72465	14.40263	0.000533	0.040557
FANCM	-0.98386	3.096697	14.33871	0.000547	0.041382
LOC121914514	-1.4138	4.380179	14.24947	0.000571	0.042516
PIMREG	-3.46765	0.296187	14.24365	0.000572	0.042516
PTTG1	-1.89098	1.597867	14.21346	0.000573	0.042516
AURKA	-2.40082	1.232734	14.19526	0.000579	0.042766
ATAD2	-1.12131	4.111023	14.17671	0.000582	0.042766
LOC121931691	-0.94426	6.339607	14.11063	0.000596	0.043528
PSRC1	-3.23559	-0.18252	14.10898	0.000598	0.043528
MYBL1	-1.16083	1.989615	14.09561	0.0006	0.043528
NCAPG	-2.36732	2.832569	14.13684	0.000605	0.043528
SOX7	-0.98075	5.611459	14.04991	0.000611	0.043528
FAM53B	-0.57071	6.135509	14.04256	0.000612	0.043528
POC1A	-0.78907	2.498836	14.03785	0.000613	0.043528
DNAAF1	-1.75278	-0.0294	14.03653	0.000614	0.043528
TPK1	-0.79962	2.630778	14.01369	0.000619	0.043739
LOC121933666	-1.36066	3.940032	13.99079	0.000627	0.044131
LOC121922034	-1.21198	2.473392	13.95524	0.000633	0.044143
TACC3	-2.29385	2.49609	14.00117	0.000633	0.044143
DTD2	-0.70921	2.028863	13.9493	0.000635	0.044143
HMMR	-2.52871	2.40169	13.97952	0.000641	0.044408
RASSF10	-1.45004	2.722752	13.87627	0.000653	0.045054
ECT2	-3.00393	2.285531	13.88162	0.000672	0.046038
LOC121915977	-0.76801	2.243763	13.77525	0.000679	0.046313
LOC121915297	-1.72977	4.888741	13.82865	0.000682	0.046385
LOC121927228	-2.75459	0.93885	13.74598	0.000691	0.046667
UBE2C	-2.10788	1.602918	13.73472	0.000692	0.046667
FAM131B	-1.08437	1.122437	13.61425	0.000722	0.048375
LOC121937179	-2.43944	1.654393	13.61936	0.000727	0.048522
PAQR4	-1.02045	5.873778	13.57823	0.000734	0.048807
RASSF1	-0.51223	5.851579	13.5425	0.000743	0.049109
PCSK1N	-1.1096	1.654504	13.52802	0.000747	0.049109
ANKDD1B	-1.31427	3.804701	13.5236	0.000751	0.049171
LOC121929179	-3.05986	-1.35959	13.49272	0.000757	0.049383
LOC121932163	-1.82466	4.267011	13.54963	0.000759	0.049383
LOC121936561	-1.15081	7.353263	13.47665	0.000765	0.049557

Table S3. Genes upregulated by exogenous testosterone in *S. virgatus* juveniles. Log$_2$FC represents the log$_2$ fold change in gene expression in the testosterone group relative to the control group. Log$_2$CPM represents the log$_2$ expression of each gene in counts per million averaged across all samples. *F* is the *F* statistic and *P*-value is the associated *P*-value, and FDR is the Benjamini-Hochberg corrected *P*-value from differential expression analyses.

Gene symbol	log$_2$FC	log$_2$CPM	*F*	*P*-Value	FDR
LOC121920525	7.001869	2.906431	76.62819	1.01E-09	1.82E-05
SCARB1	2.468346	5.941564	52.51064	1.41E-08	0.000127
LOC121935802	1.576765	2.248372	35.28213	7.73E-07	0.001903
ASPHD1	3.364983	-0.27991	35.03028	8.26E-07	0.001903
LOC121923632	4.090305	1.176806	34.77718	8.83E-07	0.001903
LOC121927973	4.153894	1.070954	34.4966	9.51E-07	0.001903
LOC121921684	4.098634	2.756634	31.6359	2.18E-06	0.003934
LOC121920741	2.503257	1.420248	29.01823	4.32E-06	0.005981
GRIN2B	3.57778	-0.36061	28.26079	7.39E-06	0.007855
SNX31	2.317904	1.715916	27.07124	7.63E-06	0.007855
LOC121920490	3.632132	1.540824	26.3341	9.56E-06	0.009066
SOX9	0.799359	7.315309	23.16917	2.54E-05	0.019869
HSD11B2	2.460629	1.297461	22.00811	3.69E-05	0.025543
LOC121918783	2.945907	0.112867	24.81752	5.38E-05	0.031263
LOC121928095	3.311558	-2.19848	22.44877	6.27E-05	0.03278
ZC3H12A	1.251573	5.239516	20.25181	6.59E-05	0.032986
IL17RB	2.194198	2.90888	20.18233	6.79E-05	0.033044
LOC121928897	2.509998	0.467754	19.7876	7.71E-05	0.034731
CEACAM5	0.978073	4.361642	19.10873	9.72E-05	0.041399
TLL1	1.496856	3.944031	19.06279	9.88E-05	0.041399
ASIC1	1.05495	3.084706	18.81338	0.000108	0.044095
B4GALNT2	3.278504	-0.34922	18.48073	0.000121	0.046004
LOC121932976	1.931837	2.13239	18.43316	0.000123	0.046004
CDKN2D	0.890978	2.84922	18.41922	0.000123	0.046004
HMGA2	1.222355	6.025239	18.30986	0.000128	0.046004
SLCO2A1	1.606476	6.119849	18.3542	0.000129	0.046004
LOC121920489	3.842305	-1.93231	19.51096	0.000129	0.046004
SDR42E2	2.064474	0.535094	18.23502	0.000132	0.046004
LOC121932389	2.094457	3.248826	18.24737	0.000133	0.046004
MMP9	1.399807	3.636249	17.89334	0.000149	0.049555

**Table S4.** Genes downregulated by exogenous testosterone in *S. virgatus* juveniles. Log$_2$FC represents the log$_2$ fold change in gene expression in the testosterone group relative to the control group. Log$_2$CPM represents the log$_2$ expression of each gene in counts per million averaged across all samples. *F* is the *F* statistic and *P*-value is the associated *P*-value, and FDR is the Benjamini-Hochberg corrected *P*-value from differential expression analyses.

| Gene symbol	log2FC	log$_2$CPM	*F*	*P*-Value	FDR
LOC121936095	-4.31963	0.853992	46.11022	5.56E-08	0.000334
KCNIP2	-1.80893	1.95214	37.71289	4.14E-07	0.001731
SPIRE2	-2.34829	2.939999	37.12358	4.80E-07	0.001731
WNT16	-3.23939	3.039412	30.52876	2.93E-06	0.004794
SYTL2	-1.14025	6.198807	29.57591	3.68E-06	0.005521
HSDL1	-2.50152	6.592025	27.43895	7.33E-06	0.007855
ADAMTS7	-0.74584	5.553597	26.99276	7.81E-06	0.007855
LOC121915612	-3.71523	0.613754	26.97779	7.85E-06	0.007855
SCUBE3	-1.4619	5.513464	26.10533	1.02E-05	0.009194
DNAAF1	-2.60662	-0.0294	24.62855	1.60E-05	0.013754
EDAR	-0.94873	3.496179	23.49686	2.29E-05	0.018719
LOC121930116	-6.35997	9.842756	23.12936	2.91E-05	0.021871
LAMA5	-0.64344	6.299943	22.53631	3.11E-05	0.022389
LOC121914699	-1.70499	4.74315	21.34265	4.65E-05	0.031006
LRRK2	-0.71796	5.830745	20.98228	5.16E-05	0.031263
KIF1A	-2.17966	1.978357	20.96771	5.19E-05	0.031263
LOC121937448	-1.09177	1.176666	20.91768	5.28E-05	0.031263
LOC121920291	-3.25916	-0.63995	22.82999	5.63E-05	0.031704
SYT5	-2.83684	-0.29257	20.55168	5.96E-05	0.032541
LOC121935103	-1.03141	5.162886	20.35424	6.37E-05	0.03278
SEMA5A	-0.96839	5.621493	19.97173	7.24E-05	0.034347
SLC1A7	-1.57603	1.255599	19.86872	7.50E-05	0.034655
LOC121932263	-1.05216	3.358006	19.19128	9.45E-05	0.041399
DENND2A	-0.71522	3.903168	18.13156	0.000137	0.04643
NEO1	-0.70854	6.35461	17.82106	0.000152	0.049912

Table S5. Results from Gene Ontology enrichment analysis testing for pathways enriched with genes that were downregulated by testosterone in *S. undulatus* juveniles. Analyses were conducted three times, examining enrichment of protein-coding genes from three reference species (source of GO terms). FDR represents the *P*-value after False Discovery Rate correction.

Source of GO terms	Biological process	Fold Enrichment	FDR
Homo sapiens	Spermine biosynthetic process	>100	0.048
	Mitotic spindle midzone assembly	40.99	0.013
	Positive regulation of ubiquitin protein ligase activity	40.99	0.013
	Regulation of attachment of spindle microtubules to kinetochore	33.40	0.002
	Kinetochore assembly	30.06	0.027
	Meiotic spindle organization	28.18	0.031
	Seminiferous tubule development	28.18	0.031
	Mitotic chromosome condensation	26.52	0.036
	Resolution of meiotic recombination intermediates	25.05	0.040
	Mitotic spindle assembly checkpoint signaling	24.24	<0.001
	Mitotic metaphase plate congression	23.57	<0.001
	Interstrand cross-link repair	18.33	0.002
	Female meiotic nuclear division	17.68	0.015
	Sister chromatid cohesion	15.65	0.004
	G2/M transition of mitotic cell cycle	15.55	<0.001
	Regulation of cell cycle checkpoint	15.34	0.004
	Mitotic cytokinesis	14.84	<0.001
	Male meiotic nuclear division	14.18	0.006
	Regulation of mitotic spindle organization	13.66	0.034
	Positive regulation of cytokinesis	13.36	0.036
	Replication fork processing	12.79	0.041
	Regulation of G2/M transition of mitotic cell cycle	12.27	<0.001
	Centrosome cycle	10.02	0.006
	Regulation of cyclin-dependent protein serine/threonine kinase activity	9.15	0.003
	Regulation of microtubule polymerization or depolymerization	8.64	0.042
	Microtubule bundle formation	7.16	0.031
Anolis carolinensis	Meiotic spindle organization	62.02	0.011
	Spindle elongation	55.13	0.013
	Mitotic spindle assembly	32.01	<0.001
	Mitotic metaphase plate congression	26.46	0.009
	Regulation of cytokinesis	21.57	<0.001
	Mitotic cytokinesis	17.41	0.030

	Meiotic nuclear division	13.95	<0.001
	Regulation of nuclear division	12.34	0.020
	Regulation of microtubule cytoskeleton organization	10.21	0.042
	Positive regulation of cell cycle process	9.73	0.004
	DNA recombination	7.35	0.047
	Regulation of mitotic cell cycle	5.56	0.031
	Positive regulation of protein modification process	4.12	0.045
Danio rerio	Kinetochore organization	60.62	0.007
	Centromere complex assembly	53.89	<0.001
	Metaphase plate congression	45.47	0.013
	Meiotic chromosome separation	45.47	0.013
	Mitotic spindle assembly	40.42	<0.001
	Mitotic sister chromatid segregation	34.64	<0.001
	Mitotic cytokinesis	21.55	0.011
	Meiosis I	16.72	0.024
	DNA recombination	12.76	<0.001
	DNA replication	9.40	0.039
	Regulation of cell cycle phase transition	9.19	0.042
	DNA repair	8.01	<0.001
	Microtubule-based movement	7.67	0.003
	Anatomical structure development	1.83	0.034
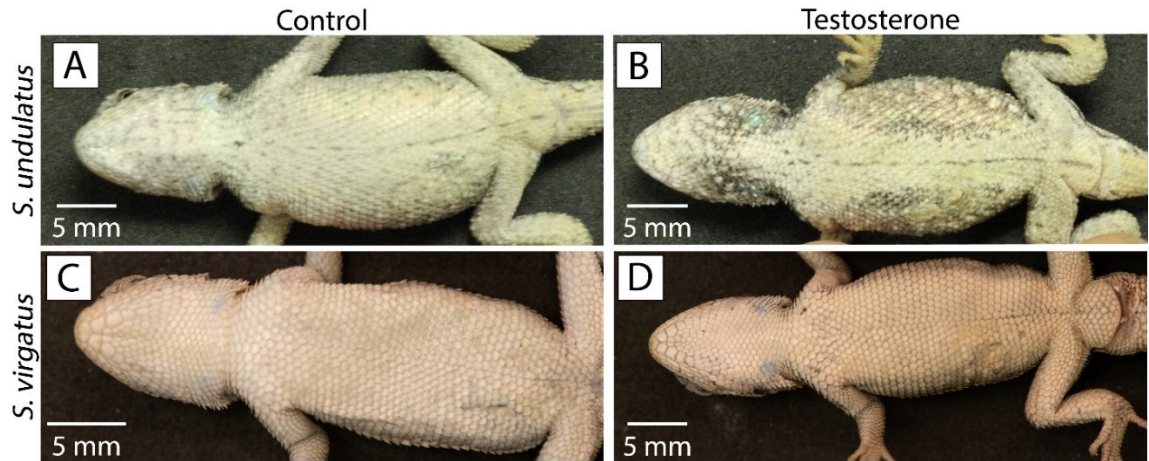
Figure S1. Representative images of the ventral surfaces of individuals in our testosterone manipulation experiment. *S. undulatus* receiving a testosterone implant developed melanized patches on their abdomens with faint specks of blue (**A**) while individuals in the control group exhibited no color development (**B**). Similar to control individuals in *S. undulatus*, no color development was observed in *S. virgatus* receiving a testosterone (**C**) or control (**D**) implant.
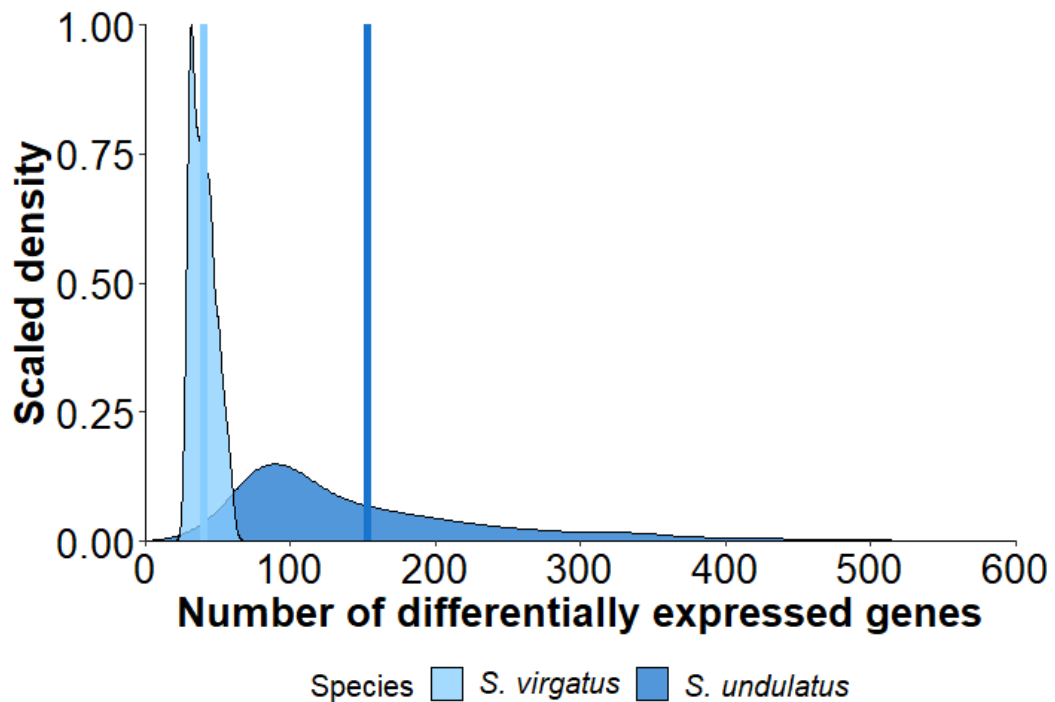
Figure S2. Density plot showing the distribution of DEGs in *S. undulatus* and *S. virgatus* when randomly dropping three *S. undulatus* libraries from differential expression analyses. The number of DEGs in response to testosterone is significantly higher in *S. undulatus* than *S. virgatus* in 96.6% of cases (1,487 out of 1,540), suggesting that the number of DEGs reported in our analyses with unequal sample sizes is not driven by greater statistical power in *S. undulatus*. Vertical lines represent the mean number of DEGs for each species.
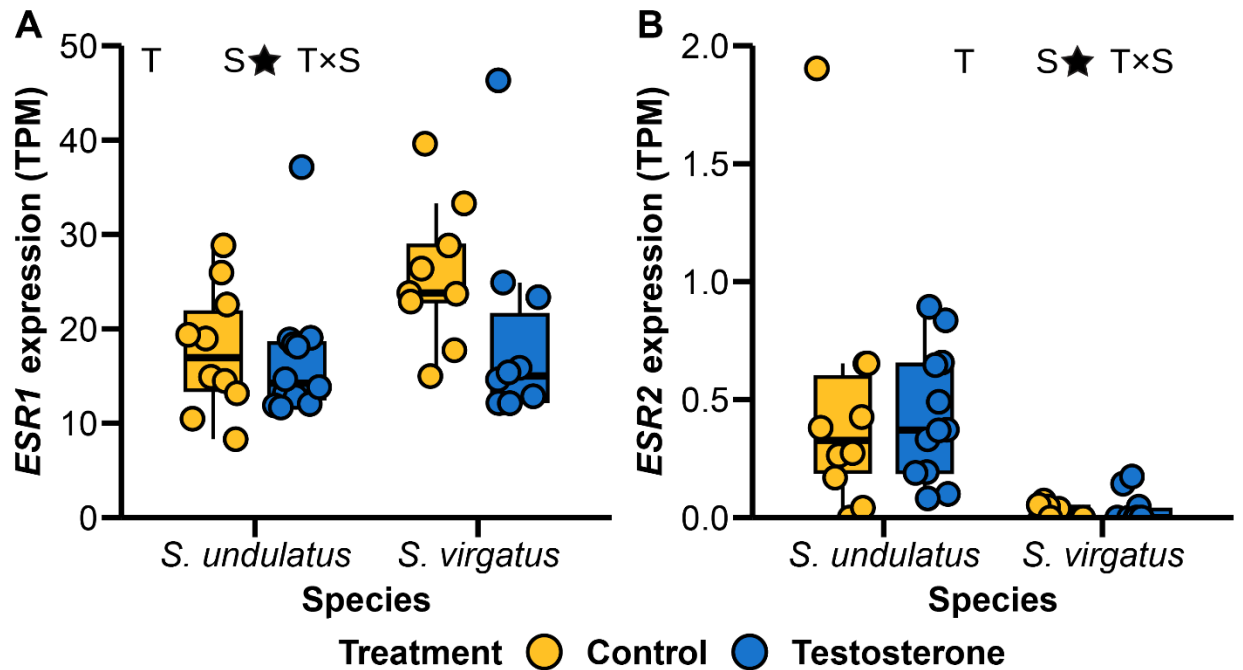
Figure S3. Gene expression (transcripts per million, TPM) as a function of species and testosterone treatment for **A**) estrogen receptor-α (*ESR1*) and **B**) estrogen receptor-β (*ESR2*). Boxplots illustrate the median (horizontal line), first and third quartiles (box edges) and 1.5 times the interquartile range (whiskers) for individual values (circles) in each group. Significant terms from ANOVA including hormone treatment (T), species (S), and treatment × species interactions (T×S) are represented by black stars to the right of each model term when $P < 0.05$.

Chapter 2:

Evolutionary loss of male-specific coloration in *Sceloporus* lizards is associated with the

loss of androgen receptor expression in skin[2]

---

[2] Robinson CD, M Milnes, IT Clifton, CL Cox, HB John-Alder, and RM Cox. In prep. Evolutionary loss of male-specific coloration in *Sceloporus* lizards is associated with the loss of androgen receptor expression in skin.

Abstract

Hormones can induce trait development in one species yet have no effect on the same trait in a closely related species. However, the underlying mechanisms contributing to these differences are unclear. Here, we test how the production of male-typical coloration in a lizard can become decoupled from androgen regulation, resulting in a derived, sexually monomorphic phenotype. The Eastern Fence Lizard (*Sceloporus undulatus*) has sexually dimorphic blue and black ventral coloration that develops when maturational increases in androgens induce melanin synthesis in males. The closely related Striped Plateau Lizard (*S. virgatus*) has sexually monomorphic white ventral skin that does not produce melanin in response to the same hormonal signal. We used immunohistochemistry to test whether the loss of ventral coloration in *S. virgatus* corresponds to the loss of androgen receptor (AR) expression in the skin, and to localize AR expression in the skin of both species. We found that ventral skin in males from the sexually monomorphic *S. virgatus* displays a reduction in AR expression, which could explain the loss of androgen sensitivity in this tissue, relative to the robust expression of AR in skin of males from the sexually dimorphic species. AR appears to be expressed in melanophores in *S. undulatus*, but we could not detect melanophore markers in the skin of *S. virgatus*. Therefore, the loss of the AR may have evolved due to loss of the AR-expressing melanophore in mature ventral skin, preventing the development of a male-typical trait and sexual dimorphism in this tissue.

Introduction

      The development of male-typical traits is facilitated by sex differences in the circulation of androgens, which induces sex-biased gene expression (van Nas et al. 2009; Peterson et al. 2013, 2014; Partridge et al. 2015; Cox et al. 2017; Hale et al. 2022). Because androgens regulate many traits simultaneously, a phenomenon referred to as hormonal pleiotropy (Finch and Rose 1995; Flatt et al. 2005), the evolution of hormonally mediated traits can be constrained if selection on one co-regulated trait acts in opposition to selection on another (Hau 2007; McGlothlin and Ketterson 2008; Ketterson et al. 2009). For a single hormonally mediated trait to evolve, the mechanistic coupling between the trait and hormone can change, which relaxes the evolutionary constraint imposed by hormonal pleiotropy (Hau 2007; Fuxjager and Schuppe 2018; Cox 2020; Cox et al. 2022). One way that this mechanistic coupling can evolve is by altering the hormonal sensitivity of a single tissue by increasing or decreasing the abundance of hormone receptors in that tissue. For example, evolutionary changes in androgen receptor (AR) abundance in specific target tissues contribute to the evolution of foot-flagging behavior in frogs (Mangiamele et al. 2016, 2018; Anderson et al. 2021), wing-snap displays in manakins (Fuxjager et al. 2015), and locomotion and push-up display behaviors in anole lizards (Johnson et al. 2018). While the connection between the evolutionary gain of elaborate displays and AR expression is well-established, it is less clear if the loss of AR expression can explain the derived loss of a trait present in the ancestral state. Here, we investigate how the evolution of tissue-specific AR abundance contributes to the evolutionary loss of male-typical ornamental coloration and its

112

implications for the evolution of sexual dimorphism in a closely related pair of lizard species.

Lizards in the genus *Sceloporus* exhibit considerable interspecific variation in sexually dimorphic, androgen-mediated traits, making this lineage well-suited for testing mechanisms underlying the evolution of these traits. For example, androgens stimulate growth in *Sceloporus* species with male-biased sexual size dimorphism (Cox and John-Alder 2005; John-Alder and Cox 2007), whereas they inhibit growth in species with female-biased sexual size dimorphism (Abell et al. 1998; Cox and John-Alder 2005; Cox et al. 2005b; Pollock et al. 2017). Similarly, androgens stimulate the production of melanin, a pigment necessary for the expression of ventral blue coloration (Morrison et al. 1995), in *Sceloporus* species that have male-typical ventral blue and black coloration (Kimball and Erpino 1971; Quinn and Hews 2003; Cox et al. 2005a, 2008; Robinson et al. 2023; Chapter 1), but androgens do not induce melanin production in species that lack ventral blue coloration (Abell 1998; Quinn and Hews 2003; Robinson et al. 2023; Chapter 1). The cellular mechanisms underlying how androgen regulation evolves to give rise to these species differences in melanin production and coloration are unresolved. However, similar differences in levels of male aggression between *Sceloporus* species are explained by differences in the distribution of the AR in neural tissues (Hews et al. 2012). Males of species exhibiting high male-specific aggression have more AR-positive nuclei in brain regions contributing to sex-specific behaviors than either conspecific females or males from species exhibiting low male-specific aggression (Hews et al. 2012). Therefore, tissue-specific changes in AR expression represent a potential mechanism by which hormonally mediated traits such as coloration can evolve.

In this study, we use adults from two *Sceloporus* species to test how the distribution and abundance of the AR in ventral skin contributes to the evolution of male traits. *Sceloporus undulatus* males develop vibrant blue coloration at sexual maturity in response to increasing levels of circulating androgens (Quinn and Hews 2003; Cox et al. 2005a, Pollock et al. 2017). In contrast, *S. virgatus* males do not develop this ventral coloration in response to either natural or experimental increases in circulating androgens (Abell 1998; Quinn and Hews 2003), suggesting that the mechanisms underlying color development have decoupled from androgen regulation in this species. Alternatively, melanophores (the cell type in which melanin synthesis occurs) could be absent in *S. virgatus* ventral skin, which would prevent color development regardless of whether the hormonal signal (testosterone) is present or not. Previous work has shown that juveniles from both species have abundant AR mRNA in ventral skin, but that testosterone regulates the expression of many more genes in ventral skin of *S. undulatus* relative to *S. virgatus* (Robinson et al. 2023; Chapter 1). Specifically, testosterone strongly upregulates the expression of melanin synthesis genes in *S. undulatus*, but not in *S. virgatus* (Robinson et al. 2023; Chapter 1). However, it is unknown how androgens induce a response in one species but not in the other. To address this issue, we first test whether the distribution and abundance of the AR in ventral skin differs between adults of these species. The low androgen sensitivity previously observed for *S. virgatus* skin could occur if the AR protein is absent or present at low levels despite abundant expression of its transcript, or if AR protein is not present in melanophores. Second, we test for the presence of unpigmented melanophores in the ventral skin of each species to determine whether this cell type is absent in *S. virgatus*. The absence of melanophores could alter

the overall transcriptional profile of the skin and potentially account for the low androgen sensitivity in *S. virgatus* previously inferred from bulk RNA sequencing (Darolti and Mank 2023). Specifically, we test for the presence of two molecular markers for melanophores, microphthalmia-associated transcription factor (MITF) and dopachrome tautomerase (DCT) (Steel et al. 1992; Opdecamp et al. 1999; Bondurand et al. 2000; Kelsh et al. 2000; Mort et al. 2015; Schartl et al. 2016), which would suggest that unpigmented melanophores are present in the dermis of *S. virgatus*. We also test for the presence of tyrosinase (TYR) as a marker of ongoing melanin synthesis (Raper 1928), which we predict will only be present in *S. undulatus* males. Based on previous bulk RNAseq data which found no species differences in the expression of *MITF* or *DCT* (Robinson et al. 2023; Chapter 1), we predict that unpigmented melanophores will be present in the skin of *S. virgatus*, but that AR will localize to melanophores in *S. undulatus*, and elsewhere in the skin of *S. virgatus*.

Methods

All procedures involving animals were approved by the University of Virginia's Animal Care and Use Committee (protocol 3896). Animals were collected under permits from New Jersey Fish & Wildlife (SC 2022068), Arizona Game & Fish (SP820881), and the U.S. Forest Service (Coronado National Forest). We collected *Sceloporus undulatus* adults from Colliers Mills Wildlife Management Area, Jackson Township, NJ (40.07889, -74.43736) on 12 April 2022 and *S. virgatus* adults from Cochise County, AZ (31.89834, -109.21800) on 17-18 May 2022. We euthanized animals in the field via rapid decapitation and pithing, then fixed tissues in 10% formalin. We fixed *S. undulatus*

carcasses whole and then later dissected skin prior to embedding. We dissected skin from

S. virgatus immediately upon euthanasia and fixed it independent from the carcass. After

48 hours in 10% formalin, we transferred tissues to 70% ethanol, where they were stored

until processing. We dehydrated tissues using a serial dilution of ethanol (90 minutes at

85%, 90 minutes at 95%, three runs of 60 minutes at 100%), cleared them using CitrSolv

(three runs of 60 minutes), and embedded them in paraffin wax under increasing vacuum

(45 minutes at 15 in/Hg, 45 minutes at 20 in/Hg, and 45 minutes at 24 in/Hg) and

constant heat (60°C). Finally, we sectioned tissues at 8 μm on a microtome.

We performed immunohistochemistry on samples from 3 individuals per sex, per

species ($N = 12$ total) to visualize the distribution and quantify the abundance of four

proteins: androgen receptor (AR), microphthalmia-associated transcription factor

(MITF), dopachrome tautomerase (DCT), and tyrosinase (TYR; see Table 1 for antibody,

sequence similarity and identity, dilution, antigen retrieval buffer, and product and lot

numbers). MITF regulates many melanophore processes, DCT contributes to regulating

melanophore survival, and tyrosinase converts tyrosine into melanin precursors (reviewed

in Park et al. 2009). Our primary antibodies were rabbit polyclonal antibodies, and we

visualized the location of these antibodies using 1:500 dilution of goat anti-rabbit IgG

cross-adsorbed Alexa Fluor™ 555 (Invitrogen™).

We followed Milnes et al. (2024) for tissue preparation, with the addition of a

bleaching step to allow for the visualization of our primary antibodies without melanin

obscuring our view. We deparaffinized slides and rehydrated tissues by soaking slides in

CitrSolv twice for 10 minutes and then in a series of ethanol baths (twice in 100% for two

minutes, 95% for two minutes, 70% for two minutes). We bleached each section by

applying 5% H_2O_2 in phosphate buffered saline for 12 hours at room temperature,

modifying a protocol from Orchard (2007). We then performed antigen retrieval (see

Table 1 for antigen retrieval buffer for each antibody) by using heat-induced epitope

retrieval under pressure at 110°C for 15 minutes. We allowed slides to cool to room

temperature and then washed slides three times in assay buffer (tris-buffered saline [TBS]

with 0.025% Triton X-100) for five minutes per wash. Next, we incubated sections in a

blocking and permeabilization buffer comprised of 10% (v/v) normal goat serum and

TBS with 0.2% Triton X-100 and 1% bovine serum albumin (BSA). Afterwards, we

added primary antibody (Table 1) diluted in assay buffer supplemented with 1% BSA and

allowed slides to incubate for 24 hours at 4°C. To remove unbound primary antibody, we

performed three washes with assay buffer for five minutes each. We then added

secondary antibody, diluted 1:500 with TBS assay buffer supplemented with 1% BSA to

each section, and incubated slides at room temperature for 1 hour. Finally, we washed

slides four times in assay buffer for three minutes each and then added a coverslip to each

slide with Invitrogen™ ProLong™ Gold Antifade Mountant with DAPI. We imaged

slides on an Olympus FLUOVIEW FV3000 confocal microscope at 60X magnification

and processed images using Fiji (ImageJ 1.52v) software (Schindelin et al. 2012).

To characterize differences in the amount of each protein present in ventral skin,

we used the Color Histogram plugin from Fiji to measure the amount of secondary

antibody fluorescence in each image by quantifying the RBG value for each pixel.

Specifically, we isolated the channel containing the secondary antibody and counted the

number of pixels with non-zero values. Therefore, a greater number of pixels above this

threshold value can be interpreted as more of the target protein distributed throughout the

image. To control for differences in the amount of tissue and cells within an image, we also quantified the amount of DAPI, which is a nuclear stain, present in each image. We used the same method as for the secondary antibody, except that we isolated the DAPI channel rather than the channel containing the secondary antibody. We then used ANCOVA to test for effects of species, sex, and their interaction on the amount of each protein, using the amount of detected DAPI as a covariate. Analyses were performed in R v4.3.2 (R Core Team 2023). Although vibrant blue ventral coloration is sexually dimorphic in *S. undulatus* and is typically only expressed by males, androgens can induce male-typical coloration in females (Cox et al. 2005; Pollock et al. 2017), and adult females occasionally exhibit male-typical ventral coloration naturally (Swierk and Langkilde 2013; Assis et al. 2022). Our sampling serendipitously included a single *S. undulatus* female with pronounced blue ventral coloration, providing an unplanned opportunity to link our immunohistochemistry data directly to color phenotype.

Results

We detected AR in the ventral skin of both sexes in both species (Fig. 1). However, AR was more abundant in *S. undulatus* than in *S. virgatus* ($F_{1,7} = 14.14$, $P = 0.007$). Similarly, AR was more abundant in males than in females ($F_{1,7} = 8.70$, $P = 0.02$). This sex difference in AR expression was primarily evident in sexually dimorphic *S. undulatus*, whereas AR levels were similarly low in both sexes for sexually monomorphic *S. virgatus,* as indicated by a significant sex-by-species interaction ($F_{1,7} = 9.43$, $P = 0.018$). In both sexes of *S. undulatus*, AR was cytosolic, and expressed primarily in the superficial pigment cell layer of the dermis (Fig. 1). Because this species has androgen-

mediated melanin synthesis, AR expression in this layer is likely occurring within melanophores, although our data cannot confirm this directly. Variation in AR expression was high among *S. undulatus* females, with the one individual female that exhibited vibrant blue ventral coloration also expressing much higher levels of AR than the other two females we sampled (Fig. 1B). If this female is excluded from the analysis, we find even more pronounced effects of species ($F_{1,6} = 52.24$, $P < 0.001$), sex ($F_{1,6} = 67.31$, $P < 0.001$), and the sex-by-species interaction ($F_{1,6} = 71.42$, $P < 0.001$). In both sexes of *S. virgatus*, AR was much less abundant than in *S. undulatus* males, with only a few deep nuclei showing any evidence of AR expression. Therefore, the expression of AR was both quantitatively and qualitatively different between species.

MITF, a molecular marker of melanophores, was expressed more highly in *S. undulatus* than in *S. virgatus* ($F_{1,7} = 19.16$, $P = 0.003$), contrary to the RNAseq results from our previous study (Table 2). Males tended to have more MITF expression than females ($F_{1,7} = 5.23$, $P = 0.056$), and sex differences in MITF expression tended to be more pronounced in *S. undulatus* than in *S. virgatus* (sex-by-species interaction: $F_{1,7} = 3.69$, $P = 0.096$), although neither of these trends were significant. In *S. undulatus* males, MITF distribution was punctate and localized to nuclei that were largely restricted to the superficial pigment layer of the dermis, matching expectations based on location of melanophores in ventral skin (Fig. 2A). The single *S. undulatus* female with vibrant blue ventral coloration was also the only female with detectable MITF staining (Fig. 2B), and the protein was largely perinuclear and located deep to the pigment cell layer, although there was also modest nuclear staining in the pigment cell layer of the dermis (Fig. 2A). Similar to what we found for AR, the exclusion of this female from analysis resulted in

more pronounced differences in MITF expression with respect to species ($F_{1,6} = 178.28$, $P < 0.001$), sex ($F_{1,6} = 127.99$, $P < 0.001$), and the sex-by-species interaction ($F_{1,6} = 111.48$, $P < 0.001$).

DCT, a second molecular marker of melanophores, was expressed at marginally higher levels in *S. undulatus* than in *S. virgatus* ($F_{1,6} = 5.59$, $P = 0.056$; $n = 2$ for *S. undulatus* females in this analysis) and at marginally higher levels in males than in females ($F_{1,6} = 4.48$, $P = 0.079$). However, there was also a significant sex-by-species interaction ($F_{1,6} = 7.69$, $P = 0.032$), with *S. undulatus* males having the highest DCT expression, which was largely absent in *S. undulatus* females and in either sex of *S. virgatus*. In *S. undulatus* males, DCT was cytosolic and located in the superficial pigment cell layer, showing a similar expression pattern to that of AR (Fig. 2C). However, unlike the pattern observed for AR and MITF, we did not detect pronounced DCT staining in the individual *S. undulatus* female that exhibited vibrant blue ventral coloration (Fig. 2C-D).

TYR, a molecular marker of ongoing melanin synthesis, was expressed more highly in *S. undulatus* than in *S. virgatus* ($F_{1,7} = 7.35$, $P = 0.030$) and more highly in males than in females ($F_{1,7} = 7.35$, $P = 0.030$). This pattern was driven by high TYR expression in *S. undulatus* males, as indicated by a significant sex-by-species interaction ($F_{1,7} = 6.05$, $P = 0.044$). In *S. undulatus* males, TYR was cytosolic and exclusively found in the superficial pigment cell layer, the same layer in which AR, MITF, and DCT localized. TYR was undetectable in all other groups, including the single *S. undulatus* female with vibrant blue coloration (Fig. 2E-F).

Discussion

We found that *S. undulatus* and *S. virgatus* differ in the amount and location of AR in the ventral dermis. Colorful *S. undulatus* individuals (all males plus one atypical female in our sample) had abundant AR expression in the ventral skin. In contrast, skin from more typical *S. undulatus* females lacking color and from both sexes of the sexually monomorphic *S. virgatus* had quantitatively less AR staining, with virtually no staining in the pigment cell layer of the dermis. AR staining appeared to localize in the superficial pigment layer along with the three melanophore markers in *S. undulatus* males, suggesting that AR is present within melanophores. In contrast, the small amount of AR staining observed in *S. virgatus* was deep to the pigment cell layer, suggesting that the weak AR signal we detected may be due to expression in a different cell type in this species. The absence of staining for MITF, DCT, and TYR further suggests that mature melanophores or their precursors are not present in the skin of adult *S. virgatus*. Therefore, the lack of androgen-mediated color development in *S. virgatus* may have evolved due to the loss of dermal AR expression, potentially mediated through the loss of the melanophores that express high levels of AR and mediate melanin synthesis in *S. undulatus*.

We detected relatively high amounts of AR in ventral skin of *S. undulatus*, which has androgen-induced melanin synthesis (Quinn and Hews 2003, Cox et al. 2005a, Pollock et al. 2017, Robinson et al. 2023; Chapter 1). Males of this species consistently expressed high levels of AR, whereas only one of three females had detectable AR expression. This hormone receptor was absent from the inferred pigment cell layer of ventral skin in both sexes of *S. virgatus*, a species that does not synthesize melanin in the

ventral regions where blue and black patches occur in *S. undulatus* (Quinn and Hews 2003; Robinson et al. 2023; Chapter 1). AR expression is necessary for the development of androgen-mediated sexually dimorphic phenotypes that occur via genomic (i.e., transcriptional) pathways, and the relative amount of AR within a tissue can evolve to facilitate the evolution of species-specific behaviors (Fuxjager et al. 2015; Mangiamele et al. 2016; Johnson et al. 2018; Mangiamele et al. 2018; Anderson et al. 2021). Experiments using cell type- or tissue-specific AR knockouts indicate that the loss of AR prevents androgen responsiveness in that cell type or tissue, resulting in a reduced magnitude of sexual dimorphism (MacLean et al. 2008; De Gendt and Verhoeven 2012; Yong et al. 2017). Testosterone influences the expression of significantly fewer genes in ventral skin of *S. virgatus* than it does in ventral skin of *S. undulatus* (Robinson et al. 2023; Chapter 1), which is consistent with our observation that AR expression is greatly reduced in ventral skin of *S. virgatus*. However, Robinson et al. (2023; Chapter 1) also found higher expression of *AR* transcript in the ventral skin of *S. virgatus* than in *S. undulatus*, albeit in juveniles.

An unexpected line of support for the contribution of the AR to the expression of blue ventral coloration comes from *S. undulatus* females. One *S. undulatus* female exhibited blue ventral coloration similar to that of males (Fig. 1B), while the other two that we sampled lacked blue color on the abdomen, which is more typical and similar to *S. virgatus*. In *S. undulatus,* females with rudimentary male-like coloration often suffer fitness consequences (Swierk and Langkilde 2013; Assis et al. 2022). Saturation of ventral color is positively correlated with circulating testosterone levels in both sexes (Assis et al. 2021), implying that the regulation of color development shares mechanistic

pathways between females and males (Cox et al. 2005; Pollock et al. 2017). Indeed, we found that this strikingly colorful female exhibited male-like levels of AR (Fig. 1B) and MITF (Fig. 2B), while the two females with white ventral coloration had low expression levels for all four proteins, similar to *S. virgatus*. Interestingly, the only melanophore marker protein present in the female with blue ventral coloration was MITF (i.e., DCT and TYR were not detectable), suggesting that mature melanophores were present in this female, but that melanin synthesis was not actively occurring. In our study population of *S. undulatus*, females have low circulating testosterone in April (John-Alder et al. 2009), the time at which we conducted our sampling. Therefore, the expression of androgen-regulated melanin synthesis genes such as *TYR* would potentially not be induced at this time (Robinson et al. 2023; Chapter 1). Collectively, evidence from *S. undulatus* females supports the hypothesis that expression of AR in the ventral skin is necessary for the production of coloration.

In *Sceloporus*, vibrant blue ventral coloration is dependent on two pigment cell types: melanophores and iridophores (Morrison et al. 1995). While iridophores are present in the sexually monomorphic ventral skin of *S. virgatus* adults, pigmented melanophores are absent (Hews and Quinn 2003; Robinson et al. 2023; Chapter 1). However, previous RNAseq data suggest that molecular markers for melanophores are expressed in the skin of *S. virgatus* juveniles (Robinson et al. 2023; Chapter 1). This result led us to predict that unpigmented melanophores are present in the skin of *S. virgatus* adults, but that AR would be absent from this cell type, preventing the induction of melanin synthesis. However, we found that MITF, DCT, and TYR were undetectable in the ventral skin of *S. virgatus* (Fig. 2), suggesting that melanophore or their precursors

are absent in the skin of *S. virgatus* adults. Reconciling RNAseq data from juveniles tested in Robinson et al. (2023; Chapter 1) with the observations in adults presented here is difficult, but a few phenomena could explain these patterns. For example, androgens and androgenic metabolites can regulate programmed cell death (Davis et al. 1999; Forger 2006, 2009; Tsukahara 2009; Waters and Simerly 2009), resulting in sexually dimorphic tissues, and patterns of sex-biased programmed cell death can evolve to alter sexually dimorphic development across species (Kijimoto et al. 2010; Hanna and Abouheif 2023). Therefore, rates of androgen-regulated cell death may have evolved to prevent the retention of melanophores into adulthood for *S. virgatus*. Alternatively, multipotent progenitor cells can express markers for multiple terminal cell types, such that the RNAseq data from juveniles (Robinson et al. 2023; Chapter 1) may have detected unspecified cell types undergoing progressive or cyclical fate restriction (Kelsh et al. 2017; Dawes and Kelsh 2021; Subkhankulova et al. 2023). If so, these multipotent progenitor cells may have been specified to develop into iridophores rather than melanophores in *S. virgatus*. While we have not tested either of these hypotheses directly, *S. virgatus* skin has a qualitatively thicker iridophore layer than that of *S. undulatus* (Robinson, personal observation), which might suggest cells specified to become melanophores (which sit deep to the iridophore layer) in *S. undulatus* become iridophores in *S. virgatus*. Similarly, disruption of melanophore development in zebrafish results higher numbers of iridophores (Lister et al. 1999), so increased melanophore cell death or differences in cell fate specification could explain this result.

The development of male traits is facilitated by the sex-biased production, circulation, and detection of steroid hormones. While changes in circulating hormone

levels can alter these traits (e.g., Husak and Lovern 2014), changes to other elements of endocrine-regulated networks comprising complex hormone-phenotype couplings can have similar evolutionary outcomes (Fuxjager and Schuppe 2018; Cox et al. 2022), resulting in different patterns of sexual dimorphism. The evolution of hormonally mediated development can be challenging because of the pleiotropic nature of hormones, but specific cell types or tissues decoupling from hormonal regulation can ease evolutionary constraints (Hau 2007; McGlothlin and Ketterson 2008; Ketterson et al. 2009; Cox 2020; Cox et al. 2022). Three lines of evidence in *Sceloporus* contribute to this perspective. First, growth rates of both *S. undulatus* and *S. virgatus* are suppressed by androgens (Abell 1998; Cox and John-Alder 2005; Cox et al. 2005b; Pollock et al. 2017). Second, androgen regulation of gene expression in the liver is largely concordant between these two species (Chapter 3). Third, decreased androgen sensitivity in *S. virgatus* skin relative to *S. undulatus* (Robinson et al. 2023; Chapter 1) and the evolution of sexually dimorphic coloration corresponds with remarkable reduction in AR (this Chapter). Together, this indicates that decoupling of hormonal regulation can occur in a tissue-specific manner to allow for evolutionary transitions in single phenotypes between closely related species.

Acknowledgements

Literature Cited

Abell A.J. 1998. The effect of exogenous testosterone on growth and secondary sexual character development in juveniles of *Sceloporus virgatus*. Herpetologica 54:533-543. (https://www.jstor.org/stable/3893445)

Anderson N.K., E.R. Schuppe, K.V. Gururaja, L.A. Mangiamele, J.C.C. Martinez, H. Priti, R. von May, D. Preininger, and M.J. Fuxjager. 2021. A common endocrine signal marks the convergent evolution of an elaborate dance display in frogs. Am Nat 198:522-539. (doi:10.1086/716213)

Assis B.A., J.D. Avery, C. Tylan, H.I. Engler, R.L. Earley, and T. Langkilde. 2021. Honest signals and sexual conflict: female lizards carry undesirable indicators of quality. Ecol Evol 11:7647-7659. (doi:10.1002/ece3.7598)

Assis B.A., J.D. Avery, R.L. Earley, and T. Langkilde. 2022. Fitness costs of maternal ornaments and prenatal corticosterone manifest as reduced offspring survival and sexual ornament expression. Front Endocrinol:801834. (doi:10.3389/fendo.2022.801834)

Bagnara J.T., J. Matsumoto, W. Ferris, S.K. Frost, W.A. Turner Jr., T.T. Tchen, and J.D. Taylor. Common origin of pigment cells. Science 203:410-415. (doi:10.1126/science.760198)

Bondurand N., V. Pingault, D.E. Goerich, N. Lemort, E. Sock, C. Le Caignec, M. Wegner, and M. Goossens. 2000. Interaction among *SOX10*, *PAX3*, and *MITF*, three genes altered in Waardenburg syndrome. Hum Mol Genet9:1907-1917. (doi:10.1093/hmg/9.13.1907)

Bronner M.E. and M. Simões-Costa. 2016. The neural crest migrating into the twenty-

    first century. Curr Top Dev Biol 116:115-134. (doi:10.1016/bs.ctdb.2015.12.003)

Cox R.M. 2020. Sex steroids as mediators of phenotypic integration, genetic correlations,

    and evolutionary transitions. Mol Cell Endocrinol 502:110668.

    (doi:10.1016/j.mce.2019.110668)

Cox R.M., C.L. Cox, J.W. McGlothlin, D.C. Card, A.L. Andrew, and T.A. Castoe. 2017.

    Hormonally mediated increases in sex-biased gene expression accompany the

    breakdown of between-sex genetic correlations in a sexually dimorphic lizard. Am

    Nat 189:315-332. (doi:10.1086/690105)

Cox R.M. and H.B. John-Alder. 2005. Testosterone has opposite effects on male growth

    in lizards (*Sceloporus* spp.) with opposite patterns of sexual size dimorphism. J Exp

    Biol 208:4679-4687. (doi:10.1242/jeb.01948)

Cox R.M., M.D. Hale, T.N. Wittman, C.D. Robinson, and C.L. Cox. 2022. Evolution of

    hormone-phenotype couplings and hormone-genome interactions. Horm Behav

    114:105216. (doi:10.1016/j.yhbeh.2022.105216)

Cox R.M., S.L. Skelly, A. Leo, and H.B. John-Alder. 2005a. Testosterone regulates

    sexually dimorphic coloration in the eastern fence lizard, *Sceloporus undulatus*.

    Copeia 2005:597-608. (doi:10.1643/CP-04-313R)

Cox R.M., S.L. Skelley, and H.B. John-Alder. 2005b. Testosterone inhibits growth in

    juvenile male eastern fence lizards (*Sceloporus undulatus*): implications for energy

    allocation and sexual size dimorphism. Physiol Biochem Zool 78:531-545.

    (doi:10.1086/430226)

Cox R.M., V. Zilberman, and H.B. John-Alder. 2008. Testosterone stimulates the expression of a social color signal in Yarrow's spiny lizard, *Sceloporus jarrovii*. J Exp Zool A Ecol Integr Physiol 309:505-514. (doi:10.1002/jez.481)

Darolti I. and J.E. Mank. 2023. Sex-biased gene expression at single-cell resolution: cause and consequence of sexual dimorphism. Evol Lett 7:145-156. (doi:10.093/evlett/qrad013)

Davis E.C., P. Popper, and R.A. Gorski. 1996. The role of apoptosis in sexual differentiation of the rat sexually dimorphic nucleus of the preoptic area. Brain Res 734:10-18. (doi:10.1016/0006-8993(96)00298-3)

Dawes J.H.P. and R.N. Kelsh. 2021. Cell fate decisions in the neural crest, from pigment cells to neural development. Int J Mol Sci 22:13531. (doi:10.3390/ijms222413531)

De Gendt K. and G. Verhoeven. 2012. Tissue- and cell-specific functions of the androgen receptor revealed through conditional knockout models in mice. Mol Cell Endocrinol 352:13-25. (doi:10.1016/j.mce.2011.08.008)

Finch C.E. and M.R. Rose. 1995. Hormones and the physiological architecture of life history evolution. Q Rev Biol 70:1-52. (doi:10.1086/418864)

Flatt T., M.-P. Tu, and M. Tatar. 2005. Hormonal pleiotropy and the juvenile hormone regulation of *Drosophila* development and life history. BioEssays 27:999-1010. (doi:10.1002/bies.20290)

Forger N.G. 2006. Cell death and sexual differentiation of the nervous system. Neuroscience 138:929-938. (doi:10.1016/j.neuroscience.2005.07.006)

Forger N.G. 2009. Control of cell number in the sexually dimorphic brain and spinal cord. J Neuroendocrinol 21:393-399. (doi:10.1111/j.1365-2826.2009.01825.x)

Fuxjager M.J. and E.R. Schuppe. 2018. Androgenic signaling systems and their role in behavioral evolution. J Steroid Biochem Mol Biol 184:47-56. (doi:10.1016/j.jsbmb.2018.06.004)

Fuxjager M.J., J. Eaton, W.R. Lindsay, L.H. Salwiczek, M.A. Rensel, J. Barske, L. Sorenson, L.B. Day, and B.A. Schlinger. 2015. Evolutionary patterns of adaptive acrobatics and physical performance predict expression profiles of androgen receptor – but not oestrogen receptor – in the forelimb musculature. Funct Ecol 29:1197-1208. (doi:10.1111/1365-2435.12438)

Hale M.D., C.D. Robinson, C.L. Cox, and R.M. Cox. 2022. Ontogenetic change in male expression of testosterone-responsive genes contributes to the emergence of sex-biased gene expression in *Anolis sagrei*. Front Physiol 13:886973. (doi:10.3389/fphys.2022.886973)

Hanna L. and E. Abouheif. 2023. Deep conservation and co-option of programmed cell death facilitates evolution of alternative phenotypes at multiple biological levels. Semin Cell Dev Biol 145:28-41. (doi:10.1016/j.semcdb.2022.05.024)

Hau M. 2007. Regulation of male traits by testosterone: implications for the evolution of vertebrate life histories. BioEssays 29:133-144. (doi:10.1002/bies.20524)

Hews D.K. and V.S. Quinn. 2003. Endocrinology of species differences in sexually dichromatic signals. Pp. 253-277 in S.F. Fox, J.K. McCoy, and T.A. Baird, eds. Lizard Social Behavior. John Hopkins University Press, Baltimore, MD.

Hews D.K., E. Hara, and M.C. Anderson. 2012. Sex and species differences in plasma testosterone and in counts of androgen receptor-positive cells in key brain regions of

Sceloporus lizard species that differ in aggression. Gen Comp Endocrinol 176:493-499. (doi:10.1016/j.ygcen.2011.12.028)

Hu S., S. Bai, Y. Dai, N. Yang, J. Li, X. Zhang, F. Wang, et al. 2021. Deubiqitination of MITF-M regulates melanocytes proliferation and apoptosis. Front Mol Biosci 8:692724. (doi:10.3389/fmolb.2021.692724)

Husak J.F. and M.B. Lovern. 2014. Variation in steroid hormone levels among Caribbean *Anolis* lizards: endocrine system convergence? Horm Behav 65:408-415. (doi:10.1016/j.yhbeh.2014.03.006)

John-Alder H.B. and R.M. Cox. 2007. Development of sexual size dimorphism in lizards: testosterone as a bipotential growth regulator. Pp. 195-204 in D.J. Fairbairn, T. Szekely, and W.U. Blanckenhorn WU, eds. Sex, Size and Gender Roles: Evolutionary Studies of Sexual Size Dimorphism. Oxford University Press, Oxford.

John-Alder H.B., R.M. Cox, G.J. Haenel, and L.C. Smith. 2009. Hormones, performance and fitness: natural history and endocrine experiments on a lizard (*Sceloporus undulatus*). Integrat Comp Biol 49:393-407. (doi:10.1093/icb/icp060)

Johnson M.A., B.K. Kircher, and D.J. Castro. 2018. The evolution of androgen receptor expression and behavior in *Anolis* lizard forelimb muscles. J Comp Physiol A 204:71-79. (doi:10.1007/s00359-017-1228-y)

Kelsh R.N., B. Schmid, and J.S. Eisen. 2000. Genetic analysis of melanophore development in zebrafish embryos. Dev Biol 225:277-293. (doi:10.1006/dbio.2000.9840)

Kelsh R.N., K.C. Sosa, J.P. Owen, and C.A. Yates. 2017. Zebrafish adult pigment stem

　　cells are multipotent and form pigment cells by a progressive fate restriction process.

　　BioEssays 39:1600234. (doi:10.1002/bies.201600234)

Ketterson E.D., J.W. Atwell, and J.W. McGlothlin. 2009. Phenotypic integration and

　　independence: hormones, performance, and response to environmental change.

　　Integrat Comp Biol 49:365-379. (doi:10.1093/icb/icp057)

Kijimoto T., J. Andrews, and A.P. Moczek. 2010. Programed cell death shapes the

　　expression of horns within and between species of horned beetles. Evol Dev 12:449-

　　458. (doi:10.1111/j.1525-142X.2010.00431.x)

Le Douarin N.M. and E. Dupin. 2018. The "beginnings" of the neural crest. Dev Biol

　　444:S3-S13. (doi:10.1016/j.ydbio.2018.07.019)

Lister J.A., C.P. Robertson, T. Lepage, S.L. Johnson, and D.W. Raible. 1999. *nacre*

　　encodes a zebrafish microphthalamia-related protein that regulates neural-crest-

　　derived pigment cell fate. Development 126:3757-3767.

　　(doi:10.1242/dev.126.17.3757)

MacLean H.E., W.S.M. Chiu, A.J. Notini, A.-M. Axell, R.A. Davey, J.F. McManus, C.

　　Ma, D.R. Plant, G.S. Lynch, and J.D. Zajac. 2008. Impaired skeletal muscle

　　development and function in male, but not female, genomic *androgen receptor*

　　knockout mice. FASEB J 22:2676-2689. (doi:10.1096/fj.08-105726)

Mangiamele L.A., M.J. Fuxjager, E.R. Schuppe, R.S. Taylor, W. Hödl, and D. Preininger.

　　2016. Increased androgenic sensitivity in the hind limb muscular system marks the

　　evolution of a derived gestural display. Proc Natl Acad Sci 113:5664-5669.

　　(doi:10.1073/pnas.1603329113)

Mangiamele L.A. and M.J. Fuxjager. 2018. Insight into the neuroendocrine basis of signal evolution: a case study in foot-flagging frogs. J Comp Physiol A 204:61-70. (doi:10.1007/s00359-017-1218-0)

McGlothlin J.W. and E.D. Ketterson. 2008. Hormone-mediated suites as adaptations and evolutionary constraints. Phil Trans Roy Soc B Biol Sci 363:1611-1620. (doi:10.1098/rstb.2007.0002)

Milnes, M.R., C.D. Robinson, A.P. Foley, C. Stepp, M.D. Hale, H.B. John-Alder, and R.M. Cox. 2024. Effects of testosterone on urogenital tract morphology and androgen receptor expression in immature eastern fence lizards (*Sceloporus undulatus*). Gen Comp Endocrinol 346:114418. (doi:10.1016/j.ygcen.2023.114418)

Moczek A.P. 2006. Pupal remodeling and the development and evolution of sexual dimorphism in horned beetles. Am Nat 168:711-729. (doi:10.1086/509051)

Morrison R.L., M.S. Rand, and S.K. Frost-Mason. 1995. Cellular basis of color differences in three morphs of the lizard *Sceloporus undulatus erythrocheilus*. Copeia 1995:397-408. (doi:10.2307/1446903)

Mort R.L., I.J. Jackson, and E.E. Patton. 2015. The melanocyte lineage in development and disease. Development 142:620-632. (doi:10.1242/dev.106567)

Niitsu S., K. Toga, S. Tomizuka, K. Maekawa, R. Machida, and T. Kamito. 2014. Ecdysteroid-induced programmed cell death is essential for sex-specific wing degeneration of the wingless-female winter moth. PLoS ONE 9:e89435. (doi:10.1371/journal.pone.0089435)

Ossip-Drahos A.G., J.R. Oyola Morales, C. Vital-García, J.J. Zúñiga-Vega, D.K. Hews, and E.P. Martins. 2016. Shaping communicative colour signals over evolutionary time. R Soc Open Sci 3:160728. (doi:10.1098/rsos.160728)

Opdecamp K., A. Nakayama, M.-T.T. Nguyen, C.A. Hodgkinson, W.J. Pavan, and H. Arnheiter. 1997. Melanocyte development in vivo and in neural crest cell cultures: crucial dependent on the Mitf basic-helix-loop-helix-zipper transcription factor. Development 124:2377-2386. (doi:10.1242/dev.124.12.2377)

Ophoff J., K. Van Proeyen, F. Callewaert, K. De Gendt, K. De Bock, A. Vanden Bosch, G. Verhoeven, P. Hespel, and D. Vanderschueren. 2009. Androgen signaling in myocytes contributes to the maintenance of muscle mass and fiber type regulation but not to muscle strength or fatigue. Endocrinology 150:3558-3566. (doi:10.1210/en.2008-1509)

Orchard G.E. 2007. Use of heat provides a fast and efficient way to undertake melanin bleaching with dilute hydrogen peroxide. Br J Biomed Sci 64:89-91. (doi:10.1080/09674845.2007.11978097)

Park H.Y., M. Kosmadaki, M. Yaar, and B.A. Gilchrest. 2009. Cellular mechanisms regulating human melanogenesis. Cell Mol Life Sci 66:1493-1506. (doi:10.1007/s00018-009-8703-8)

Partridge C., C.M.C. Rodgers, R. Knapp, and B.D. Neff. 2015. Androgen effects on immune gene expression during parental care in bluegill sunfish (*Lepomis macrochirus*). Can J Zool 93:9-13. (doi:10.1139/cjz-2014-0157).

Peterson M.P., K.A. Rosvall, C.A. Taylor, J.A. Lopez, J.-H. Choi, C. Ziegenfus, H. Tank, J.K. Colbourne, and E.D. Ketterson. 2014. Potential for sexual conflict assessed via

testosterone-mediated transcriptional changes in liver and muscle of a songbird. J Exp Biol 217:507-517. (doi:10.1242/jeb.089813)

Peterson M.P., K.A. Rosvall, J.-H. Choi, C. Ziegenfus, H. Tang, J.K. Colbourne, and E.D. Ketterson. 2013. Testosterone affects neural gene expression differently in male and female juncos: a role for hormones in mediating sexual dimorphism and conflict. PLoS One 8:e61784. (doi:10.1371/journal.pone.0061784)

Pollock N.B., S. Feigin, M. Drazenovic, and H.B. John-Alder. 2017. Sex hormones and the development of sexual size dimorphism: 5α-dihydrotestosterone inhibits growth in a female-larger lizard (*Sceloporus undulatus*). J Exp Biol 220:4068-4077. (doi:10.1242/jeb.166553)

Quinn V.S. and D.K. Hews. 2003. Positive relationship between abdominal coloration and dermal melanin density in phrynosomatid lizards. Copeia 2003:858-864. (doi:10.1643/h202-116.1)

R Core Team. 2023. R: a language and environment for statistical computing. R Foundation for Statistical Computer. Vienna, Austria.

Raper H.S. 1928. The aerobic oxidases. Physiol Rev 8:245-282. (doi:10.1152/physrev.1928.8.2.245)

Robinson C.D., M.D. Hale, T.N. Wittman, C.L. Cox, H.B. John-Alder, and R.M. Cox. 2023. Species differences in hormonally mediated gene expression underlie the evolutionary loss of sexually dimorphic coloration in *Sceloporus* lizards. J Hered 114:67-653. (doi:10.1093/jhered/esad046)

Schartl M., L. Larue, M. Goda, M.W. Bosenberg, H. Hashimoto, and R.N. Kelsh. 2016. What is a vertebrate pigment cell? Pigment Cell Melanoma Res 29:74-78. (doi:10.1111/pcmr.12409)

Schindelin J., I. Arganda-Carreras, E. Frise, V. Kaynig, M. Longair, T. Pietzsch, S. Peribisch, et al. 2012. Fiji: an open-source platform for biological-image analysis. Nature Methods 9:676-682. (doi:10.1038/nmeth.2019)

Steel K.P., D.R. Davidson, and I.J. Jackson. 1992. TRP-2/DT, a new early melanoblast marker, shows that steel growth factor (c-kit ligand) is a survival factor. Development 115:1111-1119. (doi:10.1242/dev.115.4.1111)

Subkhankulova T., K.C. Sosa, L.A. Uroshlev, M. Nikaido, N. Shriever, A.S. Kasianov, X. Yang, et al. 2023. Zebrafish pigment cells develop directly from persistent highly multipotent progenitors. Nat Commun 14:1258. (doi:10.1038/s41467-023-36876-4)

Swierk L. and T. Langkilde. 2013. Bearded ladies: females suffer fitness consequences when bearing male traits. Biol Lett 9:20130644. (doi:10.1098/rsbl.2013.0644)

Tsukahara S. 2009. Sex differences and the roles of sex steroids in apoptosis of sexually dimorphic nuclei of the preoptic area in postnatal rats. J Neuroendocrinol 21:370-376. (doi:10.1111/j.1365-2826.2009.01855.x)

van Nas A., D. GuhaThakurta, S.S. Wang, N. Yehya, S. Horvath, B. Zhang, L. Ingram-Drake, et al. 2009. Elucidating the role of gonadal hormones in sexually dimorphic gene coexpression networks. Endocrinology 150:1235-1249. (doi:10.1210/en.2008-0563)

Wang W., B.J. Kidd, S.B. Carroll, and J.H. Yoder. 2011. Sexually dimorphic regulation of the Wingless morphogen controls sex-specific segment number in *Drosophila*. Proc Natl Acad Sci 108:11139-11144. (doi:10.1073/pnas.1108431108)

Waters E.M. and R.B. Simerly. 2009. Estrogen induces caspase-dependent cell death during hypothalamic development. J Neurosci 29:9714-9718. (doi:10.1523/JNEUROSCI.0135-09.2009)

Westfall A.K., R.S. Telemeco, M.B. Grizante, D.S. Waits, A.D. Clark, D.Y. Simpson, R.L. Klabacka, et al. 2021. A chromosome-level genome assembly for the eastern fence lizard (*Sceloporus undulatus*), a reptile model for physiological and evolutionary ecology. GigaScience 10:giab066. (doi:10.1093/gigascience/giab066)

Wiens J.J. 1999. Phylogenetic evidence for multiple losses of a sexually selected character in phrynosomatid lizards. Proc R Soc Lond B Biol Sci 266:1529-1535. (doi:10.1098/rspb.1999.0811)

Yong L., Z. Thet, and Y. Zhu. 2017. Genetic editing of the androgen receptor contributes to impaired male courtship behavior in zebrafish. J Exp Biol 220:3017-3021. (doi:10.1242/jeb.161596)

Table 1. Antibodies used for immunohistological staining. Sequence similarity represents the percent of amino acid residues between the antibody and the protein sequence as inferred from the *S. undulatus* genome (Westfall et al. 2021) that are identical or physiologically similar. Percent identity represents the percent of identical amino acid residues between the antibody and the protein sequence as inferred from the *S. undulatus* genome. Dilution is the ratio in which we diluted each antibody in with assay buffer supplemented with 1% BSA. Antigen retrieval method is the condition in which we performed heat-induced epitope retrieval.

Protein	Antibody	Sequence similarity	Percent Identity	Dilution	Antigen retrieval method	Product and lot number
AR	Anti-androgen receptor	77.27%	72.73%	1:250	Tris/EDTA buffer pH 9.0	06-680; 3538089
MITF	Anti-MITF antibody	94.24%	83.45%	1:500	Sodium citrate buffer pH 6.0	PA5-82074; YI4031313
DCT	Anti-TRP2/DCT antibody	85.33%	74.67%	1:250	Sodium citrate buffer pH 6.0	ab223736; GR3379722
TYR	Anti-Tyrosinase antibody	87.23%	76.64%	1:2000	Tris/EDTA buffer pH 9.0	ab180753; GR3450821

Table 2. Result comparison from Robinson et al. (2023) RNAseq data in a testosterone manipulation experiment using juveniles and our immunohistochemistry study in adults. Predictions for this study were based on RNAseq data from Robinson et al. (2023), and deviations from expectation based on RNAseq data are indicated by an asterisk (*) in the immunohistochemistry columns. Plus signs (+) represent whether a gene is expressed (RNAseq) or a protein is present (IHC) and minus signs (-) represent that a gene (RNAseq) or protein (IHC) is not or very lowly detected.

	RNAseq				Immunohistochemistry			
	S. undulatus		*S. virgatus*		*S. undulatus*		*S. virgatus*	
	Testosterone	Control	Testosterone	Control	Male	Female	Male	Female
AR	+	+	+	+	+	+/-	-*	-*
MITF	+	+	+	+	+	+/-	-*	-*
DCT	+	+	+	+	+	-*	-*	-*
TYR	+	-	-	-	+	-	-	-
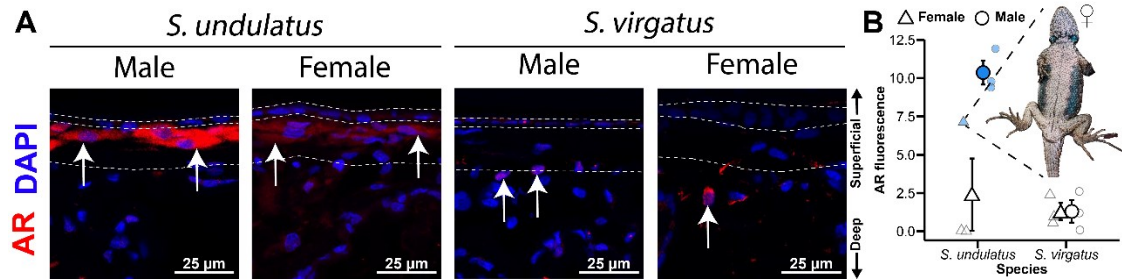
Figure 1. Immunohistochemistry staining for androgen receptor (AR) in males and females of two *Sceloporus* species. Protein localization is visualized with AlexaFluor 555 as a secondary antibody and is represented by red fluorescence and highlighted by white arrows. DAPI (blue) is used as a nuclear counterstain. White dashed lines on IHC images outline the keratinocyte layer (superficial outlined layer) and the pigment cell layer (deep outlined layer), as inferred from TYR staining in *S. undulatus* males. Fluorescence is quantified using Color Histogram in Fiji and is represented by arbitrary units, with higher values representing the presence of more pixels that are positive for secondary antibody. Small points represent individual values with the color of the point representing the phenotype of the individual. Lizard in B is a *S. undulatus* female displaying vibrant male-typical coloration. IHC image for *S. undulatus* female in panel A is from this female. Large points represent mean ± 1 SE.
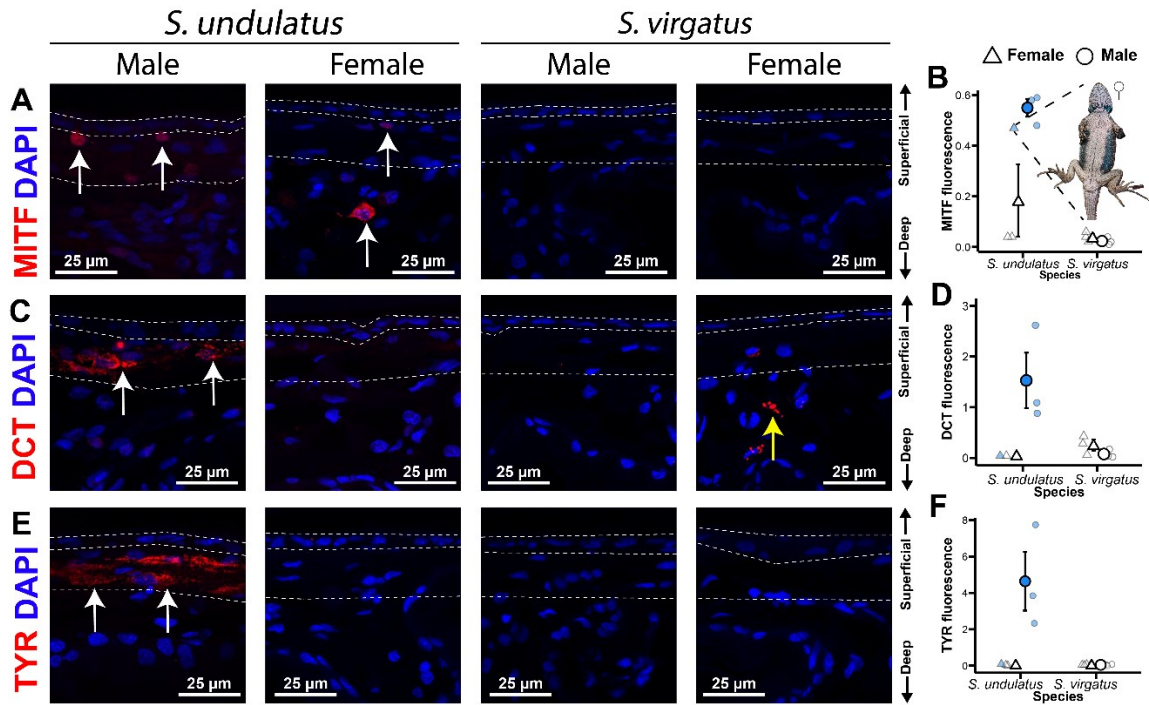
Figure 2. Immunohistochemistry staining for (A) microphthalmia-associated transcription factor (MITF), (C) dopachrome tautomerase (DCT), and (E) tyrosinase (TYR) in females and males of two *Sceloporus* species. Protein localization is visualized with AlexaFluor 555 as a secondary antibody and is represented by red fluorescence and highlighted by white arrows. DAPI (blue) is used as a nuclear counterstain. White dashed lines on IHC images outline the keratinocyte layer (superficial outlined layer) and the pigment cell layer (deep outlined area), as estimated by TYR staining in *S. undulatus* males. Fluorescence is quantified (panels B, D, F) using Color Histogram in Fiji and is represented by arbitrary units, with higher values representing the presence of more pixels that are positive for secondary antibody. Small points represent individual values with the color of the point representing the phenotype of the individual. Lizard in B is a *S. undulatus* female displaying vibrant male-typical coloration. IHC images for *S. undulatus* female in panels A, C, and E are from this female. Large points represent mean

± 1 SE. Red, punctate staining in the *S. virgatus* DCT image (highlighted by a yellow arrow) is likely an artifact and not representative of dopachrome tautomerase in the skin.

Chapter 3:

Effects of testosterone on gene expression are concordant between sexes but divergent

across species of *Sceloporus* lizards[3]

---

[3] Robinson CD, MD Hale, CL Cox, HB John-Alder, and RM Cox. In prep. Effects of

testosterone on gene expression are concordant between sexes but divergent across

species of *Sceloporus* lizards.

Abstract

Hormones mediate sexual dimorphism by regulating sex-specific patterns of gene expression, but it is unclear how much of this regulation involves sex-specific hormone levels as opposed to sex-specific transcriptomic responses to the same hormonal signal. Moreover, transcriptomic responses to hormones can evolve, but the extent to which hormonal pleiotropy in gene regulation is conserved across closely related species is not well understood. We addressed these issues by elevating testosterone levels in juvenile females and males of three *Sceloporus* lizard species prior to sexual divergence in circulating testosterone, then characterizing transcriptomic responses in the liver. In each species, more genes were responsive to testosterone in males than in females, suggesting that early developmental processes prime sex-specific transcriptomic responses to testosterone later in life. However, overall transcriptomic responses to testosterone were concordant between sexes, with no genes exhibiting sex-by-treatment interactions. By contrast, hundreds of genes exhibited species-by-treatment interactions, particularly when comparing distantly related species, suggesting evolutionary lability in gene regulation by testosterone. Collectively, our results indicate that early organizational effects may lead to sex-specific differences in the magnitude, but not the direction, of transcriptomic responses to testosterone, and that the hormone-genome interface can accrue regulatory changes over evolutionary time.

Introduction

Hormones with sex-specific patterns of secretion, such as androgens and estrogens, mediate the development of sexually dimorphic phenotypes by facilitating the sex-specific transcription of a shared autosomal genome (Rinn and Snyder 2005; van Nas et al. 2009; Partridge et al. 2015; Cox et al. 2017; Anderson et al. 2020; Oliva et al. 2020; Hale et al. 2022). Two questions about this hormonal regulation of gene expression are key to understanding the evolutionary dynamics of sexual dimorphism. First, are sex differences in gene expression achieved primarily through sexual divergence in hormone levels during maturation, or do the sexes also differ in their transcriptomic responses to the same hormonal signal? Second, to what extent are the regulatory effects of hormones evolutionarily labile across species? The first question about the sex-specificity of hormonal regulation touches on the classic endocrine paradigm of sex-specific organizational effects of hormones that occur early in development and thereby shape responsiveness to activational effects of elevated hormone levels later in life (Phoenix et al. 1959, Arnold and Breedlove 1985; Arnold 2009; McCarthy et al. 2009; Adkins-Regan 2012; Madison et al. 2015; McCarthy 2016; Anderson et al. 2022). The second question about the species-specificity of hormonal regulation is central to current debate over whether the regulatory architecture of hormonal pleiotropy acts primarily as an evolutionary constraint, or instead represents an adaptable source of evolutionary potential (Ketterson & Nolan 1999; Hau 2007; McGlothlin & Ketterson 2008; Cox et al. 2009; Ketterson et al. 2009; Hau & Wingfield 2011; Lema 2014; Fuxjager & Schuppe 2018; Cox 2020). In this study, we answer both questions by simultaneously characterizing the sex- and species-specificity of hormonally mediated gene expression in

the lizard genus *Sceloporus*, in which the hormone testosterone is known to mediate

many phenotypic sexual dimorphisms (Kimball & Erpino 1971; Klukowski et al. 1998;

Quinn & Hews 2003; Cox et al. 2005a,b; 2008; Cox & John-Alder 2005; John-Alder et

al. 2007; John-Alder & Cox 2007; Cox et al. 2008; John-Alder et al. 2009) and

underlying patterns of gene expression (Robinson et al. 2023; Chapter 1).

In many sexually dimorphic species, exogenous testosterone is sufficient to

induce male-typical phenotypes in females (Tobias et al. 1991; Rhen et al. 1999; Cox et

al. 2005a; Lahaye et al. 2012, 2014; Cox et al. 2015; Lindsay et al. 2016; Rose et al.

2022). In some of these cases, testosterone has also been shown to induce similar patterns

of genetic covariance and gene expression in each sex (Cox et al. 2017; Wittman et al.

2021). Although only a few studies have directly compared transcriptome-wide responses

to testosterone between the sexes, these studies have revealed relatively little overlap in

the specific genes identified as differentially expressed in each sex (Peterson et al. 2013,

2014; Hale et al. 2022). This apparent sex specificity could occur because early

developmental exposure to androgens, estrogens, and other factors can mediate the

strength of subsequent hormonal responsiveness by altering the availability of hormone

receptors, transcriptional cofactors, or enzymes for hormone metabolism (McAbee and

DonCarlos 1998; Bodo and Rissman 2008; Manoli and Tollkuhn 2018; Neubert da Silva

et al. 2019; Gegenhuber and Tollkuhn 2020; Lagunas et al. 2022). Therefore, early

organizational effects can predispose females and males to different transcriptional

responses to hormones later in life (Fiber and Swann 1996; Sullivan et al. 2009;

Chinnathambi et al. 2013; Peterson et al. 2013, 2014; Schweitzer et al. 2013), limiting the

phenotypic space available to each sex (Dufty et al. 2002; Adkins-Regan 2007). Studies

investigating organizational effects of embryonic hormones have focused on neural development and the subsequent activation of adult reproductive behaviors (Phoenix et al. 1959; McCarthy et al. 2009; McCarthy 2016), although evidence of organization in other tissues has been observed in other tissues and for other phenotypes (Hews and Moore 1995; Rosa-Molniar et al. 1996; Arnold 2009). Here, we explore whether this framework of sex-specific organization and activation can be extended to other tissues and to subordinate biological processes by testing for sex-specific transcriptomic responses to hormone treatments that simulate activational levels of testosterone typical of adult males.

Phenotypic responses to hormones can differ between closely related populations or species (Kitano et al. 2011; Bergeon Burns et al. 2014; Frankl-Vilches et al. 2015; Rosvall et al. 2016a,b; Cox et al. 2022a; Robinson et al. 2023). However, the evolution of transcriptional responses to a hormone regulating phenotypic development and the constraints imposed on evolution by pleiotropic gene regulation by the same hormone (hormonal pleiotropy) is poorly understood (Fuxjager et al. 2018; Cox 2020; Cox et al. 2022b; Rosvall 2022; Anderson and Renn 2023; Davidson et al. 2023). Comparing this regulatory architecture across related species can help assess the evolutionary lability of hormone-gene couplings that underlie hormonal pleiotropy (Cox et al. 2022b). This evolutionary lability is important because fitness trade-offs can arise when selection acts on multiple phenotypes regulated by the same hormone (Stearns 1989; Flatt et al. 2005; Hau 2007; Roff and Fairbairn 2007; Mauro and Ghalambor 2020), causing shifts away from fitness peaks for some traits if the regulatory effects of hormones are evolutionarily conserved (McGlothlin and Ketterson 2016; Dantzer and Swanson 2017; Wittman et al.

2021; Cox et al. 2022b). This view of hormonal pleiotropy is known as the evolutionary constraint hypothesis (Hau 2007). In contrast, the evolutionary potential hypothesis (Hau 2007) proposes that couplings between hormones and the downstream phenotypes they regulate are evolutionarily labile, thereby facilitating adaptation. For example, the evolution of testosterone-mediated phenotypes such as foot-flagging behavior in frogs (Mangiamele et al. 2016; Mangiamele and Fuxjager 2018; Anderson et al. 2021), wing-snap displays in manakin birds (Fuxjager et al. 2015), and locomotor and push-up behaviors in *Anolis* lizards (Johnson et al. 2018) result from the evolution of tissue-specific abundance of androgen receptors. Evolutionary changes in coregulator recruitment and local hormone conversion can also facilitate evolutionary changes in the hormonal sensitivity of entire tissues or cell types (Fuxjager and Schuppe 2018; Cox et al. 2022b), but much less is known about the evolution of hormonal responsiveness for individual genes and pathways within these tissues and cells. Transcriptomes provide data-rich descriptions of the pleiotropic regulatory effects of hormones (Peterson et al. 2013; Kitano et al. 2014; Peterson et al. 2014; Fuxjager et al. 2016; Cox et al. 2017; Finseth and Harrison 2018; Newhouse and Vernasco 2020; Enbody et al. 2022; Hale et al 2022; Khalil et al. 2023; Robinson et al. 2023), and therefore represent a promising framework for assessing the extent to which hormonal pleiotropy is conserved or labile across species.

In this study, we manipulated circulating testosterone levels of juvenile females and males from three species of *Sceloporus* lizards to simultaneously test for both sex- and species-specific effects of testosterone on the liver transcriptome. We used juveniles to test for effects on gene expression prior to pronounced sexual divergence in circulating

testosterone levels during maturation, thereby avoiding potential confounding effects of sex differences in endogenous testosterone. Our study is not intended to directly test the organization-activation hypothesis or the evolutionary potential-constraint hypothesis *per se*, but to provide a framework for assessing the sex- and species-specificity of hormonally mediated gene expression in a way that advances our understanding of each. If the sexes differ in early organizational effects of hormones or in other regulatory features that mediate responsiveness to elevated testosterone later in life, then we predict that (1) females and males will differ in the number and identity of differentially expressed genes, (2) transcriptome-wide correlations in the responsiveness of individual genes to testosterone will be low between the sexes, and (3) differentially expressed genes will exhibit sex-by-treatment interactions. If species-specific patterns of hormonal regulation have evolved, then we predict that (1) species will differ in the number and identity of differentially expressed genes, (2) transcriptome-wide correlations in the responsiveness of individual genes to testosterone will be low between species, (3) differentially expressed genes will exhibit species-by-treatment interactions, and (4) these patterns will be most pronounced between phylogenetically distant species.

Methods

Experimental design and sample collection

We characterized responsiveness to testosterone in three *Sceloporus* species: closely related *S. undulatus* and *S. virgatus,* which diverged ca. 12 mya, and more distantly related *S. merriami,* which diverged from the other two species ca. 30 mya (Wiens 1999; Leaché et al. 2016; Ossip-Drahos et al. 2016). We collected wild juvenile

lizards at approximately one month of age (see Table S1 for sampling locations and dates). After one month of acclimation in captivity, we split males and females of each species into two treatment groups. One treatment group received an intraperitoneal Silastic^{TM} implant containing 100 µg crystalline testosterone that was designed to consistently elevate circulating testosterone levels for the duration of the experiment, and the other treatment group received an empty implant as a control. Implant construction and surgical procedures followed previous studies (Cox et al. 2015, 2017; Wittman et al. 2021; Robinson et al. 2023; Chapter 1) and are described in the Supplemental Materials. Eight weeks after treatment, we euthanized each animal via decapitation and immediately collected blood to confirm treatment effects on circulating testosterone levels via radioimmunoassay (see Supplemental Materials). We also immediately collected liver samples into RNAlater Stabilization Solution (ThermoFisher Scientific) on ice, then refrigerated them for 24 h at 4°C and stored them at -80°C until RNA extraction. We focused on gene expression in the liver because it responds to testosterone and androgen-mediated signals, such as growth hormone, directly, and has been shown to diverge between the sexes in response to androgens across ontogeny (Cox et al. 2017; Hale et al. 2022).

RNA extraction and sequencing

We extracted RNA from livers of 72 juvenile lizards (median $n = 6$ per treatment, per sex, per species; see Table 1 for exact sample sizes in each group) using illustra™ RNAspin Mini RNA Isolation Kits (GE Healthcare) following manufacturer specifications, with detailed procedures and slight modifications described in the

Supplemental Materials. Library preparation and sequencing were carried out by the Georgia Genomics and Bioinformatics Core (University of Georgia; Athens, GA). RNA quality was assessed using an Agilent 2100 BioAnalyzer. cDNA libraries were prepared from total RNA (~500 ng per sample) using KAPA Biosystems (Wilmington, MA) RNA library preparation chemistry with poly(A) selection. Libraries were sequenced on an Illumina NextSeq 2000 (2 × 100 bp paired-end sequencing) using P3 high-output flow cells. We assessed read quality and trimmed reads using Fastp (Chen et al. 2018), then aligned reads to the *S. undulatus* genome (Westfall et al. 2021; GCA_019175285.1, SceUnd_v1.1) using subread-align (Liao et al. 2013), with *S. undulatus* transcripts as an alignment guide (GCF_019175285.1). Although the proportion of reads mapping to the *S. undulatus* genome declines with phylogenetic distance, this should not introduce any systematic bias to the estimation of sex or treatment differences in gene expression, since any mapping issues would be common to either sex or treatment. Following alignment, we assigned uniquely mapped fragments to annotated *S. undulatus* genes using featureCounts (Liao et al. 2014) to generate a matrix of read counts. We summed counts for each gene across paired and unpaired reads within each library. Many genes on the *S. undulatus* X chromosome (chromosome 10 in Westfall et al. 2021) have consistently higher expression in females than in males (unpublished data). Therefore, we excluded all genes from chromosome 10 and unplaced scaffolds to focus on the effects of testosterone on autosomal genes that are present in equal doses in both sexes. Reads are available under accession number PRJNA1051777.

Analyses of gene expression

We excluded two *S. merriami* individuals in the testosterone treatment group (one female, one male) from our gene expression analyses because their plasma testosterone levels were no longer elevated at the time of tissue collection, suggesting that their implants had exhausted (see Supplemental Materials). To test for sex, treatment, and species effects on gene expression, we conducted differential gene expression analyses on read counts using the package edgeR v3.38.4 (Robinson et al. 2010). Unless otherwise noted, we processed data independently for each species. To remove genes with low expression, we used *filterByExpr* in edgeR, retaining 13,036-13,891 genes (Table 1). We then used *robpca* in the rospca package v1.0.4 (Reynkens 2018) to conduct principal components analyses to test for outlier libraries, of which there were none. We normalized read counts using trimmed mean of M-values normalization, then used *glmQLFit* in edgeR to fit a negative binomial model to our data, specifying robust = TRUE to reduce the influence of hypervariable genes (Phipson et al. 2016). We then used *glmQLFTest* to calculate quasi-likelihood *F*-tests for paired contrasts (*e.g.*, control versus testosterone treatment, female versus male). We identified differentially expressed genes (DEGs) for each contrast as those with a Benjamini-Hochberg corrected *P*-value less than 0.05 (Benjamini and Hochberg 1995).

To characterize natural sex differences in gene expression, which are typically minor in juvenile lizards (Cox et al. 2015; Cox et al. 2022a; Hale et al. 2022; Robinson et al. 2023; Chapter 1), we first identified genes that were differentially expressed between control females and control males of each species. We view these comparisons as descriptions of natural sex differences in gene expression, not as tests of our primary

hypotheses. For comparison, we also identified genes that were differentially expressed between testosterone-treated females and testosterone-treated males of each species.

To test for sex differences in transcriptomic responses to testosterone in each species, we first identified genes that were differentially expressed between control and testosterone treatments within each sex. We then used chi-square tests with one degree of freedom to test whether females and males of each species differed in the number of genes upregulated by testosterone, downregulated by testosterone, and either up- or downregulated by testosterone. Next, we combined both sexes into a single model for each species and used *glmQLFTest* in edgeR to identify genes with a main effect of treatment on expression, and test for genes in which the response to testosterone in one sex was different than the response to testosterone in the other, as indicated by a sex-by-treatment interaction. As a measure of the overall similarity of testosterone-mediated gene expression between the sexes, we regressed $\log_2$-fold-change (the fold difference in mean expression between testosterone and control groups, hereafter $\log_2$FC) in females against the same measure of $\log_2$FC in males, each estimated from sex-specific models. We interpreted the correlation coefficients from these regressions as measures of the overall similarity of transcriptomic responsiveness to testosterone between sexes.

To test whether the transcriptomic effects of testosterone are conserved among species, we used an omnibus differential gene expression model that included read counts from all three species analysed simultaneously. Therefore, we repeated gene filtering, normalization, fitting of a negative binomial model, and calculations of quasi-likelihood *F*-tests for all 70 libraries. This method retained 15,234 genes for analysis. For each species, we estimated the $\log_2$FC between control and testosterone groups for each gene

retained in the omnibus model, then regressed $\log_2 FC$ values estimated from one species against another. We interpreted the correlation coefficients from these regressions as measures of the overall similarity of transcriptomic responsiveness to testosterone between species. Next, we tested for effects of testosterone on gene expression between species pairs by pooling data from two species and testing for differential gene expression between control and testosterone groups, constituting a main effect of treatment. We conducted a second analysis to test for differential gene expression with respect to the interaction between species and treatment. Combining these analyses allowed us to identify genes with an overall main effect of treatment (i.e., up- or down-regulated by testosterone), genes with an interaction between species and treatment (i.e., genes differentially regulated by testosterone in each species), and genes with both a main effect and an interaction (i.e., genes in which the main effect of testosterone is driven by its responsiveness in only one species). We conducted each of the above analyses separately for each sex and again with sexes pooled. We used a three-proportions Z-test to examine whether the proportion of genes exhibiting a significant species-by-treatment interaction differed between species pairs, and pairwise, two-proportion Z-tests with Holm correction (Holm 1979) as *post hoc* tests. To infer the functions of testosterone-responsive genes and pathways, we used gene ontology (GO) analysis (see Supplemental Materials for details).

Results

Treatment effects on circulating testosterone

Implants elevated plasma testosterone concentrations (treatment: $F_{1,55}$ = 192.2, P < 0.001; Fig. S1), with no effect of species ($F_{2,55}$ = 0.546, P = 0.582) or sex ($F_{1,55}$ = 0.895, P = 0.348), and no two- or three-way interactions (Supplementary Materials), suggesting that any observed differences in testosterone-mediated gene expression were largely driven by how the sexes and species responded to testosterone and not by differences in their circulating testosterone levels.

Sex differences in gene expression

Sex differences in juvenile gene expression were almost entirely absent when comparing control males and females in *S. undulatus* (1 DEG), *S. virgatus* (0 DEGs), and *S. merriami* (0 DEGs). Likewise, we did not detect any sex-biased genes when comparing juvenile females and males that received testosterone implants in each species.

Sex differences in effects of testosterone on gene expression

In all three species, significantly more genes were differentially expressed in response to testosterone in males than in females (Fig. 1; Table S2). However, the overall direction of transcriptomic response to testosterone was highly concordant between sexes in each species (Fig. 2), with significant correlations in log$_2$FC between females and males (all r > 0.45, all P < 0.001; Table 2). While the total numbers (Fig. 2A – F), relative proportions (Fig. 2G – I), and individual identities of up- and downregulated genes differed across species, no genes exhibited a significant sex-by-treatment interaction in

any species, indicating that male and female conspecifics responded similarly to testosterone (Fig. 2D – F). Within a species, 48-62% of genes that were responsive to testosterone in females were also responsive to testosterone in males (Table S3). Gene ontology results are presented in the Supplemental Materials.

Species differences in effects of testosterone on gene expression

In each species pair, testosterone consistently up- or downregulated hundreds of genes in the same direction for both species (67-93% of all DEGs; Fig. 3). However, in contrast to between-sex comparisons, between-species comparisons also revealed many genes that responded differently to testosterone (i.e., species-by-treatment interactions, 7-33% of all DEGs; Fig. 3). Some of these genes retained a main effect of treatment, indicating a species difference primarily in the magnitude of the response to testosterone (3-13% of all DEGs, Fig. 3), while others exhibited an interaction with no main effect, indicating a species difference in the direction of the response to testosterone (3-21% of all DEGs, Fig. 3). The number and proportion of differentially expressed genes exhibiting species-by-treatment interactions were relatively low between closely related *S. undulatus* and *S. virgatus,* but high in either pairwise comparison involving more distantly related *S. merriami* (three-proportions *Z*-test: $\chi^2 = 307.66$, *P* < 0.001; Fig. 3; Table 3). Likewise, transcriptome-wide correlations for responsiveness to testosterone were much lower for between-species comparisons (all *r* < 0.29) than for between-sex comparisons (all *r* > 0.45; Table 2). These correlations were higher between closely related *S. undulatus* and *S. virgatus* than between either of these two species and more distantly related *S. merriami* (Fig. 3; Table 2). Across species pairs, only 14-26% of genes

responsive to testosterone in one species were similarly responsive to testosterone in the other (Table S8). Gene ontology results are presented in the Supplemental Materials.

Discussion

Exogenous testosterone induced significantly more differentially expressed genes in juvenile males than in juvenile females in each of three *Sceloporus* lizard species. Yet, the overall effects of testosterone on the liver transcriptome were highly concordant between sexes. Further, no genes exhibited a significant sex-by-treatment interaction in any species, suggesting that testosterone regulates autosomal gene expression similarly in juvenile females and males, albeit to a greater degree in males. In contrast, many genes exhibited significant species differences in their response to testosterone, particularly between distantly related species, indicating that the regulatory coupling of testosterone to gene expression has evolved across species. These results suggest that early organizational effects may predispose males to (or prevent females from) enhanced transcriptomic responsiveness to testosterone later in life, and that the evolutionary lability of hormonally regulated gene expression may facilitate phenotypic diversification in closely related species.

In each *Sceloporus* species, we found that significantly more genes were both up- and downregulated by testosterone in males than in females. A similar sex difference in the number of differentially expressed genes was observed in the liver transcriptome of another lizard, *Anolis sagrei,* following treatment of juveniles with exogenous testosterone (Hale et al. 2022). In *A. sagrei*, exogenous testosterone masculinizes juvenile female phenotypes (Cox et al. 2015), statistical patterns of phenotypic and genetic

covariance (Cox 2020; Wittman et al. 2021), and underlying gene expression (Cox et al. 2017; Hale et al. 2022). Likewise, in *Sceloporus*, treatment of juvenile females with testosterone masculinizes ventral coloration (Cox et al. 2005) and induces the transcription of underlying genes for melanin synthesis in the ventral skin (Robinson et al. 2023; Chapter 1). Collectively, these studies indicate that phenotypic and transcriptomic effects of testosterone are broadly similar in juveniles of either sex, but that a larger portion of the transcriptome is responsive to testosterone in males (i.e., more genes are differentially expressed). Moreover, the between-sex correlation in transcriptomic responsiveness to testosterone was high in each *Sceloporus* species (Table 2), and no genes exhibited sex-by-treatment interactions (Fig. 3). Further, when we remove lowly expressed genes, which are more likely to exhibit high fold-change values and decrease the between-sex correlation, the correlations increase to greater than 0.63 for each species (Fig. S2). This stands in contrast to results from testosterone manipulation in dark-eyed juncos (*Junco hyemalis*), where hundreds of genes exhibited sex-by-treatment interactions in brain, liver, and muscle (Peterson et al. 2013, 2014). Whereas we treated juvenile females and males with identical doses of testosterone that approximated levels in adult males, adult female and male juncos were treated with different doses that approximated the respective adult maxima for each sex. Therefore, Peterson et al. (2013, 2014) observed sex-specific transcriptomic responses to testosterone when using sex-specific doses in sexually dimorphic adults, whereas we observed broadly concordant transcriptomic responses when using identical doses prior to the development of pronounced sexual dimorphism in juveniles.

Several mechanisms could explain why transcriptomic responses to testosterone are greater in juvenile males than in juvenile females in *Sceloporus.* For example, sexes could differ in androgen receptor density, transcriptional cofactor availability, binding globulins, or chromatin accessibility in the liver and other tissues (Cox 2020). Such sex differences in hormonal sensitivity could arise through early organizational effects of hormones that shape transcriptomic responses to testosterone later in life (Phoenix 1959; Dufty et al. 2002; Adkins-Regan 2007; Anderson et al. 2022). Typically, investigations into the organizing effects of sex hormones focus on behavior (Phoenix et al. 1959; McCarthy et al. 2009; McCarthy 2016). Though not linked to any specific organismal phenotype, our transcriptomic data suggest that similar organization may predispose males to stronger activational effects of testosterone, relative to females. Although our data do not clarify the underlying mechanisms that mediate this sex-specific sensitivity to testosterone or conclusively demonstrate that it arises from organizational effects of hormones *per se*, our results suggest that transcriptomes provide a promising means of directly testing for organizational and activational effects of hormones in future work.

Phenotypic diversification often involves the alteration of interactions between developmental regulators and genes (Carroll 1995; Prud'homme et al. 2007; Chen and Rajewsky 2007; Carroll 2008; Streifeld and Rausher 2009; Romero et al. 2012; Sackton et al. 2019). Such regulatory changes can break phenotypic and genetic correlations, facilitating trait evolution (Rabinowitz and Vokes 2012; Tsuboi et al. 2018; Cox 2020; McGlothlin et al. 2022). The evolutionary constraint hypothesis proposes that tight coordination between hormones and the phenotypes they regulate limits diversification, while the evolutionary potential hypothesis proposes that downstream regulatory nodes of

endocrine networks can evolve independently to limit the disruption of downstream phenotypes with shared regulatory components (Hau 2007). Although the dominant trend in our study was for genes to respond similarly to testosterone across *Sceloporus* species, we also observed many genes with species-specific responses to testosterone, suggesting that the relationship between testosterone and gene expression is evolutionary labile. Pairwise comparisons with distantly related *S. merriami* exhibited the highest proportion of genes with significant treatment-by-species interactions, as expected if changes in hormonal regulation accrue with evolutionary divergence. Because our treatments resulted in similar effects on circulating testosterone in each species (Fig. S1), we can infer that species differences in transcriptomic responses to testosterone are not due to differences in circulating hormones, but instead likely reflect the evolution of hormone-genome interactions (Cox et al. 2022b). In *Onthophagus* dung beetles, horn development involves *doublesex* (Kijimoto et al. 2012), Hedgehog signalling (Kijimoto et al. 2016), insulin signalling (Snell-Rood and Moczek 2012; Casasa and Moczek 2018), and serotonin signalling (Schwab et al. 2020). Interactions among these elements have evolved to result in novel transcriptomic regulation (Kijimoto et al. 2014; Ledón-Rettig and Moczek 2016; Ledón-Rettig et al. 2017) and different patterns of sexually dimorphic horn development (reviewed in Casasa et al. 2017). This illustrates how the principles of the evolutionary potential hypothesis extend beyond vertebrate-specific hormones such as testosterone to include other familiar examples in which relationships among the various nodes in a pleiotropically regulated endocrine network can evolve.

In *Sceloporus*, evolutionary changes in sexual dimorphism for phenotypes such as body size and coloration are associated with species differences in how underlying

physiological processes such as growth and melanin synthesis respond to testosterone (Quinn and Hews 2003; Cox and John-Alder 2005; Cox et al. 2005b; John-Alder and Cox 2007). In the case of coloration, these species differences in sexual dimorphism have been directly linked to underlying species differences in the expression of melanin synthesis genes in response to testosterone (Robinson et al. 2023; Chapter 1). Although we do not link patterns of testosterone-mediated gene expression in the liver to organismal phenotypes, our results suggest that underlying changes in the response to testosterone can evolve for many individual genes, which may facilitate the evolution of phenotypic sexual dimorphism. For example, testosterone promotes growth and stimulates the expression of insulin-like growth factor genes *IGF1* and *IGF2* in the liver of an *Anolis* lizard species that exhibits pronounced male-biased sexual size dimorphism (Cox et al. 2017). Although it is unknown whether testosterone influences the expression of these growth-promoting genes in sexually monomorphic *Anolis* species, direct comparison of monomorphic and dimorphic *Anolis* species reveal sex-by-species interactions for *IGF1* and *IGF2* expression in the liver (Cox et al. 2022a), analogous to the treatment-by-species interactions we observed for many genes in the *Sceloporus* liver. Although our gene ontology analysis revealed that a variety of metabolic processes were enriched for genes with significant species-by-treatment interactions (see Supplemental Materials), it is unclear whether and how these metabolic processes contribute to the development of species differences in organismal phenotypes.

The development of sexual dimorphism requires regulatory mechanisms that permit sex-specific expression of a shared autosomal genome, and the evolution of sexual dimorphism requires that these regulatory mechanisms can be modified in species-

specific ways. While much previous work has focused on how sexual dimorphism arises from sex differences in circulating hormone levels, ours is one of the few studies to test whether the sexes also respond differently to the same hormonal signal (Peterson et al. 2013, 2014, Mittal et al. 2021). Our results suggest that early developmental processes prime the sexes for differences in the magnitude, but not the direction, of transcriptomic response to testosterone, as expected if early organizational effects set the boundaries for responses to later activational effects of sex steroids (Dufty et al. 2002). Likewise, previous studies indicate that evolutionary changes in the magnitude of sexual dimorphism can be achieved by species-specific changes to circulating hormone levels (Swanson and Dantzer 2014; Husak and Lovern 2014; Karagic et al. 2022), but ours is one of the few studies to directly test whether species differ in their transcriptomic response to the same hormonal signal (Robinson et al. 2023; Chapter 1). We find that species differences in the response to testosterone increase with phylogenetic distance, suggesting that many of the regulatory couplings between hormones and genes evolve, and indicating considerable evolutionary lability in the transcriptomic architecture of hormonal pleiotropy.

Ethics

All procedures involving animals were approved by the University of Virginia's Animal

Care and Use Committee (protocol 3896). Animals were collected under permits from

New Jersey Fish & Wildlife (SC 2019007), Arizona Game & Fish (SP658032), the U.S.

Forest Service (Coronado National Forest), and Texas Parks & Wildlife (SPR-0719-113).

Data accessibility

Reads from RNAseq are available under BioProject ID PRJNA1051777 at the National

Center for Biotechnology Information Short Read Archive.

References

Adkins-Regan E. 2007 Hormones and the development of sex differences in behavior. *J. Ornithol*. **148**, 17-26. (doi:10.1007/s10336-007-0188-3)

Adkins-Regan E. 2012 Hormonal organization and activation: evolutionary implications and questions. *Gen. Comp. Endocrinol.* **176**, 279-285. (doi:10.1016/j.ygcen.2011.12.040)

Anderson AP, Renn SCP. 2023 The ancestral modulation hypothesis: predicting mechanistic control of sexually heteromorphic traits using evolutionary history. *Am. Nat.* **202**, 241-259. (doi:10.1086/725438)

Anderson AP, Rose E, Flanagan SP, Jones AG. 2020 The estrogen-responsive transcriptome of female secondary sexual traits in the gulf pipefish. *J. Hered.* **111**, 294-306. (doi:10.1093/jhered/esaa008)

Anderson NK, Goodwin SE, Schuppe ER, Dawn A, Preininger D, Mangiamele LA, Fuxjager MJ. 2022 Activational vs. organizational effects of sex steroids and their role in the evolution of reproductive behavior: looking to foot-flagging frogs and beyond. *Horm Behav* **146**, 105248. (doi:10.1016/j.yhbeh.2022.105248)

Anderson NK, Schuppe ER, Gururaja KV, Mangiamele LA, Martinez JCC, Priti H, von May R, Preininger D, Fuxjager MJ. 2021 A common endocrine signal marks the convergent evolution of an elaborate dance display in frogs. *Am Nat* **198**, 522-539. (doi:10.1086/716213)

Arnold AP, Breedlove SM. 1985. Organizational and activational effects of sex steroids on brain and behavior: a reanalysis. *Horm. Behav.* **19**, 469-498. (doi:10.1016/0018-506X(85)90042-X)

Arnold AP. 2009 The organizational-activational hypothesis as the foundation for a

unified theory of sexual differentiation of all mammalian tissues. *Horm Behav* **55**,

570-578. (doi:10.1016/j.yhbeh.2009.03.011)

Benjamini Y, Hochberg Y. 1995 Controlling the false discovery rate: a practical and

powerful approach to multiple testing. *J. R. Stat. Soc. Series B Stat. Methodol.* **57**,

289-300. (doi:10.1111/j.2517-6161.1995.tb02031.x)

Bergeon Burns CM, Rosvall KA, Hahn TP, Demas GE, Ketterson ED. 2014 Examining

sources of variation in HPG axis function among individuals and populations of the

dark-eyed junco. *Horm. Behav*. **65**, 179-187. (doi:10.1016/j.yhbeh.2013.10.006)

Bodo C, Rissman EF. 2008 The androgen receptor is selectively involved in organization

of sexually dimorphic social behaviors in mice. *Endocrinology* **149**, 4142-4150.

(doi:10.1210/en.2008-0183)

Carroll SB. 1995 Homeotic genes and the evolution of arthropods and chordates. *Nature*

376, 479-485. (doi:10.1038/376479a0)

Carroll SB. 2008 Evo-devo and an expanding evolutionary synthesis: a genetic theory of

morphological evolution. *Cell* **134**, 25-36. (doi:10.1016/j.cell.2008.06.030)

Casasa S, Moczek AP. 2018 Insulin signalling's role in mediating tissue-specific

nutritional plasticity and robustness in the horn-polyphenic beetle *Onthophgus taurus*.

Proc. R. Soc. Lond. B Biol. Sci. **285**, 20181631. (doi:10.1098/rspb.2018.1631)

Casasa S, Schwab DB, Moczek AP. 2017 Developmental regulation and evolution of

scaling: novel insights through the study of *Onthophagus* beetles. *Curr. Opin. Insect

Sci.* 19:52-60.

Chen K, Rajewsky N. 2007 The evolution of gene regulation by transcription factors and

   microRNAs. *Nat. Rev. Genet.* **8**, 93-103. (doi:10.1038/nrg1990)

Chen S, Y Zhou, Y Chen, and J Gu. 2018. fastp: an ultra-fast all-in-one FASTQ

   preprocessor. Bioinformatics 34:i884-i890. (doi:10.1093/bioinformatics/bty560)

Chinnathambi V, Yallampalli C, Sathishkumar K. 2013 Prenatal testosterone induces sex-

   specific dysfunction in endothelium-dependent relaxation pathways in adult male and

   female rates. *Biol. Reprod.* **89**, 1-9. (doi:10.1095/biolreprod.113.111542)

Chiver I, Schlinger BA. 2017 Clearing up the court: sex and the endocrine basis of

   display-court manipulation. *Anim. Behav.* **131**, 115-121.

   (doi:10.1016/j.anbehav.2017.07.014)

Chiver I, Schlinger BA. 2017 Sex differences in androgen activation of complex

   courtship behaviour. *Anim. Behav.* **124**, 109-117.

   (doi:10.1016/j.anbehav.2016.12.009)

Cox CL, Hanninen AF, Reedy AM, Cox RM. 2015 Female anoles retain responsiveness

   to testosterone despite the evolution of androgen-mediated sexual dimorphism. *Funct.*

   Ecol. **29**, 758-767. (doi:10.1111/1365-2435.12383)

Cox CL, Logan ML, Nicholson DJ, Chung AK, Rosso AA, McMillan WO, Cox RM.

   2022 Species-specific expression of growth-regulatory genes in 2 anoles with

   divergent patterns of sexual size dimorphism. *Integr. Org. Biol.* **4**, obac025.

   (doi:10.1093/iob/obac025)

Cox RM, Cox CL, McGlothlin JW, Card DC, Andrew AL, Castoe TA. 2017 Hormonally

   mediated increases in sex-biased gene expression accompany the breakdown of

between-sex genetic correlations in a sexually dimorphic lizard. *Am. Nat.* **189**, 315-332. (doi:10.1086/690105)

Cox RM, Hale MD, Wittman TN, Robinson CD, Cox CL. 2022 Evolution of hormone-phenotype couplings and hormone-genome interactions. *Horm. Behav.* **114**, 105216. (doi:10.1016/j.yhbeh.2022.105216)

Cox RM, John-Alder HB. 2005 Testosterone has opposite effects on male growth in lizards (*Sceloporus* spp.) with opposite patterns of sexual size dimorphism. *J. Exp. Biol.* **208,** 4679-4687. (doi:10.1242/jeb.01948)

Cox RM, Skelly SL, John-Alder HB. 2005 Testosterone inhibits growth in juvenile male eastern fence lizards (*Sceloporus undulatus*): implications for energy allocation and sexual size dimorphism. *Physiol. Biochem. Zool.* **78**, 531-545. (doi:10.1086/430226)

Cox RM, Skelly SL, Leo A, John-Alder HB. 2005 Testosterone regulates sexually dimorphic coloration in the eastern fence lizard, *Sceloporus undulatus*. *Copeia* **2005,** 597-608. (doi:10.1643/CP-04-313R)

Cox RM, Stenquist DS, Calsbeek R. 2009 Testosterone, growth and the evolution of sexual size dimorphism. *J. Evol. Biol.* **22**, 1586-1598. (doi:10.1111/j.1420-9101.2009.01772.x)

Cox RM, Zilberman V, John-Alder HB. 2008 Testosterone stimulates the expression of a social color signal in Yarrow's spiny lizard, *Sceloporus jarrovii*. *J. Exp. Zool.* **309A**, 505-514. (doi:10.1002/jez.481)

Cox RM. 2020 Sex steroids as mediators of phenotypic integration, genetic correlations, and evolutionary transitions. *Mol. Cell. Endocrinol.* **502,** 110668. (doi:10.1016/j.mce.2019.110668).

Dantzer B, Swanson EM. 2017 Does hormonal pleiotropy shape the evolution of performance and life history traits? *Integr. Comp. Biol.* **57**, 372-384. (doi:10.1093/icb/icx064)

Davidson PL, Nadolski EM, Moczek AP. 2023 Gene regulatory networks underlying the development and evolution of plasticity in horned beetles. *Curr. Opin. Insect Sci.* **60**, 101114. (doi:10.1016/j.cois.2023.101114)

Dufty AM, Clobert J, Møller AP. 2002 Hormones, developmental plasticity and adaptation. *Trends in Ecol. Evol.* **17**, 190-196. (doi:10.1016/S0169-5347(02)02498-9)

Enbody ED, Sin SYW, Boersma J, Edwards SV, Ketaloya S, Schwabl H, Webster MS, Karubian J. 2022 The evolutionary history and mechanistic basis of female ornamentation in a tropical songbird. *Evolution* **76**, 1720-1736. (doi:10.1111/evo.14545)

Fiber JM, Swann JM. 1996 Testosterone differentially influences sex-specific pheromone-stimulated Fos expression in limbic regions of Syrian hamsters. *Horm. Behav.* **30**, 455-473. (doi:10.1006/hbeh.1996.0050)

Finseth FR, Harrison RG. 2018 Genes integral to the reproductive function of male reproductive tissues drive heterogeneity in evolutionary rates in Japanese quail. *G3* **8**, 39-51. (doi:10.1534/g3.117.300095)

Flatt T, Tu M-P, Tatar M. 2005 Hormonal pleiotropy and the juvenile hormone regulation of Drosophila development and life history. *BioEssays* **27**, 999-1010. (doi:10.1002/bies.20290)

Frankl-Vilches C, Kuhl H, Werber M, Klages S, Kerick M, Bakker A, de Oliveira EHC, Reusch C, Capuano F, Vowinckel J, Leitner S, Ralser M, Timmermann B, Gahr M.

2015 Using the canary genome to decipher the evolution of hormone-sensitive gene regulation in seasonal singing birds. *Genome Biol.* **16**, 19. (doi:10.1186/s13059-014-0578-9)

Fuxjager MJ, Eaton J, Lindsay WR, Salwiczek LH, Rensel MA, Barske J, Sorenson L, Day LB, Schlinger BA. 2015 Evolutionary patterns of adaptive acrobatics and physical performance predict expression profiles of androgen receptor – but not oestrogen receptor – in the forelimb musculature. *Funct. Ecol.* **29**, 1197-1208. (doi:10.1111/1365-2435.12438)

Fuxjager MJ, Lee J-H, Chan T-M, Bahn JH, Chew JG, Xiao X, Schlinger BA. 2016 Research resource: Hormones, genes, and athleticism: effect of androgens on the avian muscular transcriptome. *Mol. Endocrin.* **30**, 254-271. (doi:10.1210/me.2015-1270)

Fuxjager MJ, Miles MC, Schlinger BA. 2018 Evolution of the androgen-induced male phenotype. *J. Comp. Phyiol. A* **204**, 81-92. (doi:10.1007/s00359-017-1215-3)

Fuxjager MJ, Schuppe ER. 2018 Androgenic signalling systems and their role in behavioral evolution. *J. Steroid Biochem. Mol. Biol.* **184**, 47-56. (doi:10.1016/j.jsbmb.2018.06.004)

Gegenhuber B, Tollkuhn J. 2020. Signatures of sex: sex differences in gene expression in the vertebrate brain. *Wiley Interdiscip. Rev. Dev. Biol.* **9**, e348. (doi:10.1002/wdev.348)

Hale MD, Robinson CD, Cox CL, Cox RM. 2022 Ontogenetic change in male expression of testosterone-responsive genes contributes to the emergence of sex-biased gene

expression in *Anolis sagrei*. *Front. Physiol.* **13**, 886973.
(doi:10.3389/fphys.2022.886973)

Hau M, Wingfield JC. 2011 Hormonally-regulated trade-offs: evolutionary variability and phenotypic plasticity in testosterone signalling pathways. In: Flatt T, Heyland A, editors. Mechanisms of life history evolution. Oxford, UK : Oxford University Press. p. 349-361. (https://hdl.handle.net/11858/00-001M-0000-0028-48B8-1)

Hau M. 2007 Regulation of male traits by testosterone: implications for the evolution of vertebrate life histories. *BioEssays* **29**, 133-144. (doi:10.1002/bies.20524)

Hews DK, Moore MC. 1995 Influence of androgens on differentiation of secondary sex characters in tree lizards, *Urosaurus ornatus*. *Gen. Comp. Endocrinol.* **97**, 86-102. (doi:10.1006/gcen.1995.1009)

Holm S. 1979 A simple sequentially rejective multiple test procedure. *Scand Stat* **6**, 65-70. (https://www.jstor.org/stable/4615733)

Husak JF, Lovern MB. 2014 Variation in steroid hormone levels among Caribbean *Anolis* lizards: endocrine system convergence? *Horm. Behav.* **65**, 408-415. (doi:10.1016/j.yhbeh.2014.03.006)

John-Alder HB, Cox RM, Haenel GJ, Smith LC. 2009 Hormones, performance and fitness: natural history and endocrine experiments on a lizard (*Sceloporus undulatus*). *Integr. Comp. Biol.* **49**, 393-407. (doi:10.1093/icb/icp060)

John-Alder HB, Cox RM, Taylor EN. 2007 Proximate developmental mediators of sexual dimorphism in size: case studies from squamate reptiles. *Integr. Comp. Biol.* **47**, 258-271. (doi:10.1093/icb/icm010)

John-Alder HB, Cox RM. 2007 Development of sexual size dimorphism in lizards: testosterone as a bipotential growth regulator. In: Sex, Size and Gender Roles: Evolutionary Studies of Sexual Size Dimorphism. Eds: DJ Fairbairn, WU Blanckenhorn, and T Szekely. Oxford University Press, London.

Johnson MA, Kircher BK, Castro DJ. 2018 The evolution of androgen receptor expression and behavior in *Anolis* lizard forelimb muscles. *J. Comp. Physiol. A* **204**, 71-79. (doi:10.1007/s00359-017-1228-y)

Karagic N, Härer A, Meyer A, Torres-Dowdall J. 2022 Thyroid hormone tinkering elicits integrated phenotypic changes potentially explaining rapid adaptation of colour vision in cichlid fish. *Evolution* **76**, 837-845. (doi:10.1111/evo.14455)

Ketterson ED, Atwell JW, McGlothlin JW. 2009 Phenotypic integration and independence: hormones, performance, and response to environmental change. *Integr. Comp. Biol.* **49**, 365-379. (doi:10.1093/icb/icp057)

Ketterson ED, Nolan Jr. V. 1999 Adaptation, exaptation, and constraint: a hormonal perspective. *Am. Nat.* **154**, S4-S25. (http://www.jstor.org/stable/10.1086/303280)

Khalil S, Enbody ED, Frankl-Vilches C, Welklin JF, Koch RE, Toomey MB, Sin SYW, Edwards SV, Gahr M, Schwabl H, Webster MS, Karubian J. 2023 Testosterone coordinates gene expression across different tissues to produce carotenoid-based red ornamentation. *Mol. Biol. Evol.* **40**, msad056. (doi:10.1093/molbev/msad056)

Kijimoto T, Moczek AP, Andrews J. 2012 Diversification of *doublesex* function underlies morph-, sex-, and species-specific development of beetle horns. *Proc. Natl. Acad. Sci. U. S. A.* **109**, 20526-20531. (doi:10.1073/pnas.1118589109)

Kijimoto T, Moczek AP. 2016 Hedgehog signalling enables nutrition-responsive inhibition of an alternative morph in a polyphenic beetle. *Proc. Natl. Acad. Sci. U. S. A.* **113**, 5982-5987. (doi:10.1073/pnas.1601505113)

Kijimoto T, Snell-Rood EC, Pespeni MH, Rocha G, Kafadar K, Moczek AP. 2014 The nutritionally responsive transcriptome of the polyphenic beetle *Onthophagus taurus* and the importance of sexual dimorphism and body region. *Proc. R. Soc. Lond. B Biol. Sci.* **281**, 20142084. (doi:10.1098/rspb.2014.2084)

Kimball FA, Erpino MJ. 1971 Hormonal control of pigmentary sexual dimorphism in *Sceloporus occidentalis*. *Gen. Comp. Endocrinol*. **16**, 375-384. (doi:10.1016/0016-6480(71)90050-5)

Kitano J, Kawagishi Y, Mori S, Peichel C, Makino T, Kawata M, Kusakabe M. 2011 Divergence in sex steroid hormone signaling between sympatric species of Japanese threespine stickleback. *PLoS ONE* **6**, e29253. (doi:10.1371/journal.pone.0029253)

Klukowski M, Nelson CE, Jenkinson NM. 1998 Effects of testosterone on locomotor performance and growth in field-active northern fence lizards, *Sceloporus undulatus hyacinthinus*. *Physiol. Zool.* **71**, 506-514. (https://www.jstor.org/stable/10.1086/515949)

Lagunas N, Fernández-García JM, Blanco N, Ballesta A, Carrillo B, Arevalo M-A, Collado P, Pinos H, Grassi D. 2022 Organizational effects of estrogens and androgens on estrogen and androgen receptor expression in pituitary and adrenal glands in adult male and female rats. *Front. Neuroanat.* **16**, 902218. (doi:10.3389/fnana.2022.902218)

Lahaye SEP, Eens M, Darras VM, Pinxten R. 2012 Testosterone stimulates the expression of male-typical socio-sexual and song behaviors in female budgerigars (*Melopsittacus undulatus*): An experimental study. *Gen. Comp. Endocrinol.* **178**, 82-88. (doi:10.1016/j.ygcen.2012.04.021)

Lahaye SEP, Eens M, Darras VM, Pinxten R. 2014 Bare-part color in female budgerigars changes from brown to structural blue following testosterone treatment but is not strongly masculinized. *PLoS ONE* **9**, e86849. (doi:10.1371/journal.pone.0086849)

Leaché AD, Banbury BL, Linkem CW, Nieto-Montes de Oca A. 2016. Phylogenomics of a rapid radiation: is chromosomal evolution linked to increased diversification in North American spiny lizards (genus *Sceloporus*)? *BMC Evol. Biol.* **16**, 63. (doi:10.1186/s12862-016-0628-x)

Ledón-Rettig CC, Moczek AP. 2016 The transcriptomic basis of tissue- and nutrition-dependent sexual dimorphism in the beetle *Onthophagus taurus*. *Ecol. Evol.* **6**, 1601-1613. (doi:10.1002/ece3.1933)

Ledón-Rettig CC, Zattara EE, Moczek AP. 2017 Asymmetric interactions between *doublesex* and tissue- and sex-specific target genes mediate sexual dimorphism in beetles. *Nat. Commun.* **8**, 14593. (doi:10.1038/ncomms14593)

Lema SC. 2014 Hormones and phenotypic plasticity in an ecological context: linking physiological mechanisms to evolutionary processes. *Integrat. Comp. Biol.* **54**, 850-863. (doi:10.1093/icb/icu019)

Liao Y, Smyth GK, Shi W. 2013 The Subread aligner: fast, accurate and scalable read mapping by seed-and-vote. *Nucleic Acid Res.* **41**, e108. (doi:10.1093/nar/gkt214)

Liao Y, Smyth GK, Shi W. 2014 featureCounts: an efficient general purpose program for assigning sequence reads to genomic features. *Bioinformatics* **30**, 923-930. (doi:10.1093/bioinformatics/btt656)

Lindsay WR, Barron DG, Webster MS, Schwabl H. 2016 Testosterone activates sexual dimorphism including male-typical carotenoid but not melanin plumage pigmentation in a female bird. *J. Exp. Biol.* **219**, 3091-3099. (doi:10.1242/jeb.135384)

Madison FN, Rouse Jr. ML, Balthazart J, Ball GF. 2015 Revising song behavior phenotype: testosterone driven induction of singing and measures of song quality in adult male and female canaries (*Serinus canaria*). *Gen. Comp. Endocrinol.* **215**, 61-75. (doi:10.1016/j.ygcen.2014.09.008)

Mangiamele LA, Fuxjager MJ, Schuppe ER, Taylor RS, Hödl W, Preininger D. 2016 Increased androgenic sensitivity in the hind limb muscular system marks the evolution of a derived gestural display. *Proc. Natl. Acad. Sci. U. S. A.* **113**, 5664-5669. (doi:10.1073/pnas.1603329113)

Mangiamele LA, Fuxjager MJ. 2018 Insight into the neuroendocrine basis of signal evolution: a case study in foot-flagging frogs. *J. Comp. Physiol. A* **204**, 61-70. (doi:10.1007/s00359-017-1218-0)

Manoli D, Tollkuhn J. 2018. Gene regulatory mechanisms underlying sex differences in brain development and psychiatric disease. *Ann. N. Y. Acad. Sci.* **1420**, 26-45. (doi:10.1111/nyas.13564)

Mauro AA, Ghalambor CK. 2020 Trade-offs, pleiotropy, and shared molecular pathways: a unified view of constraints on adaptation. *Integr. Comp. Biol.* **60**, 332-347. (doi:10.1093/icb/icaa056)

McAbee MD, DonCarlos LL. 1998 Ontogeny of region-specific sex differences in androgen receptor messenger ribonucleic acid expression in the rat forebrain. *Endocrinology* **139**, 1738-1745. (doi:10.1210/endo.139.4.5940)

McCarthy MM, Wright CL, Schwarz JM. 2009. New tricks by an old dogma: mechanisms of the organizational/activational hypothesis of steroid-mediated sexual differentiation of brain and behavior. *Horm Behav* **55**, 655-665. (doi:10.1016/j.yhbeh.2009.02.012)

McCarthy MM. 2016 Multifaceted origins of sex differences in the brain. *Philos. Trans. R. Soc. Lond. B Biol. Sci.* **371**, 20150106. (doi:n10.1098/rstb.2015.0106)

McGlothlin JW, Ketterson ED. 2008 Hormone-mediated suites as adaptations and evolutionary constraints. *Philos. Trans. R. Soc. Lond. B. Biol. Sci.* **363**, 1611-1620. (doi:10.1098/rstb.2007.0002)

McGlothlin JW, Ketterson ED. 2016 Hormonal pleiotropy and the evolution of correlated traits. In: Snowbird: Integrative Biology and Evolutionary Diversity in the Junco. Eds: ED Ketterson and JW Atwell. University of Chicago Press, Chicago, Illinois, USA.

McGlothlin JW, Kobiela ME, Wright HV, Kolbe JJ, Losos JB, and Brodie III ED. 2022 Conservation and convergence of genetic architecture in the adaptive radiation of *Anolis* lizards. *Am. Nat.* **200**, 207-220. (doi:10.1086/721091)

Mittal K, Henry PFP, Cornman RS, Maddox C, Basu N, Karouna-Renier NK. 2021 Sex- and developmental stage-related differences in the hepatic transcriptome of Japanese quail (*Coturnix japonica*) exposed to 17β-trenbolone. *Environ. Toxicol. Chem.* **40**, 2559-2570. (doi:10.1002/etc.5143)

Neubert da Silva G, Curi TZ, Tolouei SEL, Passoni MT, Hey GBS, Romano RM,
Martino-Andrade AJ, Dalsenter PR. 2019 Effects of diisopentyl phthalate exposure
during gestation and lactation on hormone-dependent behaviours and hormone
receptor expression in rats. *J. Neuroendocrinol.* **31**, e12816.

Newhouse DJ, Vernasco BJ. 2020 Developing a transcriptomic framework for testing
testosterone-mediated handicap hypotheses. *Gen. Comp. Endocrinol.* **298**, 113577.
(doi:10.1016/j.ygcen.2020.113577)

Oliva M, Muñoz-Aguirre M, Kim-Hellmuth S, Wucher V, Gewirtz ADH, Cotter DJ,
Parsana P, Kasela S, Balliu B, Viñuela A, et al. 2020 The impact of sex on gene
expression across human tissues. *Science* **369**, eaba3066.
(doi:10.1126/science.aba3066)

Ossip-Drahos AG, Oyola Morales JR, Vital- García C, Zúñiga-Vega JJ, Hews DK,
Martins EP. 2016 Shaping communicative colour signals over evolutionary time. *R.
Soc. Open Sci.* **3**, 160728. (doi:10.1098/rsos.160728)

Partridge C, Rodgers CMC, Knapp R, Neff BD. 2015 Androgen effects on immune gene
expression during parental care in bluegill sunfish (*Lepomis macrochirus*). *Can. J.
Zool.* **93**, 9-13. (doi:10.1139/cjz-2014-0157).

Peterson MP, Rosvall KA, Choi J-H, Ziegenfus C, Tang H, Colbourne JK, Ketterson ED.
2013 Testosterone affects neural gene expression differently in male and female
juncos: a role for hormones mediating sexual dimorphism and conflict. *PLoS ONE* **8**,
e61784. (doi:10.1371/journal.pone.0061784)

Peterson MP, Rosvall KA, Taylor CA, Lopez JA, Choi J-H, Ziegenfus C, Tang H,
Colbourne JK, Ketterson ED. 2014. Potential for sexual conflict assessed via

testosterone-mediated transcriptional changes in liver and muscle of a songbird. *J. Exp. Biol.* **217**, 507-517. (doi:10.1242/jeb.089813)

Phipson B, Lee S, Majewski IJ, Alexander ES, Smyth GK. 2016 Robust hyperparameter estimation protects against hypervariable genes and improves power to detect differential expression. *Ann. App. Stat.* **10** 946-963. (doi:10.1214/16-AOAS920)

Phoenix CH, Goy RW, Gerall AA, WC Young AA. 1959 Organizing action of prenatally administered testosterone propionate on the tissues mediating mating behavior in the female guinea pig. *Endocrinology* **65**, 369-382. (doi:10.1210/endo-65-3-369)

Prud'homme B, Gompel N, Carroll SB. 2007 Emerging principles of regulatory evolution. *Proc. Natl. Acad. Sci. U. S. A*. **104**, 8605-8612. (doi:10.1073/pnas.0700488104)

Quinn VS, Hews DK. 2003 Positive relationship between abdominal coloration and dermal melanin density in phrynosomatid lizards. *Copeia* **2003**, 858-864. (doi:10.1643/h202-116.1)

R Core Team. 2022 R: a language and environment for statistical computing. R Foundation for Statistical Computing. Vienna, Austria.

Rabinowitz AH, Vokes SA. 2012 Integration of the transcriptional networks regulating limb morphogenesis. *Dev. Biol.* **368**, 165-180. (doi:10.1016/j.ydbio.2012.05.035)

Reynkens T. 2018 rospca: robust sparse PCA using ROSPCA algorithm. R package version 1.0.4.

Rhen T, Ross J, Crews D. 1999 Effects of testosterone on sexual behavior and morphology in adult female leopard geckos, *Eublepharis macularius*. *Horm. Behav.* **36**, 119-128. (doi:10.1006/hbeh.1999.1530)

Rinn JL, Snyder M. 2005 Sexual dimorphism in mammalian gene expression. *Trends Genet.* **21**, 298-305. (doi:10.1016/j.tig.2005.03.005)

Robinson CD, Hale MD, Wittman TN, Cox CL, John-Alder HB, Cox RM. 2023 Species differences in hormonally mediated gene expression underlie the evolutionary loss of sexually dimorphic coloration in *Sceloporus* lizards. *J. Hered.* **114**, 637-653. (doi:10.1093/jhered/esad046)

Robinson MD, McCarthy DJ, and Smyth GK. 2010 edgeR: a Bioconductor package for differential expression analysis of digital gene expression data. *Bioinformatics* **26**, 139-140. (doi:10.1093/bioinformatics/btp616)

Roff DA, Fairbairn DJ. 2007 The evolution of trade-offs: where are we? *J. Evol. Biol.* **20**, 433-447. (doi:10.1111/j.1420-9101.2006.01255.x)

Romero IG, Ruvinsky I, Gilad Y. 2012 Comparative studies of gene expression and the evolution of gene regulation. *Nat. Rev. Genet.* **13**, 505-516. (doi:10.1038/nrg3229)

Rosa-Molinar E, Fritzsch B, Hendricks SE. 1996 Organizational-activational concept revisited: sexual differentiation in an atherinomorph teleost. *Horm. Behav.* **30**, 563-575. (doi:10.1006/hbeh.1996.0059)

Rose EM, Haakenson CM, Stennette K, Patel A, Gaind S, Shank BD, Madison FN, Ball GF. 2022 Neuroendocrine and behavioral response to testosterone-induced female song in canaries (*Serinus canaria*). *Physiol. Behav.* **250**, 113782. (doi:10.1016/j.physbeh.2022.113782)

Rosvall KA, Bergeon Burns CM, Jayaratna SP, Dossey EK, Ketterson ED. 2016 Gonads and the evolution of hormone phenotypes. *Integr. Comp. Biol.* **56**, 225-234. (doi:10.1093/icb/icw050)

Rosvall KA, Bergeon Burns CM, Jayaratna SP, Ketterson ED. 2016 Divergence along the
gonadal steroidogenic pathway: implications for hormone-mediated phenotypic
evolution. *Horm. Behav.* **84**, 1-8. (doi:10.1016/j.yhbeh.2016.05.015)

Rosvall KA. 2022 Evolutionary endocrinology and the problem of Darwin's tangled
bank. *Horm. Behav*. **146**, 105246. (doi:10.1016/j.yhbeh.2022.105246)

Sackton TB, Grayson P, Cloutier A, Hu Z, Liu JS, Wheeler NE, Gardner PP, Clarke JA,
Baker AJ, Clamp M, et al. 2019 Convergent regulatory evolution and loss of flight in
paleognathous birds. *Science* **364**, 74-78. (doi:10.1126/science.aat7244)

Schwab DB, Newsom KD, Moczek AP. 2020 Serotonin signalling suppresses the
nutrition-responsive induction of an alternate male morph in horn polyphenic beetles.
J. Exp. Zool. A Ecol. Integr. Physiol. **333**, 660-669. (doi:10.1002/jez.2413)

Schweitzer C, Goldstein MH, Place NJ, Adkins-Regan E. 2013 Long-lasting and sex-
specific consequences of elevated egg yolk testosterone for social behavior in
Japanese quail. *Horm. Behav.* **63**, 80-87. (doi:10.1016/j.yhbeh.2012.10.011)

Snell-Rood EC, Moczek AP. 2012 Insulin signalling as a mechanism underlying
development plasticity: the role of FOXO in a nutritional polyphenisms. *PLoS ONE*
7, e34857. (doi:10.1371/journal.pone.0034857)

Stearns SC. 1989 Trade-offs in life-history evolution. *Funct. Ecol.* **3**, 259-268.
(doi:10.2307/2389364)

Streisfeld MA, Rausher MD. 2009 Genetic changes contributing to the parallel evolution
of red floral pigmentation among *Ipomoea* species. *New Phytol.* **183**, 751-763.
(doi:10.1111/j.1469-8137.2009.02929.x)

Sullivan DA, Jensen RV, Suzuki T, Richards SM. 2009 Do sex steroids exert sex-specific and/or opposite effects on gene expression in lacrimal and meibomian glands? *Molec. Vision* **15**, 1553-1572. (http://www.molvis.org/molvis/v15/a166)

Swanson EM, Dantzer B. 2014. Insulin-like growth factor-1 is associated with life-history variation across Mammalia. *Proc. R. Soc. Lond. B Biol. Sci.* **281**, 20132458. (doi:10.1098/rspb.2013.2458)

Tobias ML, Marin ML, Kelley DB. 1991 Temporal constraints on androgen directed laryngeal masculinization in *Xenopus laevis*. *Dev. Biol.* **147**, 260-270. (doi:10.1016/S0012-1606(05)80023-5)

Tsuboi M, van der Bijl W, Kopperud BT, Erritzøe J, Voje KL, Kotrschal A, Yopak KE, Collin SP, Iwaniuk AN, Kolm N. 2018 Breakdown of brain-body allometry and the encephalization of birds and mammals. *Nat. Ecol. Evol.* **2**, 1492-1500. (doi:10.1038/s41559-018-0632-1)

van Nas A, GuhaThakurta D, Wang SS, Yehya N, Horvath S, Zhang B, Ingram-Drake L, Chaudhuri G, Schadt EE, Drake TA, et al. 2009 Elucidating the role of gonadal hormones in sexually dimorphic gene coexpression networks. *Endocrinology* **150**, 1235-1249. (doi:10.1210/en.2008-0563)

Westfall AK, Telemeco RS, Grizante MB, Waits DS, Clark AD, Simpson DY, Klabacka RL, Sullivan AP, Perry GH, Sears MW, et al. 2021 A chromosome-level genome assembly for the eastern fence lizard (*Sceloporus undulatus*), a reptile model for physiological and evolutionary ecology. *GigaScience* **10**, giab066. (doi:10.1093/gigascience/giab066)

Wiens JJ. 1999 Phylogenetic evidence for multiple losses of a sexually selected character

in phrynosomatid lizards. *Proc. R. Soc. Lond. B Biol. Sci.* **266**, 1529-1535.

(doi:10.1098/rspb.1999.0811)

Wittman TN, Robinson CD, McGlothlin JW, Cox RM. 2021 Hormonal pleiotropy

structures genetic covariance. *Evol. Lett.* **5**, 397-407. (doi:10.1002/evl3.240)

Table 1. Sample sizes for analysis in each species, sex, and treatment group. We extracted RNA from liver from 72 individuals, but two *S. merriami* libraries in the testosterone treatment group (one female, one male) were removed from analyses (not included here) because they were subsequently determined to have implants that were exhausted. The number of genes retained for analysis after filtering for low expression is indicated for each species.

Species	Control			Testosterone			Genes retained
	Females	Males	Total	Females	Males	Total	
S. undulatus	6	6	12	6	7	13	13,891
S. virgatus	6	6	12	6	6	12	13,772
S. merriami	6	5	11	5	5	10	13,036

Table 2. Correlation coefficients and 95% confidence intervals for the effects of testosterone on differential gene expression ($\log_2$FC) estimated between sexes of a species or between species (estimated separately for females, males, and both sexes pooled). Asterisks indicate statistical significance (*$P < 0.05$, **$P < 0.001$).

Between sexes			Between species			
Species	**r**		**Species dyad**	**r in females**	**r in males**	**r in both**
S. undulatus	0.461** 0.447 – 0.474		*S. undulatus* vs *S. virgatus*	0.131** 0.115 – 0.147	0.178** 0.163 – 0.193	0.285** 0.270 – 0.300
S. virgatus	0.450** 0.436 – 0.463		*S. undulatus* vs *S. merriami*	0.141** 0.125 – 0.157	0.172** 0.157 – 0.188	0.202** 0.186 – 0.217
S. merriami	0.551** 0.539 – 0.563		*S. virgatus* vs *S. merriami*	0.015 -0.001 – 0.031	0.154** 0.139 – 0.170	0.141** 0.125 – 0.156

Table 3. Results from *post hoc* analyses after a significant three-proportions *Z*-test examining whether the proportion of genes exhibiting a significant species-by-treatment interaction differed between species pairs. The number of DEGs with a significant interaction is represented in the "Pair" columns. Value in parentheses represent the proportion of genes with an interaction out of the total number of genes with a significant main effect or interaction. χ^2 values are from *post hoc* two-proportion *Z*-tests and P_{adj} represents the adjusted *P*-value after Holm correction.

Species Pair 1	Pair 1 DEGs	Species Pair 2	Pair 2 DEGs	χ^2	P_{adj}
S. undulatus vs *S. virgatus*	92 (0.067)	*S. undulatus* vs *S. merriami*	375 (0.286)	211.63	< 0.001
S. undulatus vs *S. virgatus*	92 (0.067)	*S. virgatus* vs *S. merriami*	579 (0.330)	300.94	< 0.001
S. undulatus vs *S. merriami*	375 (0.286)	*S. virgatus* vs *S. merriami*	579 (0.330)	6.63	0.010
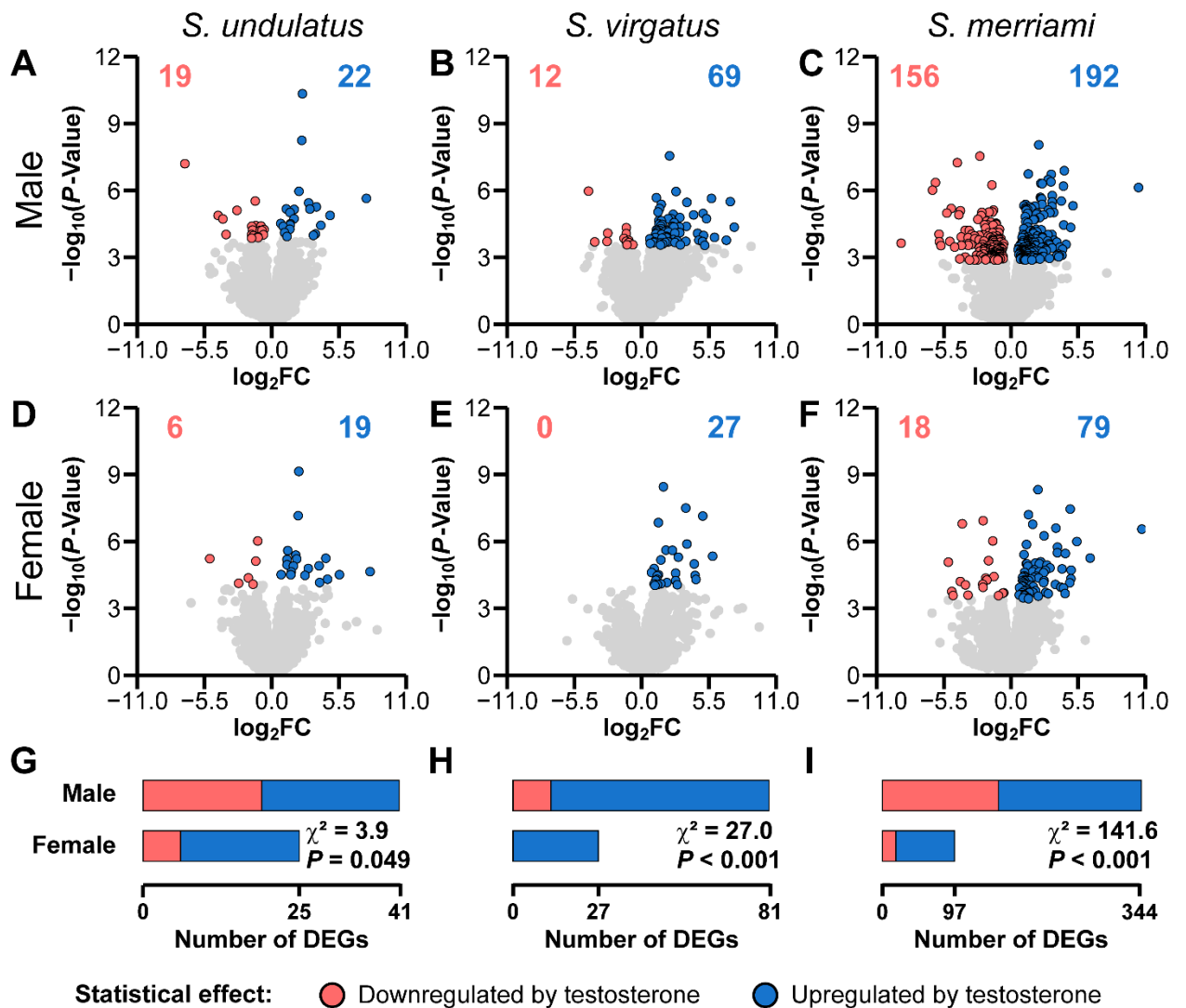
Figure 1. Volcano plots of the $-\log_{10}P$-value for the effect of testosterone on gene expression against the $\log_2$-fold change (FC) between testosterone and control groups for (**A** – **C**) males and (**D** – **F**) females in three species: *S. undulatus* (left column), *S. virgatus* (middle column), and *S. merriami* (right column). Each plot represents output from sex- and species-specific models. Points represent individual genes, and positive values along the X-axis represent genes that are more highly expressed in the testosterone group (upregulated by testosterone) whereas negative values represent genes that are more highly expressed in the control group (downregulated by testosterone). Colored

points represent genes that are significantly differentially expressed between treatment groups after *P*-value correction, and the number of significantly up- and downregulated genes is presented in the upper corners of each plot. (**G** – **I**) Chi-squared tests for sex differences in the total number of differentially expressed genes are shown alongside quantitative summaries of the number of up- and downregulated genes in each sex.
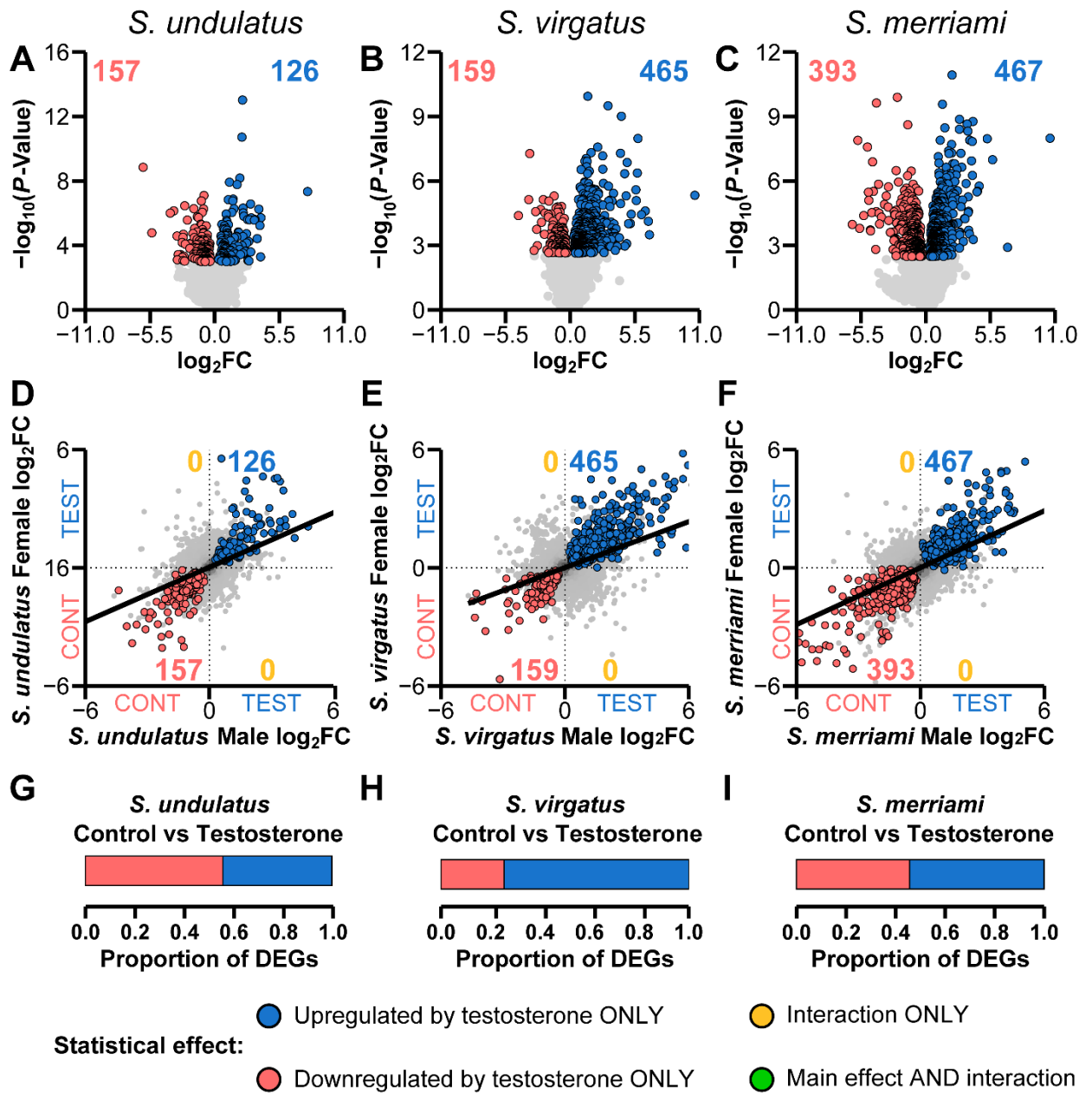
Figure 2. (**A** – **C**) Volcano plots of the $-\log_{10}P$-value for the effect of testosterone on gene expression against the $\log_2$-fold change (FC) between testosterone and control groups for (**A**) *S. undulatus*, (**B**) *S. virgatus*, and (**C**) *S. merriami*. Each plot represents output from species-specific models where sexes are combined. Points represent individual genes, and positive values along the X-axis represent genes that are more highly expressed in the testosterone group (upregulated by testosterone) whereas negative values represent genes

that are more highly expressed in the control group (downregulated by testosterone). Colored points represent genes that are significantly differentially expressed between treatment groups after Benjamini-Hochberg correction, and the number of significantly up- and downregulated genes is represented in the upper corners of each plot. (**D** – **F**) Relationship between male and female response to testosterone (log$_2$FC) for **D**) *S. undulatus*, **E**) *S. virgatus*, and **F**) *S. merriami*, where the log$_2$FC for each sex is estimated from sex-specific models. Blue and red points represent autosomal genes that have a significant effect of testosterone across sexes (same colorful points from **A** – **C**; TEST = testosterone implant; CONT = control implant). No genes have a significant sex-by-treatment interaction. (**G** – **I**) Bars representing the proportion of genes that are significantly upregulated (blue) or downregulated (red) by testosterone out of the total number of DEGs for **G**) *S. undulatus*, **H**) *S. virgatus*, and **I**) *S. merriami*.

A
S. virgatus Male log₂FC vs S. undulatus Male log₂FC — 11, 281, 168, 0

B
S. merrami Male log₂FC vs S. undulatus Male log₂FC — 29, 263, 310, 15

C
S. merrami Male log₂FC vs S. virgatus Male log₂FC — 64, 444, 248, 110

D
S. virgatus Female log₂FC vs S. undulatus Female log₂FC — 0, 138, 59, 0

E
S. merrami Female log₂FC vs S. undulatus Female log₂FC — 14, 72, 49, 3

F
S. merrami Female log₂FC vs S. virgatus Female log₂FC — 6, 131, 46, 9

G
S. virgatus log₂FC vs S. undulatus log₂FC — 42, 699, 537, 4

H
S. merrami log₂FC vs S. undulatus log₂FC — 126, 441, 494, 78

I
S. merrami log₂FC vs S. virgatus log₂FC — 138, 711, 462, 222

J *virgatus* vs *undulatus* — Male, Female, Both — Proportion of DEGs

K *merriami* vs *undulatus* — Male, Female, Both — Proportion of DEGs

L *merriami* vs *virgatus* — Male, Female, Both — Proportion of DEGs

Statistical effect:
- Upregulated by testosterone ONLY (blue)
- Downregulated by testosterone ONLY (red)
- Interaction ONLY (yellow)
- Main effect AND interaction (green)

189

Figure 3. Relationship between experimentally induced gene expression across pairwise combinations of species, assessed for (**A** – **C**) males, (**D** – **F**) females, and (**G** – **I**) both sexes. For all axes in panels **A** – **I**, log$_2$FC represents the log$_2$-fold change of gene expression of individuals receiving a testosterone implant relative to individuals receiving a control implant from an omnibus model containing all three species. Positive values indicate that a gene is upregulated by testosterone while negative values indicate that a gene is downregulated by testosterone. Genes with a significant main effect of treatment or a species-by-treatment interaction after *P*-value correction are represented by colored points. The line represents the slope from a linear regression, showing the relationship of testosterone-induced gene expression across the entire liver transcriptome in pairwise comparisons. Panels **A** – **C** represent models that only include males, panels **D** – **F** represent models that only include females, and panels **G** – **I** represent models that include both sexes. Values in panels **A** – **I** represent the number of genes with that effect. Genes with a significant main effect and interaction are not numerically represented in **A** – **I**. All regression lines are significant at *P* < 0.001 except panel **F** (*P* = 0.059, dashed line). Panels **J** – **L** summarize the proportion of DEGs for each statistical effect from all nine comparisons.

Supplementary Materials

Animal collection and husbandry

Animals for the testosterone manipulation experiment were collected from the wild at approximately one month of age. We collected 30 (15 per sex) juvenile *S. undulatus*, 42 (21 per sex) juvenile *S. virgatus*, and 30 (16 female, 14 male) juvenile *S. merriami* (Table S1). We housed each lizard individually in a small terrarium (18 x 35 x 27 cm plastic cage) at the University of Virginia in dedicated animal space. Each cage contained sand as a substrate, a brick for basking, a 15-cm segment of PVC as a shelter, and a petri dish with aquarium gravel and deionized water, filled daily, for drinking. We placed each cage under two fluorescent bulbs to provide UV light (ReptiSun 10.0 UVB; Zoo Med Laboratories, Inc.) and one incandescent bulb to provide focused heat (Bulbrite 45W 120V R20 Spot Reflector Bulb) for basking. The combination of focused heat and a room set to an ambient temperature of 21°C provided a thermal gradient within each cage from 24°C to 31°C when basking lights were on. We set room and UV lights to a 12:12 light-dark cycle, and set timers on spot bulbs such that they provided 9 h of basking time each day. We rotated cages among shelves weekly to mitigate potential placement effects from thermal stratification. Finally, we fed each lizard 5 – 7 crickets (*Gryllodes sigillatus,* 0.25-inch size, Ghann's Cricket Farm, Augusta, GA) three times per week.

Hormone implants and surgical procedures

For our hormone manipulation experiment, we built slow-release implants using 4 mm pieces of Silastic™ tubing (Dow Corning, Midland, MI, USA; 0.058 inner diameter x 0.077 outer diameter). One end was sealed using 100% waterproof silicone gel (General

Electric; Boston, MA) and allowed to cure. We then added 1 µL of either (1) testosterone

dissolved into dimethyl sulfoxide (DMSO) at a concentration of 100 µg µL^{-1}

(testosterone implant), or (2) pure DMSO (control implant), sealing the open side with

silicone gel. We allowed DMSO to diffuse out of these implants over five days, leaving

either 100 µg of crystallized testosterone in the treatment implant or an empty lumen in

the control implant. This amount of hormone was chosen so that implants would elevate

circulating testosterone to levels typical of breeding adult males of each species (Cox and

John-Alder 2005; Cox et al. 2005; John-Alder et al. 2009; Hews et al. 2012). We fasted

animals for two days prior to surgical implantation. Immediately before surgery, we

administered a 1 µL subcutaneous injection of 0.25% Sensoricaine (Bupivacaine HCl) in

the lower abdomen for local anesthesia and analgesia. We then held animals at -20°C for

3-5 minutes to immobilize them (assessed via loss of righting response) prior to surgery,

which we performed on a semi-frozen gel pack at room temperature. We sanitized the

lower abdomen with alternating swabs of antiseptic (chlorohexidine gluconate 4%

solution) and isopropyl alcohol. Finally, we made a 3-5 mm lateral incision in the lower

abdomen, placed the appropriate implant (sterilized in 100% ethanol) into the body

cavity, and sealed the incision using cyanoacrylate surgical adhesive (VetClose®, Butler

Schein Animal Health, Dublin, OH, USA). We allowed animals to recover in sterile

plastic containers overnight before returning them to their home cages.

Quantification of Circulating Testosterone

We used radioimmunoassay to quantify testosterone levels (Smith and John-Alder

1999). We extracted hormones from 20 µl samples of plasma twice with diethyl ether,

dried these extracts under streamed ultra-pure nitrogen, and reconstituted them in phosphate-buffered saline with gelatin. We then assayed each sample using a radiolabel of tritiated testosterone (PerkinElmer Life Science Inc.) and a rabbit-derived testosterone antiserum at a 1:18,000 dilution. Intra-assay variation was $4.8 \pm 0.7\%$ (mean $\pm$ 1SD), inter-assay coefficient of variation was 6.6%, and the limit of detection was 6.5 pg. To assess whether our implant treatment successfully raised circulating testosterone to similar levels in each sex and species, we used ANOVA with sex, species, and treatment as predictors with all two- and three-way interactions. Two individuals treated with exogenous testosterone (one *S. merriami* female, one *S. merriami* male) were removed from this and all subsequent analyses because their circulating testosterone concentrations were substantially lower than levels observed in other individuals from the testosterone treatment group and similar to concentrations in the control group, suggesting their implants had been depleted of hormone by the time we sampled blood and liver. All of the two- and three-way interactions were nonsignificant (sex-by-species: $F_{2,55} = 2.03$, $P = 0.141$; sex-by-treatment: $F_{1,55} = 0.777$, $P = 0.382$; species-by-treatment: $F_{2,55} = 0.884$, $P = 0.419$; sex-by-species-by-treatment $F_{2,55} = 2.855$, $P = 0.066$).

To infer the functions of testosterone-responsive genes and pathways, we used gene ontology (GO) analysis (Ashburner et al., 2000; The Gene Ontology Consortium et al., 2021), specifically using the PANTHER Overrepresentation Test (PANTHER17.0; GO Ontology database doi:10.5281/zenodo.6799722) with Fisher's exact test to examine GO biological processes. Within each species, we tested separately for biological processes that were enriched for genes upregulated by testosterone and for genes downregulated by testosterone. To maximize power, we only conducted analyses on gene

groupings from models with the sexes combined. For each dyadic species pair, we tested separately for biological processes that were enriched for genes consistently upregulated by testosterone, for genes consistently downregulated by testosterone, and for genes with significant treatment-by-species interactions.

In species-specific models, GO analysis identified multiple biological processes significantly enriched for genes that were downregulated by testosterone in *S. undulatus* (9 processes, Table S3), upregulated by testosterone in *S. virgatus* (21 processes, Table S4), and both up- and downregulated by testosterone in *S. merriami* (32 processes upregulated by testosterone, 11 processes downregulated by testosterone, Table S5 – S6). Generally, each species exhibited unique GO terms, although "system development" was enriched for genes downregulated by testosterone in *S. undulatus* and for genes upregulated by testosterone in *S. virgatus*.

In each species dyad, gene ontology analysis identified biological processes that were enriched for genes consistently up- or downregulated in both species (Tables S8 – S13), with "cellular response to hormone stimulus" consistently enriched for downregulated genes. When considering genes with a significant species-by-treatment interaction, no biological processes were enriched for the relatively small number of genes that responded differently in *S. undulatus* and closely related *S. virgatus.* However, several biological processes were enriched for the larger numbers of genes that responded differently to testosterone in contrasts involving either of these species and distantly related *S. merriami* (Tables S14 – S15). Specifically, processes related to lipids and metabolism were enriched, such as "monocarboxylic acid metabolic process", "lipid

biosynthetic process", "cellular lipid metabolic process", "carnitine metabolic process", "intracellular lipid transport", and "triglyceride metabolic process".

Supplementary References

Ashburner M, Ball CA, Blake JA, Botstein D, Butler H, Cherry JM, Davis AP, Dolinski K, Dwight SS, Eppig JT, Harris MA, Hill DP, Issel-Tarver L, Kasarskis A, Lewis S, Matese JC, Richardson JE, Ringwald M, Rubin GM, Sherlock G. 2000. Gene ontology: tool for the unification of biology. Nature Genetics 25:9.

Cox RM and HB John-Alder. 2005. Testosterone has opposite effects on male growth in lizards (*Sceloporus* spp.) with opposite patterns of sexual size dimorphism. Journal of Experimental Biology 208:4679-4687.

Cox RM, SL Skelly, A Leo, and HB John-Alder. 2005. Testosterone regulates sexually dimorphic coloration in the eastern fence lizard, *Sceloporus undulatus*. Copeia 2005:597-608.

John-Alder HB, RM Cox, GJ Haenel, and LC Smith. 2009. Hormones, performance and fitness: natural history and endocrine experiments on a lizard (*Sceloporus undulatus*). Integrative and Comparative Biology 49:393-407.

Hews DK, E Hara, and MC Anderson. 2012. Sex and species differences in plasma testosterone and in counts of androgen receptor-positive cells in key brain regions of *Sceloporus* lizard species that differ in aggression. General and Comparative Endocrinology 176:493-499.

Smith LC and HB John-Alder. 1999. Seasonal specificity of hormonal, behavioral, and coloration responses to within- and between-sex encounters in male lizards (*Sceloporus undulatus*). Hormones and Behavior 36:39-52.

The Gene Ontology Consortium. 2021. The gene ontology resource: enriching a GOld mine. Nucleic Acid Res. 49:D325-D334.
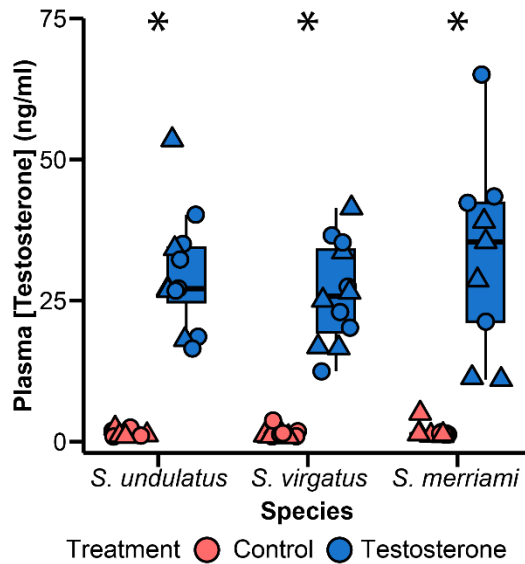
Figure S1. Circulating levels of plasma testosterone for each species eight weeks after implantation. Each point represents an individual, with females represented by triangles and males represented by circles, and boxplots illustrate the median (horizontal line), first and third quartiles (box limits), and 1.5 times the interquartile range (whiskers) for each treatment group within a species (sexes are combined and represented by different symbols only for illustrative purposes). Implants elevated circulating levels of testosterone similarly across all three species, with no effect of sex and no significant two- or three-way interactions among sex, species, or treatment.

Supplementary Tables

Table S1. Location and sampling dates for the three species used in this study.

Coordinates represent points using the WGS84 Coordinate System.

Species	Location	Coordinates	Dates
S. merriami	Brewster/Presidio Counties, TX	29.55564, -103.79169	10 - 12 August 201
S. undulatus	Ocean County, NJ	40.07889, -74.43736	7 September 2019
S. virgatus	Cochise County, AZ	31.89834, -109.21800	26 September 2019

Table S2. Results of chi-squared tests for sex differences in the number of differentially expressed genes (DEGs) in response to testosterone in each species.

Species	DEG category	DEGs in	DEGs in	χ^2	*P*
S. undulatus	Downregulated	6	19	6.8	0.009
	Upregulated	19	22	0.2	0.64
	Combined	25	41	3.9	0.049
S. virgatus	Downregulated	0	12	12.0	< 0.001
	Upregulated	27	69	18.4	< 0.001
	Combined	27	81	27.0	< 0.001
S. merriami	Downregulated	18	156	109.4	< 0.001
	Upregulated	79	192	47.1	< 0.001
	Combined	97	348	141.6	< 0.001

Table S3. Number of genes with shared identity between females and males within a species. Values in the "Females" and "Males" columns represent the number of genes responsive to testosterone. Values in the "Shared" and "% Females" columns indicate the number and proportion of share genes that are differentially expressed in response to testosterone between sexes.

Species	DEG category	Female	Males	Shared	%
S. undulatus	Downregulated	6	19	2	33.3
	Upregulated	19	22	10	52.6
	Combined	25	41	12	48.0
S. virgatus	Downregulated	0	12	---	---
	Upregulated	27	69	14	51.9
	Combined	27	81	14	51.9
S. merriami	Downregulated	18	156	13	72.2
	Upregulated	79	192	48	60.8
	Combined	97	348	61	62.3

Table S4. Results from Gene Ontology enrichment analysis testing for enriched pathways from genes downregulated by testosterone in *S. undulatus* juveniles. Analyses were conducted examining over-enrichment of protein-coding genes from *Homo sapiens*.

Biological Process	Fold Enrichment	FDR
Positive regulation of axon extension involved in axon guidance	72.33	2.40E-02
Cellular response to salt stress	63.29	2.74E-02
Inositol phosphate metabolic process	21.78	3.52E-02
Regulation of morphogenesis of an epithelium	12.98	3.48E-02
Positive regulation of endothelial cell migration	9.46	3.47E-02
Cell-cell adhesion	4.04	2.41E-02
Tube morphogenesis	3.95	5.08E-03
Epithelium development	3.06	1.13E-02
System development	2.14	3.57E-03

Table S5. Results from Gene Ontology enrichment analysis testing for enriched pathways from genes upregulated by testosterone in *S. virgatus* juveniles. Analyses were conducted examining over-enrichment of protein-coding genes from *Homo sapiens*.

Biological process	Fold Enrichment	FDR
Negative regulation of hormone secretion	6.64	1.86E-02
L-alpha-amino acid transmembrane transport	6.39	4.19E-02
Cholesterol metabolic process	5.98	6.53E-04
Acylglycerol metabolic process	5.11	3.28E-02
Ceramide metabolic process	5.06	3.46E-02
Negative regulation of establishment of protein localization	4.49	3.53E-02
Monocarboxylic acid transport	4.05	3.72E-02
Cellular lipid catabolic process	4.02	1.13E-02
Regulation of neuron apoptotic process	3.69	1.28E-02
Negative regulation of protein kinase activity	3.62	3.18E-02
Response to hypoxia	3.07	4.22E-02
Lipid transport	3.04	1.41E-02
Lipid biosynthetic process	3.03	7.06E-05
Small molecule biosynthetic process	3.02	1.58E-03
Phosphorylation	2.39	1.01E-03
Response to organic cyclic compound	2.17	1.59E-02
Organophosphate metabolic process	2.16	1.38E-02
Carboxylic acid metabolic process	2.12	3.01E-02
Intracellular signal transduction	1.75	3.73E-02
Protein modification process	1.55	4.64E-02
System development	1.46	3.84E-02

Table S6. Results from Gene Ontology enrichment analysis testing for enriched pathways from genes upregulated by testosterone in *S. merriami* juveniles. Analyses were conducted examining over-enrichment of protein-coding genes from *Homo sapiens*.

Biological process	Fold Enrichment	FDR
Succinate transmembrane transport	27.6	4.37E-02
Mitochondrial ADP transmembrane transport	27.6	4.34E-02
Cadmium ion transmembrane transport	27.6	4.32E-02
NADH metabolic process	16.98	2.30E-02
Carnitine metabolic process	16.98	2.28E-02
Fatty acid transmembrane transport	15.77	2.75E-02
NADPH regeneration	13.8	3.98E-02
Diacylglycerol metabolic process	12.74	2.93E-03
Acylglycerol biosynthetic process	11.83	3.91E-03
Tricarboxylic acid cycle	10.04	8.40E-03
Mitochondrial electron transport, NADH to ubiquinone	9.6	8.78E-04
Sulfur compound catabolic process	8.95	1.33E-02
Pyruvate metabolic process	7.77	3.77E-04
Proton motive force-driven mitochondrial ATP synthesis	7.76	1.03E-03
Purine nucleoside bisphosphate biosynthetic process	7.29	1.21E-02
Ribonucleoside bisphosphate biosynthetic process	7.29	1.20E-02
Glycerolipid catabolic process	7.29	1.19E-02
Long-chain fatty acid transport	7.03	1.41E-02
Gluconeogenesis	6.76	4.33E-02
Acyl-coA metabolic process	6.67	4.30E-04
Fatty acid beta-oxidation	6.44	2.20E-02
Triglyceride metabolic process	5.52	4.31E-02
Organophosphate catabolic process	5.2	6.20E-04
Positive regulation of small molecule metabolic process	4.19	1.40E-02
Sodium ion transmembrane transport	4.12	2.87E-02
Positive regulation of lipid metabolic process	3.87	2.50E-02
Proton transmembrane transport	3.78	4.70E-02
Regulation of carbohydrate metabolic process	3.5	2.94E-02
Glycerophospholipid metabolic process	2.88	3.83E-02
Alcohol metabolic process	2.68	4.82E-02
Chemical homeostasis	2.02	2.82E-02
Cellular response to oxygen-containing compound	1.83	4.18E-02

Table S7. Results from Gene Ontology enrichment analysis testing for enriched pathways from genes downregulated by testosterone in *S. merriami* juveniles. Analyses were conducted examining over-enrichment of protein-coding genes from *Homo sapiens*.

Biological process	Fold Enrichment	FDR
Ras protein signal transduction	4.11	4.86E-02
Extracellular matrix organization	3.52	5.15E-02
Lipid biosynthetic process	2.99	3.94E-03
Enzyme-linked receptor protein signaling pathway	2.63	2.02E-02
Cellular lipid metabolic process	2.19	5.04E-02
Response to endogenous stimulus	1.99	2.29E-02
Tissue development	1.81	4.95E-02
Phosphorus metabolic process	1.79	4.96E-02
Animal organ development	1.68	1.35E-02
Cellular localization	1.63	4.99E-02
System development	1.53	4.96E-02

Table S8. Number of genes with shared identity between species dyads. Values in the "Species 1" (top species in "Species pair" column) and "Species 2" (bottom species in "Species pair" column) columns represent the number of genes responsive to testosterone. Values in the "Shared" and "% Species 1" columns indicate the number and proportion of share genes that are differentially expressed in response to testosterone between species.

Species	DEG category	Species	Species 2	Share	% Species
S. undulatus	Downregulated	157	159	23	14.6
S. virgatus	Upregulated	126	465	50	39.7
	Combined	283	624	73	25.7
S. undulatus	Downregulated	157	393	25	15.9
S. merriami	Upregulated	126	467	34	27.0
	Combined	283	860	59	20.8
S. virgatus	Downregulated	159	393	19	11.9
S. merriami	Upregulated	465	467	67	14.4
	Combined	624	860	86	13.9

Table S9. Results from Gene Ontology enrichment analysis testing for enriched pathways from genes upregulated by testosterone in *S. undulatus* and *S. virgatus* juveniles. Analyses were conducted examining over-enrichment of protein-coding genes from *Homo sapiens*.

Biological process	Fold Enrichment	FDR
Tricarboxylic acid cycle	7.54	3.39E-02
Purine nucleotide metabolic process	2.36	2.31E-02
Organophosphate biosynthetic process	2.28	8.11E-03
Phosphorylation	1.97	7.87E-03
Amide metabolic process	1.95	2.33E-02
Carboxylic acid metabolic process	1.9	2.99E-02
Transmembrane transport	1.82	4.86E-03
Organonitrogen compound biosynthetic process	1.82	2.33E-03
Cellular catabolic process	1.82	1.69E-02
Organic substance catabolic process	1.62	1.83E-02
Cellular nitrogen compound biosynthetic process	1.59	4.56E-02
Protein modification process	1.49	2.31E-02

Table S10. Results from Gene Ontology enrichment analysis testing for enriched pathways from genes downregulated by testosterone in *S. undulatus* and *S. virgatus* juveniles. Analyses were conducted examining over-enrichment of protein-coding genes from *Homo sapiens*.

Biological process	Fold Enrichment	FDR
Norrin signaling pathway	38.03	3.07E-02
Positive regulation of vascular endothelial growth factor signaling pathway	31.69	1.25E-03
Positive regulation of endothelial cell chemotaxis	13.52	4.81E-02
Cellular modified amino acid metabolic process	4.85	8.33E-03
Extracellular matrix organization	3.67	8.04E-04
Positive regulation of angiogenesis	3.67	2.68E-02
Cellular response to transforming growth factor beta stimulus	3.58	4.81E-02
Cell-substrate adhesion	3.56	2.14E-02
Positive regulation of lipid metabolic process	3.55	4.95E-02
Axon guidance	3.47	8.06E-03
Transmembrane receptor protein serine/threonine kinase signaling pathway	3.38	2.04E-02
Regulation of MAP kinase activity	3.33	4.88E-02
Angiogenesis	3.13	2.65E-03
Response to steroid hormone	2.81	3.81E-02
Regulation of epithelial cell proliferation	2.73	1.58E-02
Response to peptide hormone	2.72	1.62E-02
Wound healing	2.7	2.89E-02
Regulation of endopeptidase activity	2.69	3.85E-02
Cellular response to hormone stimulus	2.68	2.49E-03
Positive regulation of kinase activity	2.59	1.45E-02
Regulation of neuron projection development	2.59	1.15E-02
Regulation of actin filament-based process	2.5	4.33E-02
Positive regulation of hydrolase activity	2.4	1.12E-02
Monocarboxylic acid metabolic process	2.33	2.82E-02
Cell migration	2.22	2.55E-03
Positive regulation of intracellular signal transduction	1.97	1.81E-02
Epithelium development	1.89	2.27E-02
Positive regulation of protein metabolic process	1.74	3.09E-02
Phosphate-containing compound metabolic process	1.62	4.56E-02
Regulation of biological quality	1.54	9.50E-03
Animal organ development	1.53	1.20E-02

Table S11. Results from Gene Ontology enrichment analysis testing for enriched pathways from genes upregulated by testosterone in *S. undulatus* and *S. merriami* juveniles. Analyses were conducted examining over-enrichment of protein-coding genes from *Homo sapiens*.

Biological process	Fold Enrichment	FDR
Protein oxidation	14.7	3.92E-02
Diacylglycerol metabolic process	12.86	7.89E-04
Mitochondrial electron transport, NADH to ubiquinone	12.46	5.96E-07
Proton motive force-driven mitochondrial ATP synthesis	11.94	5.49E-09
Triglyceride biosynthetic process	11.37	2.33E-02
Tricarboxylic acid cycle	8.69	1.92E-02
Mitochondrial respiratory chain complex I assembly	7.7	4.34E-04
NAD metabolic process	6.82	4.68E-02
Hexose biosynthetic process	6.43	2.71E-02
Glycerolipid catabolic process	6.31	2.89E-02
Neutral amino acid transport	6.19	3.08E-02
Carboxylic acid transmembrane transport	5.84	6.90E-06
Acyl-coA metabolic process	4.72	2.89E-02
Proton transmembrane transport	4.58	1.06E-03
Glucose metabolic process	4.38	1.24E-02
Monocarboxylic acid transport	4.11	5.87E-03
Glycerophospholipid biosynthetic process	3.51	7.96E-03
Alcohol metabolic process	2.61	3.92E-02
Regulation of lipid metabolic process	2.58	3.26E-02
Monocarboxylic acid metabolic process	2.47	6.43E-03
Negative regulation of signal transduction	1.74	4.32E-02
Response to oxygen-containing compound	1.62	4.30E-02
Response to organic substance	1.51	2.52E-02

Table S12. Results from Gene Ontology enrichment analysis testing for enriched pathways from genes downregulated by testosterone in *S. undulatus* and *S. merriami* juveniles. Analyses were conducted examining over-enrichment of protein-coding genes from *Homo sapiens*.

Biological process	Fold Enrichment	FDR
Positive regulation of vascular endothelial growth factor signaling pathway	23.67	8.89E-03
Peptide cross-linking via chondroitin 4-sulfate glycosaminoglycan	23.67	4.80E-02
Barbed-end actin filament capping	14.2	2.38E-03
Hepatocyte apoptotic process	13.52	3.69E-02
Cholesterol biosynthetic process	8.95	4.24E-03
Wound healing, spreading of cells	8.45	4.15E-02
Positive regulation of extracellular matrix organization	8.16	4.60E-02
Sprouting angiogenesis	6.98	2.55E-03
Wnt signaling pathway, planar cell polarity pathway	6.93	3.37E-02
Acyl-coA biosynthetic process	6.76	3.68E-02
Positive regulation of glucose metabolic process	6.76	3.66E-02
Positive regulation of phosphatidylinositol 3-kinase signaling	6.2	1.17E-03
Positive regulation of endothelial cell migration	5.31	1.68E-03
Cell-matrix adhesion	4.87	1.00E-03
Positive regulation of neuron projection development	4.58	9.44E-04
Organ growth	4.22	3.80E-02
Negative regulation of cellular response to growth factor stimulus	4.14	4.19E-02
Cellular response to transforming growth factor beta stimulus	3.94	6.66E-03
Regulation of axonogenesis	3.92	6.90E-03
Branching morphogenesis of an epithelial tube	3.8	2.45E-02
Response to glucocorticoid	3.64	3.20E-02
Bone development	3.6	5.12E-03
Extracellular matrix organization	3.43	1.14E-03
Kidney development	3.12	2.65E-03
Muscle tissue development	2.98	3.06E-03
Heart morphogenesis	2.97	1.84E-02
Regulation of angiogenesis	2.97	8.42E-03
Transmembrane receptor protein tyrosine kinase signaling pathway	2.91	9.29E-04
Axon guidance	2.83	4.96E-02

Muscle cell differentiation	2.8	2.98E-02
Regulation of epithelial cell proliferation	2.67	8.95E-03
Ossification	2.63	4.63E-02
Regulation of lipid metabolic process	2.55	2.66E-02
Cellular response to hormone stimulus	2.41	8.16E-03
Embryonic organ development	2.27	3.99E-02
Cell junction organization	2.23	3.12E-02
Actin cytoskeleton organization	2.18	3.70E-02
Cellular lipid metabolic process	2.11	2.40E-03
Cell population proliferation	2.08	2.05E-02
Negative regulation of developmental process	2.06	4.68E-03
Positive regulation of cell differentiation	2.04	7.29E-03
Positive regulation of cell population proliferation	2.04	4.00E-03
Positive regulation of phosphorylation	2.03	1.93E-02
Protein phosphorylation	2	3.98E-02
Chemical homeostasis	2	1.18E-02
Negative regulation of signal transduction	1.76	2.48E-02
Regulation of catalytic activity	1.66	9.56E-03
Intracellular signal transduction	1.64	3.91E-02
Regulation of protein metabolic process	1.5	3.02E-02

Table S13. Results from Gene Ontology enrichment analysis testing for enriched pathways from genes upregulated by testosterone in *S. virgatus* and *S. merriami* juveniles. Analyses were conducted examining over-enrichment of protein-coding genes from *Homo sapiens*.

Biological process	Fold Enrichment	FDR
Intestinal epithelial cell development	9.79	4.20E-02
Diacylglycerol metabolic process	9.04	2.50E-03
Acylglycerol catabolic process	8.1	4.38E-03
Tricarboxylic acid cycle	7.12	8.65E-03
Regulation of hormone biosynthetic process	7.05	4.77E-02
Glycerophospholipid catabolic process	6.63	2.71E-02
Modified amino acid transport	5.62	1.30E-02
L-alpha-amino acid transmembrane transport	4.81	1.58E-02
Ceramide biosynthetic process	4.64	3.49E-02
Phosphatidylinositol phosphate biosynthetic process	4.38	2.73E-02
Pyruvate metabolic process	4.14	3.61E-02
Transport across blood-brain barrier	4.1	1.37E-02
Cellular modified amino acid metabolic process	3.32	3.58E-02
Sodium ion transmembrane transport	3.29	1.75E-02
Glucose metabolic process	3.18	4.75E-02
Secondary alcohol metabolic process	3.14	3.59E-02
Monocarboxylic acid transport	3.11	1.83E-02
Proton transmembrane transport	3.02	3.46E-02
Negative regulation of secretion by cell	3.02	3.43E-02
Import across plasma membrane	2.81	4.14E-02
Carboxylic acid catabolic process	2.64	1.71E-02
Purine nucleotide biosynthetic process	2.54	3.24E-02
Purine ribonucleotide metabolic process	2.4	8.49E-03
Small molecule biosynthetic process	2.36	1.17E-03
Regulation of lipid metabolic process	2.25	2.58E-02
Angiogenesis	2.25	3.31E-02
Lipid transport	2.19	3.83E-02
Carbohydrate derivative biosynthetic process	2	1.12E-02
Protein phosphorylation	1.91	1.12E-02
Negative regulation of apoptotic process	1.78	1.32E-02
Chemical homeostasis	1.74	2.70E-02
Negative regulation of signal transduction	1.58	3.73E-02
Response to oxygen-containing compound	1.57	6.94E-03
Response to organic substance	1.46	3.11E-03

| Regulation of multicellular organismal process | 1.46 | 9.17E-04 |

Table S14. Results from Gene Ontology enrichment analysis testing for enriched pathways from genes downregulated by testosterone in *S. virgatus* and *S. merriami* juveniles. Analyses were conducted examining over-enrichment of protein-coding genes from *Homo sapiens*.

Biological process	Fold Enrichment	FDR
Positive regulation of ryanodine-sensitive calcium-release channel activity	22.99	2.81E-02
Positive regulation of fibroblast proliferation	6.71	3.79E-02
Positive regulation of phosphatidylinositol 3-kinase signaling	5.54	2.73E-02
Cellular modified amino acid metabolic process	4.5	3.68E-02
Extracellular matrix organization	3.37	1.01E-02
Angiogenesis	3.04	1.20E-02
Regulation of endopeptidase activity	2.91	2.94E-02
Cellular response to hormone stimulus	2.54	1.69E-02
Regulation of neuron projection development	2.53	3.26E-02
Regulation of anatomical structure morphogenesis	2.44	7.12E-04
Enzyme-linked receptor protein signaling pathway	2.35	1.73E-02
Positive regulation of cell migration	2.32	4.69E-02
Cell adhesion	2.25	2.62E-03
Response to organic cyclic compound	2.08	2.76E-02
Negative regulation of developmental process	1.97	4.85E-02
Cytoskeleton organization	1.94	1.18E-02
Cell projection organization	1.86	3.66E-02
Tissue development	1.71	2.94E-02
Phosphorus metabolic process	1.66	4.43E-02
Animal organ development	1.57	1.12E-02
Regulation of multicellular organismal process	1.51	3.12E-02
Negative regulation of cellular process	1.48	1.23E-03

Table S15. Results from Gene Ontology enrichment analysis testing for enriched pathways from genes exhibiting a significant treatment × species interaction from a model containing *S. undulatus* and *S. merriami*. Analyses were conducted examining over-enrichment of protein-coding genes from *Homo sapiens*.

Biological process	Fold Enrichment	FDR
Monocarboxylic acid metabolic process	2.92	2.74E-02
Lipid biosynthetic process	2.86	1.68E-02
Cellular lipid metabolic process	2.42	1.76E-02
Phosphate-containing compound metabolic process	1.98	2.13E-02

Table S16. Results from Gene Ontology enrichment analysis testing for enriched pathways from genes exhibiting a significant treatment × species interaction from a model containing *S. virgatus* and *S. merriami*. Analyses were conducted examining over-enrichment of protein-coding genes from *Homo sapiens*.

Biological process	Fold Enrichment	FDR
Carnitine metabolic process	17.37	6.23E-03
Cholesterol biosynthetic process	12.2	3.01E-05
Sphingoid metabolic process	10.26	3.04E-02
Cellular modified amino acid biosynthetic process	9.03	4.56E-02
Acyl-coA biosynthetic process	8.6	2.72E-03
Intracellular lipid transport	7.18	1.52E-02
Fatty acid beta-oxidation	6.02	1.53E-02
Triglyceride metabolic process	5.81	9.34E-03
Long-chain fatty acid transport	5.75	4.18E-02
Sphingolipid biosynthetic process	4.73	8.06E-03
Regulation of heart rate	4.38	2.29E-02
Heart process	4.1	3.38E-02
Regulation of mitochondrion organization	3.5	3.44E-02
Monocarboxylic acid biosynthetic process	3.45	2.34E-02
Glycerolipid biosynthetic process	3.23	1.19E-02
Cellular response to external stimulus	2.89	5.77E-03
Regulation of small molecule metabolic process	2.59	3.03E-02
Phospholipid metabolic process	2.52	3.02E-02
Response to nutrient levels	2.36	1.77E-02
Regulation of cell growth	2.33	4.27E-02
Intracellular chemical homeostasis	2.25	1.76E-02
Response to organic cyclic compound	2.18	1.78E-03
Cellular response to endogenous stimulus	1.95	2.01E-03
Response to hormone	1.94	3.93E-02
Response to organonitrogen compound	1.92	1.39E-02
Response to lipid	1.9	3.97E-02
Positive regulation of cellular component organization	1.9	7.84E-03
Cellular response to oxygen-containing compound	1.89	6.76E-03
Regulation of protein phosphorylation	1.77	4.69E-02
Cellular response to organic substance	1.63	2.00E-02
Response to stress	1.45	1.04E-02
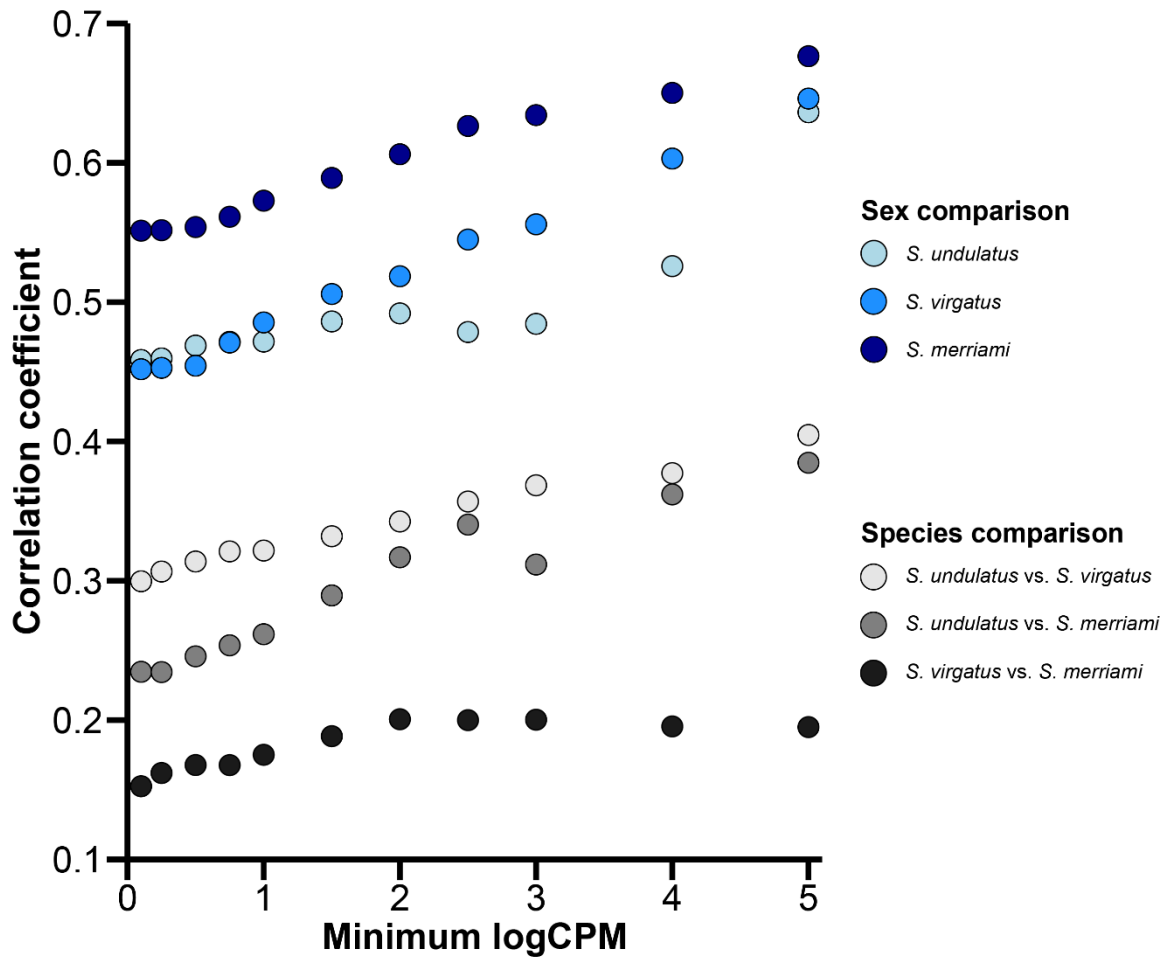
Figure S2. Correlations between male and female $\log_2$-fold change in response to testosterone for sex comparisons within a species (dots with blue hues) and species-level $\log_2$-fold change in response to testosterone in pairwise species comparison (dots with gray hues). We subset the data to include only genes expressed above a threshold (the minimum logCPM represented on the X-axis) and recalculated the correlation of gene expression to remove the effect of lowly expressed genes having high variance in $\log_2$-fold change. As the minimum logCPM becomes more stringent, the correlation of gene expression in response to testosterone increases.